Design and Testing of a Liquid Nitrous Oxide and Ethanol Fueled Rocket Engine

by

Stewart H. Youngblood

Submitted in Partial Fulfillment
of the Requirements for the Degree of
Master of Science in Mechanical Engineering
with Specialty in Explosive Engineering

New Mexico Institute of Mining and Technology
Socorro, New Mexico
August, 2015

ABSTRACT

A small-scale, bi-propellant, liquid fueled rocket engine and supporting test infrastructure were designed and constructed at the Energetic Materials Research and Testing Center (EMRTC). This facility was used to evaluate liquid nitrous oxide and ethanol as potential rocket propellants. Thrust and pressure measurements along with high-speed digital imaging of the rocket exhaust plume were made. This experimental data was used for validation of a computational model developed of the rocket engine tested.

The developed computational model was utilized to analyze rocket engine performance across a range of operating pressures, fuel-oxidizer mixture ratios, and outlet nozzle configurations. A comparative study of the modeling of a liquid rocket engine was performed using NASA CEA and Cantera, an open-source equilibrium code capable of being interfaced with MATLAB. One goal of this modeling was to demonstrate the ability of Cantera to accurately model the basic chemical equilibrium, thermodynamics, and transport properties for varied fuel and oxidizer operating conditions. Once validated for basic equilibrium, an expanded MATLAB code, referencing Cantera, was advanced beyond CEAs capabilities to predict rocket engine performance as a function of supplied propellant flow rate and rocket engine nozzle dimensions.

Cantera was found to comparable favorably to CEA for making equilibrium calculations, supporting its use as an alternative to CEA. The developed rocket engine performs as predicted, demonstrating the developed MATLAB rocket engine model was successful in predicting real world rocket engine performance. Finally, nitrous oxide and ethanol were shown to perform well as rocket propellants, with specific impulses experimentally recorded in the range of 250 to 260 seconds.

Keywords: Rocket Engine, Nitrous Oxide, Ethanol, Propellant, NASA CEA, Cantera, Computational Modeling, Test Facility

ACKNOWLEDGMENTS

I would like to thank Dr. Michael J. Hargather for being my adviser and mentor for the past two years. He has provided me countless opportunities and support to hone my skills as a designer, experimentalists, and researcher. With out his support, I would not be where I am today nor would this research have been possible. I would also like to thank Mark Grubelich and Venner Saul for their invaluable support and advice in the development of this research. Their support has allowed me to grow in skill and knowledge beyond anything I thought possible.

Thank you to my parents, Nathan and Anne, for their unwavering support both in life and professional pursuits. Their love and enthusiasm have guided me to never quit, enjoy my work, and always continue to improve myself professionally and personally. My work these past years is a testament to their support and teachings, and it is a privilege to dedicate this work to them as well as to my grandfathers, Malcolm Stewart and Walt Youngblood.

To all my friends, thank you for your invaluable support and tolerance of my idiosyncrasies. I would like to extend a special thanks to my best friends Ben Jensen, Paul Galindo, Zach Yohanas, and Alexander Menke. You gentleman have been instrumental in helping me to achieve and become who I am today. Your constant intellectual stimulation, badgering, and support have been invaluable these past seven years. I would also like to extend a special thanks to my childhood mentor, Michael Sheppard. Your enthusiasm for science and understanding the world has inspired me to chase my dreams and the skills you taught have allowed me to continue to succeed in engineering.

CONTENTS

LIST OF TABLES

LIST OF FIGURES

This thesis is accepted on behalf of the faculty
of the Institute by the following committee:

Dr. Michael J. Hargather
_____
Academic Advisor

Dr. Michael J. Hargather

_____
Research Advisor

Mark C. Grubelich
_____
Committee Member

Dr. Seokbin Lim
_____
Committee Member

_____
Committee Member

I release this document to New Mexico Institute of Mining and Technology

Stewart Youngblood   August 25 2015
_____
Student Signature   Date

CHAPTER 1

INTRODUCTION

1.1   Research Motivation

The steady advancement in space exploration has resulted in an expansion of focus on available propulsion technologies and methods to improve them. For liquid fueled rocket engines, this includes not only improvement and development of new rocket engine designs but also expansion of conventional and development of new propellants.

In order to develop new rocket engine technologies, significant testing is required to establish viability of the concept and develop reliable system designs. The development of new propulsion technologies falls in two fields: theoretical and experimental. Large scale testing is expensive, which is where small-scale laboratory tests and dedicated test facilities become important when establishing new rocket propulsion technologies. Small scale test facilities permit performance testing of new technologies and propellants and permit the testing of novel designs and propellants economically and safely. Before a design or concept can see experimental testing, a theoretical and analytical analysis is generally performed to evaluate the potential use. For rocket engines, computational models are important to evaluate the performance of both the engine design itself and also the propellants employed. While advance computationally modeling can be performed initially, simplified computational models can provide reasonable insight to the potential performance and viability of a design or propellant[1]. However, a middle ground between simplified and advance models yields the potential of better design capabilities and faster evaluation of concepts in the initial phase of the research before extensive efforts are put forward with advanced computational fluid dynamic work (CFD).

The dangers of rocket use to personnel are not only present in the launch, but also in the handling of the propellants used. The current workhorse propellant hydrazine, has found use in space propulsion dating back to World War 2. While it has been used successfully, hydrazine is a toxic substance, with carcinogenic, inhalation, and skin contact hazards[2]. The use of hydrazine can expose operators to significant hazard during fueling of the propulsion system. Alternate propellants are being investigated that are less hazardous to personnel, but also do not require advanced propellant supply systems to use[3]. Simplifying propellants supply systems for a rocket engine decreases flight weight, chance

of failure, and cost. This improves reliability, efficiency, and economical viability. The environmental factor requires not only an understanding of the potential negative effects rocket launches have on the environment, but also forward thinking in beginning to develop methods to mitigate their environmental impact[4]. Improving rocket engine performance with conventional propellants is important, but focus on the development of new propellants that produce exhaust that is less environmentally damaging has begun to receive interest[5].

The development of new test facilities and computational models is therefore important in continuing to support new developments in the field of space propulsion. The development of a hardened facility designed to test systems with a possibility of failure while mitigating potential system loss and damage is invaluable. A facility of this nature and the resultant experimental data gathered, when combined with new computational modeling techniques, yields the ability to provide a hands on teaching tool to educate propulsion engineers.

1.2   Literature Review

The scope of this research spans two main areas: computational modeling of rocket engine performance, and the design, construction, and experimental testing of rocket engines and supporting test facilities. Since research and development of modern rocket engines and research relating to the field have existed for well over a century, it has been important to review the past work to gain insight in what has been successful, what has failed, and potential areas that have not seen extensive research that are important to investigate.

With the second portion of this research focused on the development of a rocket engine and supporting test facility, a review of past systems is invaluable. This is because it is important to become familiar with technologies and designs that have been shown to work, and learn from and avoid others mistakes. Nitrous oxide and ethanol have the potential as rocket engine propellants, from both a performance and safety standpoint [3][5]. Being the principal propellants for this research, a look at previous work using nitrous oxide and ethanol as propellants is necessary. Applying design ideas or concepts that proved successful in past research allows focus to be directed to the design and development of new approaches or design features. In dealing with new system design elements, it has been important to become familiar with the hazards of the propellants to be used, specifically nitrous oxide, and to design accordingly. A review of research papers, reports of nitrous oxide accidents, and industry standards for handling of nitrous oxide and system design provides this insight.

1.2.1 Computational Modeling

Modeling efforts of rocket engines has been extensive in both analytical and computational realms, with the available research tending to fall into two categories: a simplified methodology for performing analysis, and then advance computational fluid dynamic models. Work by Gordon and Mcbride[6] in their Chemical Equilibrium with Applications (CEA) program is representative of a modeling approach that relies on a simplified methodology.

Gorden and Mcbride's developed computational model is a multipurpose tool capable of performing equilibrium calculations for reacting species as well rocket engine performance, shock, and detonation calculations. Chemical equilibrium is generally calculated using one of two equivalent methods: using equilibrium constants or minimization of Gibbs free energy of a system. CEA uses the minimization of free energy method as this allows each species to be treated independently without specifying a set of reactions prior to making calculations. The governing Gibbs free energy equations are dependent on the state of the species mixture being analyzed, and hte total Gibbs free energy of the system is dependent on the quantity and the Gibbs free energy of the individual species present in the mixture. For this reason an iterative approach is required to solve the equations, with CEA using a Newton-Raphson method to solve the equations. An initial estimate is made of the state of the system, and through the iterative procedures corrections are made to these initial estimations for system composition, Lagrangian multipliers, moles of the species present, and if necessary temperature.

Advance computational fluid dynamics models that are capable of solving two or three dimensional reacting flows through the rocket engine combustion chamber and nozzle rely on heavy computational power, such as the three-dimensional Atlas rocket plume analysis by Alexeenko et al.[7]. The introduction of more powerful computational fluid dynamics (CFD) modeling programs has allowed research and theories to be tested that are out of the realm of simplified modeling approaches, including further advancing CFD models. Munday et al.[8] demonstrated the usefulness of CFD to analyze supersonic flow in converging-diverging nozzles, while Gaddam and Subramanya[9] applied CFD past the exit of the nozzle to analyze rocket exhaust plumes and study acoustic events within the rocket engine. Bauer et al. [10] demonstrated the important application of CFD for simplified model validation. Bauer's group used CFD to validate an engineering model of a rocket exhaust plume they developed. By using the validated engineering model, Bauer's group was able to decreasing computation time, allowing for more advance models to run as computational resources are now available.

Advanced modeling using analytical equations without the need for computational modeling has also be performed. Using the Navier-Stokes equations, Alden and Habert[11] formulated a three-dimensional, gas dynamic model of exhaust plumes for rockets operating at high altitudes. The assumption of symmetry and non-reacting exhaust composition was necessary to maintain simplicity

of the equations. Despite this assumption, Habert demonstrated the effectiveness of an analytical exhaust plume model.

While the effects or reacting chemical species in the gas flow are generally accounted for, real world thermo-physical effects are often left out of modeling. Effects such as heat transfer, propellant droplet vaporization and burning, reaction rates of the chemical species, etc, are only found in the most advanced computational models even though simplified models have been developed in other fields to account for these effects. Abramzon's[12] work on improving the classic droplet vaporization model, as explained by Turns[13], and Aggarwal and Mongia's[14] development of a high pressure, multi-component droplet vaporization model for gas turbine are examples of work performed in advancing combustion modeling that is applicable to rocket engine modeling. Viskanta and Munguc[15] provide a detailed analysis procedure for accounting for radiative heat transfer in combustion systems, which is applicable to modeling the combustion processes in a rocket engine combustion chamber. Simpler computational models of rocket engines seem to have stagnated in development, focusing largely on the use of the NASA CEA developed in the mid 1990s, with the majority of computational modeling involving the use of computational fluid dynamic programs. After identifying this gap, it is apparent that work must be performed to help close the gap between simple and advanced models, and develop new methodologies and strategies for performing this research.

With the intent to use Goodwin's[16] equilibrium and thermodynamic and transport property calculator, Cantera, applications of Cantera in rocket engine modeling were investigated. Though specific research using Cantera in rocket performance analysis is lacking, Cantera has been shown to provide good results when compared to other computational programs such as Chemkin[17]. Cantera has been used in performing equilibrium calculations in the modeling of deflagration to detonation transition of nitrous oxide and ethylene mixtures by Venktech et al.[18]. Both of these studies demonstrated that Cantera provides results that compare well to hand calculations, other equilibrium codes, and experimental data. However, the use of equilibrium codes, such as Cantera, for multi-phase reaction scenarios are only a successful endeavor if quality thermodynamic and transport property data is available for phases present that the available reaction mechanism files may lack.

Both ethanol and nitrous oxide have been used in computational modeling efforts. Lawerence Livermore National Laboratories developed a reaction mechanism for gaseous ethanol combustion[19], and work by Lindbolm[1] used CEA to analyze nitrous oxide performance as a propellant with selected fuels. There is well established data and polynomial fits for chemical species, with ethanol represented by authors such as Dillon and Penoncello[20] and Wilhoit et al.[21] and nitrous oxide represented by the work performed by IHS[22]. These collections of data can be combined with equilibrium modeling codes, such as Cantera, to allow calculations to be performed with liquid and gaseous phases present.

1.2.2 Rocket Engine Design

Research from the 1960s on the design and construction of rocket engines focuses on assembly or supportive infrastructure for rocket engine testing, with fewer investigations on new developments and "next-generation" research in the field. Fox[23] on the use of cavitating venturis for flow control in rocket engines and Krzycki's[24] guide on design and construction of a small scale rocket engine are representative of the mindset of the time to support rather than advance rocket engine or system design. As the research progresses towards the late 1990s and early 2000s, the focus shifts from a supportive point of view of current rocket technology to that of a development of new concepts, including areas such as new propellants, nozzle designs, and ignition methods. This shift in focus coincides with the significant increase in interest in space exploration, especially in the development of private industry support. Work by authors such as Hagemann, et al.[25], who discusses the development of new nozzle designs to increase performance and Law[Law2012], who presents ideas of next generation fuels for chemical propulsion use, including ethanol, are presenting work to benefit the space exploration community by advancing the current technology.

Beyond interest in new propellants for improved performance and efficiency, safety and environmental effects have become a concern. These research efforts are being supported by development of laboratory scale test facilities by corporate and government interests such as the more reliable igniter design by Repas[26] from NASA or Peretz et al.[27] from Israel with their construction of a hybrid rocket motor testing facility. Academic groups are also supporting these research efforts, with test facilities and research conducted by universities such as Purdue[28] and Stanford University[29][30]. These academic facilities range in size and capabilities, but the combined testing capabilities cover the spectrum of hybrid, liquid, and solid rockets.

Of particular interest is the High Pressure Laboratory (HPL) located at Maurice Zucrow Laboratories at Purdue University. Constructed in 1965, the HPL was specifically designed to test experimental solid rocket motors. A renovation in 2001 expanded the facility so it could continue its experimental Liquid rocket engine and gas turbine testing. Currently, the facility has onsite bulk liquid oxygen (LOX) storage and a 63 gallon, 5000psi run tank for their blow down propellant supply system. A blow down system functions by isolating the propellant in a storage tank rate for high pressure, and then pressurizing the tank with high pressure nitrogen. An outlet at the bottom of the tank allows the propellant, in this case LOX, to flow through a cavitating venturi and main supply valve to the rocket engine as the nitrogen gas above pushes it out of the tank[28]. The need for a pump is eliminated as the high pressure nitrogen gas performs the work of pushing the liquid propellant to the rocket engine, simplifying system operation. The HPL has bulk liquid nitrogen storage onsite of 2500 gallons to supply the propellant blow down systems as well as supply the purge systems for blowing out the rocket engine or propellant systems with gaseous nitrogen. The liquid nitrogen is also used in cooling of the LOX during transfer from the bulk storage

to the 63 gallon run tank.

The HPL data collection and control systems are PC-based and operate on the National Instruments (NI) computational architecture using NI Labview software. This permits remote control and data acquisition of experiments at the facility. The NI Labview software is configured for auto sequencing of the test operation with timing inputted by the operator prior to the start of the test. Automated aborts are included in the system that are based on pressure and temperature measurements. All operations are remotely controlled from a control room equipped with remote camera observation of the test setup. This isolates the operators providing protection and adequate safety from the physical test operations [28]. While the design of Purdue's HPL is on a significantly larger scale than the rocket engine test facility developed in the present research, the information on its operation is invaluable as the HPL shares the same end goal for testing of experimental rocket engines designs. The propellant supply and operating system design, operation protocols, safety procedures, and hardening of the facility are well suited to application for other test facilities and is valuable in the design and construction of new facilities.

Of particular interest for a new rocket propellant has been nitrous oxide. One proponent of nitrous oxide has been Zakirov et al.[3], who has identified the benefits to using nitrous oxide are its high vapor pressure and relatively safe nature with regards to manufacturing and handling. The high vapor pressure lends the potential of simplifying the propulsion system by allowing the nitrous oxide to self pressurize its holding tank and drive itself to the rocket engine[3]. However, this method of operation can result in flow rate problems and safety concerns due to the possibility of gaseous nitrous oxide bubbles present in the liquid flow, and therefore should be avoided[31]. Nitrous oxide has potential use in both hybrid rocket engines and liquid bi-propellant rocket engines[32]. At Stanford, nitrous oxide was used successfully, and without incident, with a hybrid rocket engine constructed and operated by Waxman's group[29]. In Japan, a rocket engine and supporting test facility were actually constructed by Tokudome et al.[33].

Tokudome et al. investigated the use of nitrous oxide and ethanol as propellants as well as novel rocket engine construction methods. The rocket engine body was constructed of fiber-reinforced ceramic composite and was slightly over 203mm (8") in length and 65mm (2.6") in diameter. The engine was water cooled and was shown to operate successfully for up to thirty second firings despite the temperature at the nozzle throat exceeding the upper temperature limit of the composite material by $200K(360\ ^\circ F)$. While the engine body itself was designed to operate using only radiative cooling, water cooling was used to estimate heat flux through the combustion chamber and nozzle walls. Similar to Purdue's HPL facility, a liquid propellant blow down system was used. Gaseous helium was used as the push gas to drive the propellants out of the run tank. The use of ethanol and nitrous oxide for Tokudome's test setup proved successful, with the rocket engine operating with thrust outputs in the 2kN(225lbs) range with a vacuum specific impulse of 294 seconds[33]. Tokudome et al. demon-

strated the application of using the combination of nitrous oxide and ethanol as rocket propellants and system design for their use.

1.2.3 Test Facility Design

While the work performed at Purdue, Stanford, and Japan provide examples of successful test facilities, they do not address the specific techniques required for safely designing systems and facilities to operate for novel propellants. With the shift in focus to new concept development, the need for evaluation of hazards and safety for these ideas is important. Cocchiaro and Ward's[34] report for the Department of Defense on safety standards for energetic liquids programs is a valuable asset in evaluating hazards of new propellants. While nitrous oxide is not specifically discussed, the hazards of liquid oxygen are discussed in regards to fire and explosive hazards. Storage criteria and standoff distances are also included which assist in laying out the facility floor plan. It is important to be conscious of facility layout with regards to explosive power and standoff distances as the need for safety of personnel and prevention of a chain reaction explosive event amongst the propellants and other energetic stored on-site is of the up most importance. This explosive power present on-site is a combination of both the propellant and compressed gases stored onsite[35]. Regarding nitrous oxide use as a rocket propellant, several accidents have occurred internationally. Investigations by Merrill[36] and Munke[37] show that with the right stimulus, nitrous oxide can be driven to a decomposition event and cause an explosion, which has resulted in loss of life.

Merrill details past research on nitrous oxide decomposition events. While little hazard testing has been conducted on nitrous oxide, it has been found that nitrous oxide is most likely to decompose when contaminated with minute quantities for fuel, either being lubricants from pumps and valves or system contamination due to machining and assembly[36]. For this reason, Merrill supports treating nitrous oxide systems the same as oxygen systems, suggesting that the guidelines for oxygen system design be observed for nitrous oxide system design. This is due to the strict requirements for oxygen systems to be free of contaminants[38]. While decomposition events have been observed with nitrous oxide-fuel mixtures in both the gas and liquid phases, the gas phase mixtures were found to be the most sensitive. It was determined experimentally that gas phase nitrous oxide and fuel mixtures could detonate by the use of an electric bridge wire while liquid phase mixtures required "heavy detonator charges" to be initiated. Of concern is also the adiabatic compression of nitrous oxide, as would be case of opening a high pressure supply valve to a lower pressure nitrous oxide side. Merrill details past work that showed that while decomposition of pure nitrous oxide at $10\,^{\circ}C\,(50\,^{\circ}F)$ contained in a 51 mm (2 inch) diameter tube occurred for compression rates of 6.9 MPa/second (1000 psi/second). Merrill goes on to suggest that general operating procedures should dictate pressurization rates of nitrous oxide significantly less than 6.9 MPa/second (1000 psi/second), especially when the system is above $10\,^{\circ}C\,(50\,^{\circ}F)$, but does not provide a

actual value for what this rate should be. The lack of detail in maximum compression rate exemplifies how the reaction mechanisms of nitrous oxide are still relatively unknown and more hazard testing of nitrous oxide is needed to better understand the decomposition mechanism of nitrous oxide[36].

Several technical documents exist for designing systems for use with, and proper handling procedures of, nitrous oxide. One of these documents is produced by the European Industrial Gas Association[39] and provides detailed procedures and outlines proper practices for using nitrous oxide, and Advanced Specialty Gas Equipment[40] provides a nitrous oxide compatibility table for common materials. These procedures outline the need to design systems for nitrous oxide service with the same requirements of liquid and gaseous oxygen systems. With the knowledge that nitrous oxide should be treated as similar liquid oxygen, technical documents such as the oxygen system cleaning procedures detailed by the Compressed Gas Association[41] are important when designing systems for nitrous oxide use, and when preparing custom or machined parts for use that will be exposed to nitrous oxide.

While being aware of the hazards of nitrous oxide and designing accordingly to mitigate them, it is also important to have a reference for the explosive power of the nitrous oxide stored in the system. The quantified explosive power of nitrous oxide is not only for useful in blast mitigation and facility design, but for safety protocols including clearance distances from the test site and personnel limits on site. The explosive power is quantified by accounting for two events: the energy release from the nitrous oxide decomposition event, and the stored energy of the compressed gas in the tank containing the nitrous oxide. Estimation of the TNT weight equivalence of a nitrous oxide decomposition event can be made using the methods detailed by Cooper[42], and Dewey's[43] research on calculating the TNT equivalence of the decomposition of nitrous oxide. Another detailed resource on TNT equivalence estimation is Yang's[44] work on analytical approaches to determining the effects of flammable gas mixtures. Assuming the reactants of the system react completely to products, the heat of reaction can be solved for by using the heat of formations of the species. Once the heat of reaction is known, it is divided by the energy release of TNT and the resultant scaling factor is multiplied by the weight of the energetic material being compared to TNT. This yields a TNT weight equivalence of the energetic material. While a value for nitrous oxide was not observed during the review of the available literature, the methodology detailed by Cooper and Dewey can be applied to nitrous oxide to calculate a TNT equivalence of the material as detailed later in this research.

The TNT equivalence of the stored energy within a pressure vessel can be estimated by the analysis techniques presented by Crowl[45] and Paulsen[35]. Crowl and Paulsen outline four accepted methods for estimating the explosive energy of a pressurized system and detail the benefits and limitation of the methods. The four methods include: The Brode method, isentropic expansion, isothermal expansion, and thermodynamic availability. The Brode method looks at the energy required to raise the pressure of a gas in constant volume system of the surrounding ambient pressure to the burst pressure of the vessel[45]. The Brode

8

method is considered the simplest and is thought to more closely predict the potential explosive energy close to the point of origin of the explosion. The isentropic expansion method assumes the gas expands isentropically to its final state. The isentropic method produces a low value for the energy of the explosion, and is considered thermodynamically inconsistent since the isentropic gas expansion will result in the gas reaching a very low temperature at its final state. The isothermal method assumes the gas expands isothermally, and results in the highest energy release predictions because it assumes all the energy of the compressed gas is available to perform work. Finally, the thermodynamic availability method is representative of the maximum mechanical energy extractable from a system as it moves into equilibrium with the environment[45]. Figure 1.1 shows how each of the method's predictions vary as a function of vessel pressure. Once an explosive
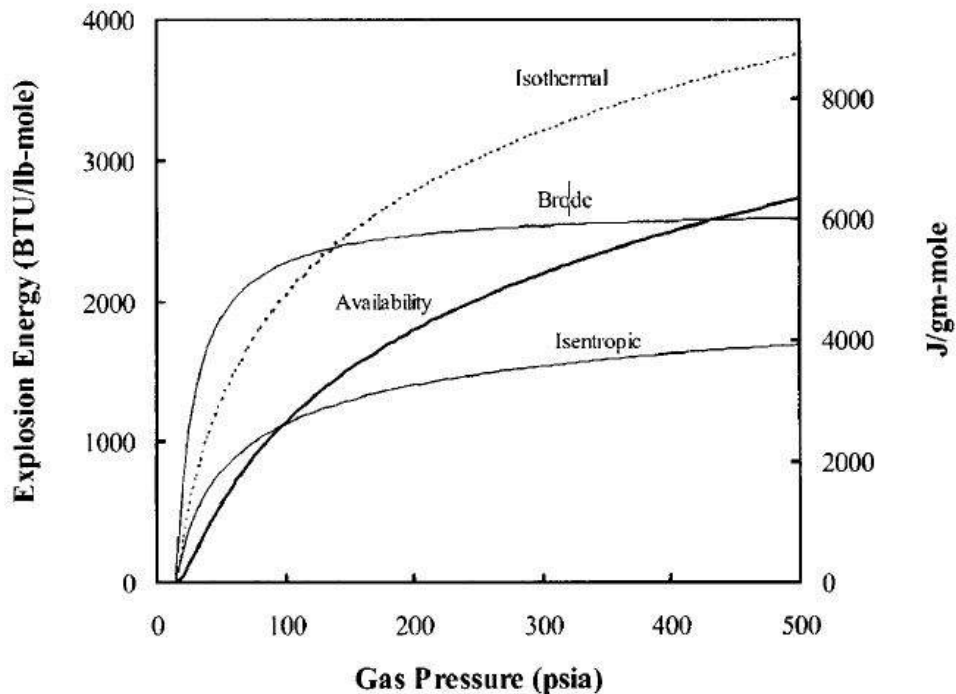
Figure 1.1: Energy release as a function of vessel gas pressure

energy estimation is found, the value can be divided by the explosive energy release of TNT yielding a TNT equivalence. This is the method detailed by Paulsen, who uses 4850 KJ/Kg for the explosive energy content of TNT, slightly higher than Cooper's value of 4522 KJ/Kg[42]. While each method predicts different results, all four continue to find use in explosive energy estimations of compressed gas systems[45]. The methodologies presented by Crowl and Paulsen are also applicable for quantifying the stored energy in gas cylinders which are commonly present at test facilities and may fail in the event of an accident, contributing to the explosive blast.

1.3 Objectives of the Present Research

The present research is focused on expanding rocket engine computational modeling methods and establishing a test facility for evaluation of novel rocket engine designs and propellants at New Mexico Tech. Specifically, the research is focused on developing the equipment and methods for evaluating the performance and potential of liquid nitrous oxide and ethanol as rocket propellants. These propellants will be evaluated for use with a bi-propellant liquid fueled rocket engine. The performance analysis will involve collecting data on rocket engine thrust output, temperature, chamber pressure, and exiting exhaust gas characteristics using thermocouples, piezo-transducers, and schlieren visualization with digital high-speed photography. The data will be used to calculate rocket performance parameters detailed by Sutton[2]. The calculated results and experimental data will then be compared to the computational model developed alongside the experimental work discussed.

In the field of rocket engine modeling, Gorden and Mcbrides CEA is generally accepted as the base standard for rocket performance modeling[6]. The present research looks to develop a computational model that expands on CEA, with the goal of accounting for combustion phenomenon not normally present in computational work. These phenomenon will include the effects of vaporization of the injected propellant droplets in the combustion chamber and chemical kinetics of the reacting combusting gases in the rocket engine. The present work will use Cantera to perform all chemical equilibrium, thermodynamic, and transport property calculations. While computational results from Cantera have not been validated against CEA in previous research, Cantera has been shown to perform well when compared to other equilibrium calculating programs such as Chemkin[17]. The idea of using Cantera in place of CEA has been discussed before [46], and the present work will expand on this. First, Cantera will be compared to CEA for equilibrium and flow property calculations, and following this a computational model will be developed in the MATLAB environment referencing Cantera for flow property calculations. The present work thus intends to establish Cantera as an acceptable alternative to CEA for equilibrium and flow property calculations, and then use Cantera in the development of a computational model that will be advanced past CEA's capabilities for rocket performance calculations, yielding new methods for predicting rocket engine performance using computational analysis.

The present research will investigate the requirements for safely designing a laboratory-scale rocket engine and supporting propellant supply system for testing nitrous oxide and ethanol as rocket propellants and provide experimental data for performance analysis. With past research discussed detailing the construction and operation of rocket engine test facilities, the present work will build off of past test facilities designs while incorporating unique safety features to minimize operator risk and potential damage to the test facility. The test facility is designed with in a modular to minimize total system loss and localize potential damage in the event of a system failure.

Experimental data will be collected of the developed rocket engine, to include thrust, chamber pressure, and propellant mass flow rates. These will be used in evaluating the specific impulse of nitrous oxide and ethanol and validation of the computational model developed.

The methods outlined of the present research will provide new engineering methods and computational models to account for combustion phenomenon. In addition, a test facility and lab-scale rocket engine will be constructed that will provide the capability of testing novel propellants and rocket engine designs. These will provide an improved methodology for analyzing rocket engine and rocket propellant performance.

CHAPTER 2

COMPUTATIONAL MODELING

Computational modeling is important for studying combustion systems because of the large number of non-linear equations and variables present that require solving simultaneously. The difficulty lies in solving the chemical equilibrium equations for reacting species. The most common computational code for these problems is the NASA CEA code.

NASA Lewis CEA (Chemical Equilibrium with Applications) is a well-known and widely-used computational program for performing chemical equilibrium and rocket performance calculations[6]. CEA uses the minimization of free energy method as this allows each species to be treated independently without specifying a set of reactions prior to making calculations. The governing Gibbs free energy equations are dependent on the quantity and state of the species mixture being analyzed. For this reason an iterative approach is required to solve the equations, with CEA using a Newton-Raphson method to solve the equations. An initial estimate is made of the state of the system, and through the iterative procedures corrections are made to these initial estimations for system composition, Lagrangian multipliers, moles of the species present, and if necessary temperature.

This method of "guess and check" is effective, but can result in the code making large corrections which result in divergence from the solution. This results from either a poor estimation at the start of the solution procedure, or the code attempting to make extremely large increase in moles of species present in minute amounts. The problem of large corrections resulting in solution divergence is mitigated by a control factor that is based on empirical rules that have been shown to provide satisfactory results[6].

In the event that the iterative process used by CEA must also iterate temperature, as is the case with combustion problems and rocket engine performance calculations, CEA is also capable of accounting for the presence of species in either the gas, liquid, or solid phase. CEA maintains the requirement that the presence of a condensed species that was not previously present will decrease the Gibbs energy of the system. To maintain simplicity in the calculations, if there are multiple species which pass the test of decreasing the Gibbs energy of the system, the species with the largest decrease of the Gibbs energy is included per iterative step. This process continues until all condensed species that may be present are accounted for. Determination of the phase of the resultant condensed

species is handled by a set of criteria that are a function of the melting temperature of the species. Depending on where the resultant temperature of the system lies in relation to the melting temperature of the species will determine whether the species exists in a solid or liquid phase.

To perform these calculations, CEA references input files that contain thermodynamic data and transport property data for the chemical species present. Specific data set files can be used or created for these calculations or a standard NASA species data set may be used if the test scenario and reacting species fall within the NASA data set applicability range[6]. Test scenarios may be inputted using a a GUI interface or using a command console to run a test scenario file. However, the interfacing of CEA with other programs to expand CEA's capabilities or to use CEA for performing equilibrium calculations within a computational model can prove challenging as CEA is designed to function as a standalone program.

Cantera is an open source chemical equilibrium calculation code developed at the California Institute of Technology. Cantera is an object based software tool for solving chemically reacting flow problems involving thermodynamics, transport processes, and chemical kinetics, and was designed to be accessed by various environments, including C++, Fortan 90, MATLAB, and Python[16]. Reaction mechanism files, containing thermodynamic, transport process, and chemical kinetics data, are referenced by Cantera when it makes chemical equilibrium calculations and flow property calculations. These reaction mechanism data files allow a predefined data file or or custom created data file for a specific reaction process to be used. Unlike CEA, Cantera is purely a chemical equilibrium and flow property solving software, relying on modeling codes in MATLAB or other computational languages to reference Cantera to perform chemical reaction and flow property calculations. While more computational work is necessary in performing thermodynamic and transport property calculations when using Cantera, Cantera provides the freedom to create advanced models of thermodynamic flow systems. For this reason, Cantera was chosen to be model the performance of a liquid nitrous oxide and ethanol fueled rocket engine.

Using Cantera for performing equilibrium calculations in rocket performance modeling has been discussed before[46], but Cantera has not formally been presented as an acceptable alternative to CEA. A primary goal of this work is to demonstrate Cantera's ability to provide comparable results to CEA for equilibrium and flow property calculations. With Cantera shown to be acceptable for equilibrium and flow property calculations, the developed MATLAB rocket engine model, referencing Cantera, is then be shown to provide comparable results to CEA for rocket performance calculations. The developed MATLAB/Cantera rocket engine model is then advanced beyond CEAs capabilities. The effects of propellant flow rate on engine performance are incorporated here. The computational rocket engine model was written using the MATLAB R2013a environment with Cantera interfaced within the environment. The graphic user interface (GUI) version of CEA was used for making calculations with CEA.

2.1 NASA CEA and Cantera Equilibrium

To compare the capabilities of Cantera to CEA for calculating equilibrium, a direct comparison of different reaction scenarios was performed. Reaction scenarios were chosen for a gas phase mixture of nitrous oxide and ethanol. Both CEA and Cantera solve for chemical equilibrium, and the respective programs' results were compared using a percent difference, using Equation 2.1.

$$Difference = \frac{\beta_{Cantera} - \beta_{CEA}}{\beta_{CEA}} * 100 \tag{2.1}$$

Where β is the property being compared. This method yields a standard sign convention of the resultant values. A positive percent difference indicates that the value Cantera predicted was higher than that of the prediction by CEA. A negative percent difference indicates a lower value predicted by Cantera.

The scenarios for comparison were chosen to be reasonably representative of conditions seen in rocket combustion processes, with the selection based on results from the literature [2][33][47]. A direct comparison was performed using a short MATLAB script to reference Cantera's equilibrium and flow property functions and direct user input into the GUI version of CEA for these predetermined conditions. The MATLAB/Cantera equilibrium script can be found in Appendix C.1.

The reaction scenarios include three different stoichiometric mixtures reacting to equilibrium at five different pressures starting at an initial mixture temperature of 298K (76.73F). Three oxidizer and fuel ratios (O/F) were chosen as defined by Equation 2.2:

$$O/F = \frac{M_{Oxidizer}}{M_{Fuel}} \tag{2.2}$$

The O/F ratios were:stoichiometric (O/F=5.7), fuel rich at fifty percent deviation from stoichiometric (O/F=2.85) , and oxidizer rich at fifty percent deviation from stoichiometric (O/F = 8.55). The equilibrium calculations were made across a pressure range of one atmosphere (0.101MPa, 14.7psi) to 100 atmo in 25 atm steps. These reaction scenarios are outlined in table 2.1.

Equilibrium was calculated assuming constant enthalpy and pressure of the gas mixture. This method of equilibrium was chosen as it most closely represents the combustion conditions in the rocket engine combustion chamber [48], and is what CEA assumes for making its equilibrium calculations. The developed MATLAB/Cantera rocket engine model also uses the same assumption when solving for chemical equilibrium rocket performance calculations. The calculated results were tabulated and compared. Final temperature, enthalpy, entropy, internal energy, Gibbs function, and specific heat (Cp) were chosen for being representative of thermodynamic property calculations. Density was chosen as representative of the transport property calculations. The properties chosen to compare were based on the need to review the capabilities of each respective code not

14

Table 2.1: Reaction simulations for equilibrium calculations. 15 total simulations performed

Initial Temperature	Gas Mixture Stoichiometry	Initial Pressure
$298K(76.7°F)$	2.85	0.101MPa (14.7psi)
		2.53MPa (367psi)
		5.06MPa (735psi)
		7.60MPa (1101psi)
		10.13MPa (1470psi)
$298K(76.7°F)$	5.7	0.101MPa (14.7psi)
		2.53MPa (367psi)
		5.06MPa (735psi)
		7.60MPa (1101psi)
		10.13MPa (1470psi)
$298K(76.7°F)$	8.55	0.101MPa (14.7psi)
		2.53MPa (367psi)
		5.06MPa (735psi)
		7.60MPa (1101psi)
		10.13MPa (1470psi)

only for equilibrium calculations, but also for calculating thermodynamic properties and transport properties. The properties reviewed are also properties used in making calculations in the rocket engine model, as discussed in the following section.

For initial comparison, the standard NASA thermodynamic and transport process data file is used with CEA. Cantera uses a modified data file based on a Lawrence Livermore National Labs (LLNL) developed reaction mechanism file for ethanol combustion [19]. While an initial comparison with a reformatted mechanism file that contains the same NASA thermodynamic and transport process data used by CEA would be ideal for direct comparison purposes, interfacing the NASA mechanism file into Cantera proved unsuccessful. Ultimately, the NASA data files used by CEA could not be properly converted to the proper file format for Cantera's use. In reviewing the LLNL mechanism file, it was found that a considerable portion of the thermodynamic data was based on the same NASA data and polynomials used by CEA[19]. For species not found in the NASA data set, custom data was supplied or extrapolated from other sources and included in the mechanism file by LLNL. The transport property data supplied was sourced from Sandia's CHEMKIN transport data base[19]. While the LLNL mechanism file is specific to detailed modeling of ethanol combustion, the data's similarity to the data sets used by CEA provided confidence that the LLNL file would be a suitable alternative to direct implementation of the NASA data files used by CEA with Cantera. Future research will investigate incorporating

chemical kinetics into the LLNL mechanism file for use with Cantera.

2.1.1 CEA and Cantera Equilibrium Comparison Results

The tables below present the percentage difference between the results produced by Cantera, using the modified LLNL mechanism file, and the results produced by CEA for constant enthalpy and pressure equilibrium. Tables 2.2. and 2.3 show the results of the reaction simulations at a mixture stoichiometry of O/F=2.85 (fuel-rich). Tables 2.4 and 2.5 show the results stochiometric (O/F=5.7). Finally, tables 2.6 and 2.7 show the results of the reaction simulations at a mixture stoichiometry of O/F = 8.55 (oxidizer-rich).

Table 2.2: Difference between Cantera's and CEA's results for equilibrium calculated for a gas mixture O/F = 2.85

Pressure (MPa, psi)	Temperature	Enthalpy	Internal Energy
0.101 (14.7)	0.14%	0.03%	0.14%
2.53 (367)	0.15%	0.03%	0.15%
5.06 (735)	0.15%	0.03%	0.16%
7.60 (1102)	0.15%	0.03%	0.16%
10.13 (1470)	0.15%	0.03%	0.16%

Table 2.3: Difference between Cantera's and CEA's results for equilibrium calculated for a gas mixture O/F = 2.85, cont.

Pressure (MPa, psi)	Entropy	Gibbs	Density	Cp
0.101 (14.7)	0.00%	0.14%	0.12%	0.37%
2.53 (367)	0.00%	0.15%	0.15%	0.41%
5.06 (735)	0.00%	0.15%	0.15%	0.41%
7.60 (1102)	0.00%	0.15%	0.15%	0.41%
10.13 (1470)	0.00%	0.15%	0.15%	0.41%

The two properties that exhibited large deviations between the results produced by Cantera and CEA were internal energy and specific heat (Cp). The maximum deviation observed being 0.919 percent less than CEA's result for the internal energy calculated by Cantera at 10.13 MPa (1470 psi) and a mixture stoichiometry of 5.7. For temperature, enthalpy, entropy, Gibbs function, and density calculations, the calculated values exhibited less than a 0.2 percent difference for all reaction simulations.

Table 2.4: Difference between Cantera's and CEA's results for equilibrium calculated for a gas mixture O/F = 5.7

Pressure (MPa, psi)	Temperature	Enthalpy	Internal Energy
0.101(14.7)	-0.11%	0.00%	-0.92%
2.53 (367)	-0.14%	0.00%	-0.80%
5.06 (735)	-0.15%	0.00%	-0.79%
7.60 (1102)	-0.16%	0.00%	-0.80%
10.13 (1470)	-0.16%	0.00%	-0.80%

Table 2.5: Difference between Cantera's and CEA's results for equilibrium calculated for a gas mixture O/F = 5.7, cont.

Pressure (MPa, psi)	Entropy	Gibbs	Density	Cp
0.101(14.7)	0.01%	-0.10%	0.07%	0.45%
2.53 (367)	0.01%	-0.14%	0.15%	0.56%
5.06 (735)	0.01%	-0.15%	0.00%	0.59%
7.60 (1102)	0.01%	-0.15%	0.17%	0.60%
10.13 (1470)	0.01%	-0.16%	0.17%	0.60%

Table 2.6: Difference between Cantera's and CEA's results for equilibrium calculated for a gas mixture O/F = 8.55

Pressure (MPa, psi)	Temperature	Enthalpy	Internal Energy
0.101 (14.7)	0.12%	0.00%	0.37%
2.53 (367)	0.15%	0.00%	0.62%
5.06 (735)	0.15%	0.00%	0.69%
7.60 (1102)	0.16%	0.00%	0.74%
10.13 (1470)	0.16%	0.00%	0.77%

Table 2.7: Difference between Cantera's and CEA's results for equilibrium calculated for a gas mixture O/F = 8.55, cont.

Pressure (MPa, psi)	Entropy	Gibbs	Density	Cp
0.101 (14.7)	0.00%	0.12%	0.08%	0.35%
2.53 (367)	0.01%	0.15%	0.14%	0.44%
5.06 (735)	0.01%	0.15%	0.14%	0.46%
7.60 (1102)	0.01%	0.16%	0.15%	0.47%
10.13 (1470)	0.01%	0.16%	0.15%	0.47%

The predicted mass fractions for the three stoichiometric cases at 0.101MPa (14.7psi) were compared in an effort to identify any trends or potential causes of the differences in property prediction between the two programs. Seven major species were chosen for comparison based on their making up at least 98% of the gas composition. It was found that the two codes' compared well for the predicted mass fractions of the gas mixture at an of O/F = 5.7. The largest difference observed for the O/F = 5.7 case was the OH mass fraction which was found to exhibit a 5.3% difference between Cantera and CEA's predictions. This data is presented in Table 2.8.

Table 2.8: Difference between Cantera and CEA equilibrium mass fraction predictions for a gas mixture O/F = 5.7

Species	CEA Mass Fractions	Cantera Mass Fractions	Difference
CO	0.094	0.094	-0.06%
CO2	0.137	0.137	0.02%
H2O	0.134	0.135	0.2%
NO	0.016	0.016	2.14%
N2	0.534	0.534	0.03%
OH	0.026	0.025	5.34%
O2	0.046	0.047	1.38%
Other	0.012	0.012	-

For the next two scenarios of an O/F = 8.55 and O/F = 2.85, presented in Tables 2.9 and 2.10 respectively, large differences were observed upwards of 50%. While this was initially concerning, it was found that CEA was consistent in predicting almost 98% of the gas mixture mass across the seven chosen species. While Cantera's predictions varied significantly, the seven chosen species for review also made up the majority of the mixtures mass.

Table 2.9: Difference between Cantera and CEA equilibrium mass fraction predictions for a gas mixture O/F = 8.55

Species	CEA Mass Fractions	Cantera Mass Fractions	Difference
CO	0.043	0.042	-2.3%
CO2	0.132	0.081	-38.6%
H2O	0.100	0.151	51%
NO	0.022	0.02	-9.0%
N2	0.559	0.540	-3.4%
OH	0.023	0.034	47.8%
O2	0.108	0.092%	14.8%
Other	0.014	0.04	-

Table 2.10: Difference between Cantera and CEA equilibrium mass fraction predictions for a gas mixture O/F = 2.85

Species	CEA Mass Fractions	Cantera Mass Fractions	Difference
CO	0.265	0.207	-21.8%
CO2	0.079	0.040	-49.3%
H2O	0.164	0.199	21.3%
NO	0.000	0.000	0%
N2	0.471	0.369	21.5%
OH	0.004	0.004	0%
O2	0.000	0.000	0%
Other	0.017	0.0161	-

While the differences in predicted equilibrium compositions for the fuel rich and oxidizer rich scenarios were concerning, the engine was to be designed to operate slightly fuel rich near an O/F = 5.7. Because Cantera predicted well for both equilibrium species composition and mixture properties near stoichiometric, it was concluded that modeling in the stoichiometric region would provide acceptable results.

The source of difference for the values calculated is believed to be a result of the differences in the thermodynamic and transport property data between the modified LLNL mechanism file used by Cantera and the NASA data file used by CEA. The modified LLNL file uses NASA thermodynamic and transport data for part of its chemical species data, however some of the chemical species included use data that is LLNL specific, such as the inclusion of species not found in the NASA data set[19]. This chemical species data is open source as is the overall LLNL mechanism file. These small differences in data and the inclusion of species in the LLNL mechanism file not present in the CEA data set not only resulted in differences in the calculations of the thermodynamic properties, but also in differences in the predicted equilibrium composition of the gas mixtures.

The results presented above demonstrate not only Cantera's ability to provide comparable and often near exact results as the results produced by CEA, but that the modified LLNL mechanism file provides adequate results. The data presented demonstrates the potential of Cantera as an alternative to CEA for making equilibrium calculations, and that Cantera is acceptable for use in the development of the MATLAB based rocket engine modeling code.

For simplicity in making calculations, 100% pure ethanol was assumed. Experimentally, 99.9% ethanol was used for testing due to manufacturing limitations, with the remaining 0.1% consisting of pure water and negligible contaminants [49]. This was confirmed by preliminary testing at EMRTC using a portable Raman spectrometer upon receipt of the ethanol fuel[50]. The difference between the ethanol concentration used computationally of 100% pure and the 99.9% ethanol used experimentally would alter the comparative results to

some degree. However, a difference of 0.1% was of such a small degree, that the effects on the gas mixture predictions would be negligible. A comparison was performed for an ethanol and nitrous oxide mixture with an O/F = 5.7 for 100% ethanol and 99.9% ethanol. The 5 major species present were compared, and the results tabulated in Table 2.11.

Table 2.11: Equilibrium species composition difference between Cantera predictions for 100% ethanol versus 99.9% ethanol. Calculations made for an O/F of 5.7 at 0.101MPa (14.7psi) and $298K(76.7° F)$.

Species	100% Pure Mass Frac.	99.9% Pure Mass Frac.	Difference
H2O	0.192	0.194	0.83%
N2	0.489	0.489	0.16%
CO2	0.079	0.080	0.2%
O2	0.037	0.037	0.00%
OH	0.037	0.037	0.00%

It can be seen that for 4 of the major species, the resultant difference was less than 0.2%, with the largest difference observed being 0.83% for the water (H2O) mass fraction predicted. This supports the theory that while a difference exists between using 100% instead 99.9% ethanol, the actual difference was of small enough size that it could be assumed to be negligible.

2.2 MATLAB/Cantera Rocket Engine Model

The developed MATLAB/Cantera rocket engine model code shares the same assumptions that govern CEA's rocket performance calculations:

- One-dimensional forms of the continuity, energy, and momentum equations.

- Steady-state operation.

- Homogeneous mixing.

- Adiabatic and complete combustion.

- Isentropic flow through the nozzle.

- Zero velocity at the combustion chamber inlet.

- Infinite area combustor.

- Ideal gas behavior

In addition the same governing equations for rocket performance apply to both codes, sourced from Mcbride and Gorden[6] and Huzel and Huang[47]. The performance parameters include characteristic exhaust velocity (C^*), thrust coefficient (C_F), area ratio of the nozzle (A_{exit}/A^*), exit velocity of the gas from the nozzle (V_{exit}), and specific impulse (I_{sp}):

$$C^* = \frac{\left(P_{inf} * A^* * g_c\right)}{\dot{m}} \tag{2.3}$$

$$C_F = \frac{V}{C^*} \tag{2.4}$$

$$\frac{A_{exit}}{A^*} = \frac{\rho^* * V^*}{\rho_{exit} * V_{exit}} \tag{2.5}$$

$$V_{exit} = \sqrt{2 * \left(h_\circ - h_{exit}\right)} \tag{2.6}$$

$$I_{sp} = \frac{V_{exit}}{g_c} \tag{2.7}$$

Initial inputs for both codes are pre-combustion propellant temperature, propellants, mixture ratio, chamber pressure, and the ambient pressure (or nozzle back pressure). In CEA, these values are inputted using the CEA user interface. For the MATLAB/Cantera model, the values are inputted in the main script function. CEA uses the standard NASA data file, and solves for flow properties in three steps, shown in Figure 2.1.
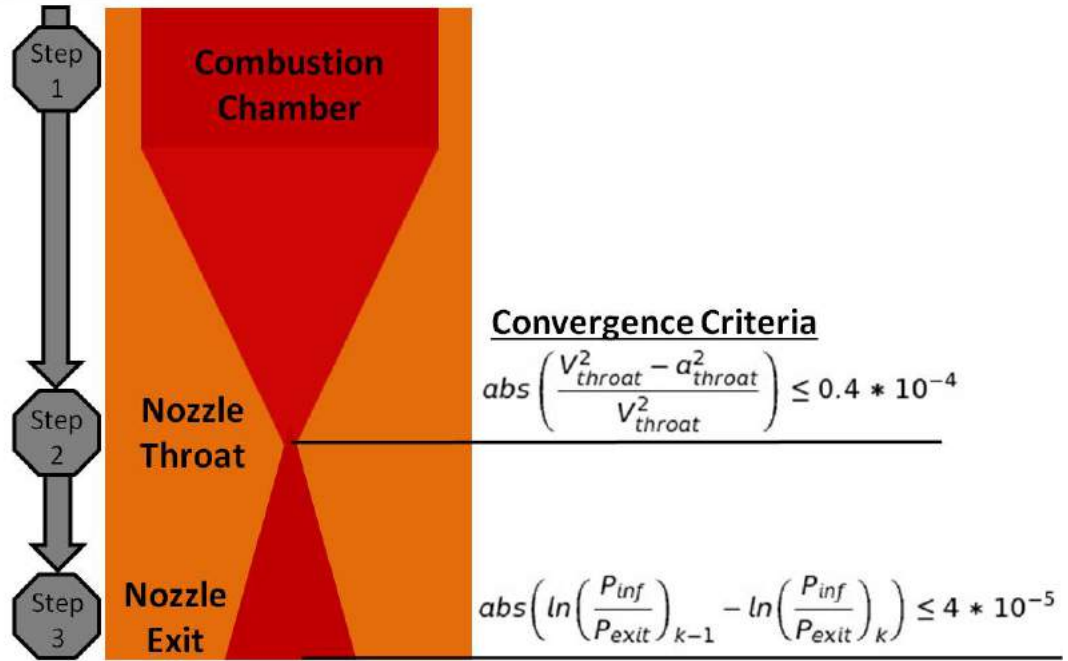
Figure 2.1: NASA CEA rocket engine solution method

With the governing assumptions and inputs for initial state, constant enthalpy and pressure equilibrium of the propellant gas mixture is calculated for the combustion chamber, completing step 1. The resultant calculated thermodynamic and transport properties are used in the following steps as the stagnation properties of the rocket for nozzle throat and exit calculations. Throat conditions are calculated by an iterative method to determine the pressure for which the area ratio is a minimum (or alternatively, the flow conditions for which the gas velocity is equal to the local speed of sound of the flow at the throat). Equilibrium is calculated for the gas flow through the nozzle during this iteration process. The initial guess for the gas state at the nozzle throat is made using the approximate formula shown as Equation 2.8:

$$\frac{P_o}{P_{throat}} = \left(\frac{\gamma + 1}{2}\right)^{\frac{\gamma}{(\gamma - 1)}} \tag{2.8}$$

Equation 2.8 is an estimate found in many references, including Sutton's book[2][6], and is derived for a Mach Number of 1 (choked flow condition) from the isentropic flow equation for pressure:

$$\frac{P_o}{P_{throat}} = \left(1 + \frac{\gamma - 1}{2}M^2\right)^{\frac{\gamma}{(\gamma - 1)}} \tag{2.9}$$

Equation 2.8 is exact only when γ is constant from the combustion chamber exit to the nozzle throat. An initial guess of the throat state is made using γ as solved for at the end of the combustion chamber in Step 1. After the initial guess is made, CEA continues to iterate the pressure at the throat, P_{throat}, and solve for equilibrium while holding the entropy at the throat constant, or equal to the stagnation entropy solved for at the point of combustion. The test for convergence is:

$$abs\left(\frac{V_{throat}^2 - a_{throat}^2}{V_{throat}^2}\right) \leq 0.4 * 10^{-4} \tag{2.10}$$

Here the gas velocity of the throat, or gas exiting the converging section of the nozzle, is compared against the local speed of sound calculated for the iterated gas state. This is equivalent to ensuring that the Mach number at the throat is within $1 \pm 0.2 * 10^{-4}$

The exit condition at the nozzle is determined using two separate methods depending on whether an area ratio or pressure ratio were assigned. If an area ratio is assigned, the pressure ratio between nozzle exit and throat is iterated in accordance to the assigned area ratio, with convergence determined when:

$$abs\left(ln\left(\frac{P_{inf}}{P_{exit}}\right)_{k-1} - ln\left(\frac{P_{inf}}{P_{exit}}\right)_{k}\right) \leq 4 * 10^{-5} \tag{2.11}$$

where the updated pressure ratio guess is compared to the previous guess, with convergence when the difference is less than $4 * 10^{-5}$. For the scenarios analyzed in this research, the pressure ratio is assigned (perfectly expanded for the test cases). CEA solves for the exit gas conditions by solving for equilibrium of the gas flow at the pressure that corresponds to the assigned pressure ratio and the stagnation entropy determined at the combustion point previously in step 1.

The MATLAB/Cantera rocket engine model follows a similar iteration method, with a solution being found at the same points as CEA. The iteration method differs, however, in regards to what is used for determining convergence. Figure 2.2 depicts the computational methodology and corresponding convergence criteria used by the MATLAB/Cantera model. The first step taken by the model is to find the combustion chamber properties. Through MATLAB, Cantera is instructed to solve for equilibrium at constant enthalpy and pressure. of the propellant gas mixture, and the resultant properties are used as the stagnation properties for later calculations. The second step is to calculate the throats properties. The MATLAB/Cantera initialization and data processing script can be found in Appendix D.2.1.

The throat properties are solved for using a "guess and check" iterative method. A gas flow temperature is guessed, and the pressure iterated, using a bisection iterative method, until the entropy at the throat is within a predefined tolerance of the stagnation entropy. Equilibrium is calculated for each iteration and the mass specific enthalpy and the local speed of sound at the throat are compared against the mass specific stagnation enthalpy. Convergence at the throat is
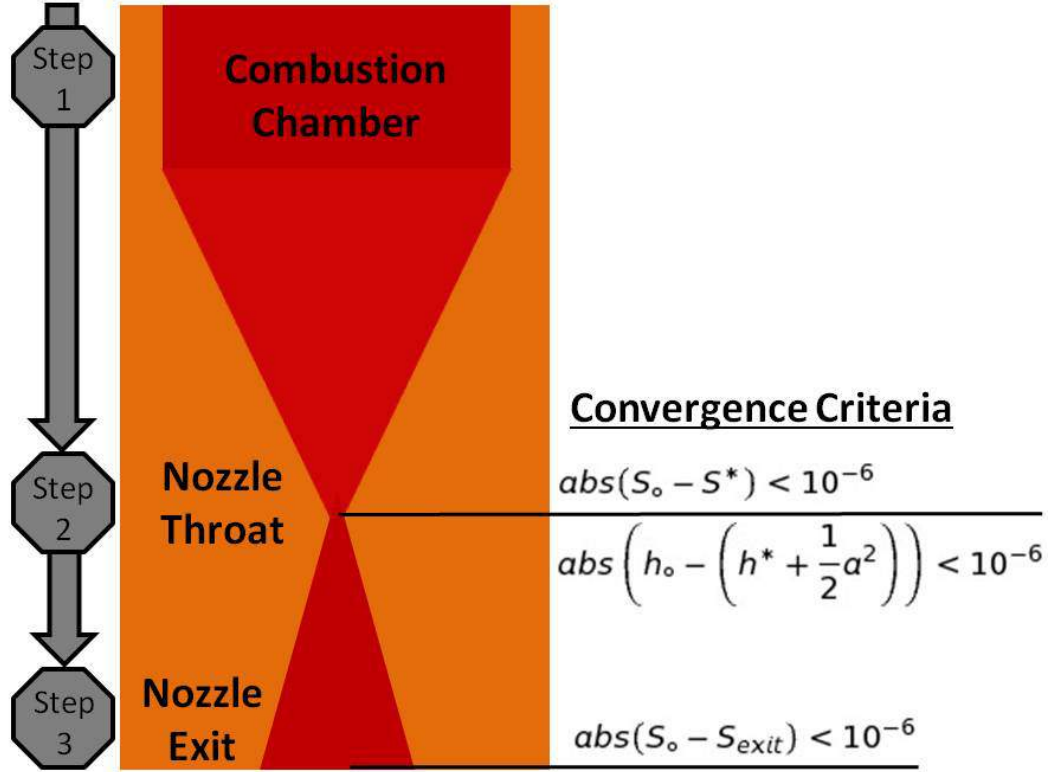
Figure 2.2: MATLAB/Cantera Computational rocket engine solution method

determined once two conditions are met:

$$abs\left(S_\circ - S^*\right) < 10^{-6} \tag{2.12}$$

$$abs\left(h_\circ - \left(h^* + \frac{1}{2}a^2\right)\right) < 10^{-6} \tag{2.13}$$

The third and final step is solving for the flow properties at the nozzle exit. The exit properties are calculated by assuming the gas flow exiting the nozzle is perfectly expanded, such that the pressure of the gas flow is equal to the ambient pressure (back pressure). A bisection method iterates the gas temperature from the nozzle throat to the nozzle exit. Equilibrium of the gas flow is calculated for that temperature and the exit pressure. The entropy of the exiting gas is then compared against the stagnation entropy of the flow. Convergence at the nozzle exit is determined when:

$$abs\left(S_\circ - S_{exit}\right) < 10^{-6} \tag{2.14}$$

The MATLAB/Cantera rocket engine model script can be found in Appendix D.2.2. The throat property and exit property scripts can be found in Appendix D.4.1 and D.4.2, respectively.

Test scenarios were chosen for the rocket performance calculations that would be solved by both CEA and Cantera. These scenarios were chosen to check the applicability of the MATLAB/Cantera code across a range of rocket operating conditions. The conditions for each simulation can be found in table 2.12 . The performance properties chosen for comparison were chamber temperature, throat temperature, exit temperature, exit Mach number, area ratio, characteristic exhaust velocity, coefficient of thrust, and specific impulse. Each mixture ratio is simulated at each of the four chamber pressures.

Table 2.12: Rocket simulations. 12 total simulations performed

Initial Propellant Temperature	Mixture Ratio (O/F)	Chamber Pressure
$298K(76.7°F)$	2.85	1.72MPa (250psi) 3.45MPa (500psi) 5.17MPa (750psi) 6.89MPa (1000psi)
$298K(76.7°F)$	5.7	1.72MPa (250psi) 3.45MPa (500psi) 5.17MPa (750psi) 6.89MPa (1000psi)
$298K(76.7°F)$	8.55	1.72MPa (250psi) 3.45MPa (500psi) 5.17MPa (750psi) 6.89MPa (1000psi)

2.2.1 MATLAB/Cantera Model and CEA Comparison Results

Tables 2.13, 2.14, and 2.15 present the difference between the rocket performance results produced by the MATLAB/Cantera rocket engine model compared to the results from CEA. For all three mixture stoichiometries, the temperature calculations were a main source of difference and these differences carried through to later calculations. It is believed that the methods of integration used

Table 2.13: Difference between Cantera's and CEA's results for rocket performance calculated for a gas mixture stoichiometry of 2.85.

Chamber						
Pressure	Temperature			Area				
(Mpa, psi)	Chamber	Throat	Exit	Ratio	C*	CF	Isp
6.89 (1000)	-2.84%	-3.65%	-3.98%	-0.67%	-0.74%	-0.17%	-0.97%
5.17 (750)	-2.81%	-3.27%	-3.98%	-0.82%	-0.63%	-0.26%	-0.96%
3.45 (500)	-2.76%	-3.25%	-3.96%	-0.75%	-0.70%	-0.17%	-0.93%
1.72 (250)	-2.67%	-3.21%	-3.87%	-0.61%	-0.78%	-0.01%	-0.88%

Table 2.14: Difference between Cantera's and CEA's results for rocket performance calculated for a gas mixture stoichiometry of 5.7

Chamber						
Pressure	Temperature			Area				
(Mpa, psi)	Chamber	Throat	Exit	Ratio	C*	CF	Isp
6.89 (1000)	0.29%	-0.17%	-3.10%	-2.74%	0.60%	-0.29%	0.23%
5.17 (750)	0.29%	-0.16%	-2.24%	-1.99%	0.49%	-0.11%	0.32%
3.45 (500)	0.28%	-0.19%	-1.04%	-1.17%	0.60%	-0.15%	0.39%
1.72 (250)	0.26%	-0.20%	-0.09%	-0.38%	0.54%	0.00%	0.46%

are different enough from the methods used by CEA to produce noticeable difference in calculated temperatures. Specifically, the convergence criteria for the calculating the nozzle throat and exit flow states. However, at a stoichiometric mixture of 5.7, the results from the MATLAB/Cantera model compared well to CEA. Despite a near four percent difference in the calculated exit temperature, the characteristic exhaust velocity, thrust coefficient, and specific impulse all compare within 1% to the values produced by CEA. These results demonstrated that the methods used by the MATLAB/Cantera model for modeling rocket performance are acceptable and provide comparable results to CEA.

Table 2.15: Difference between Cantera's and CEA's results for rocket performance calculated for a gas mixture stoichiometry of 8.55

Chamber							
Pressure		Temperature		Area			
(Mpa, psi)	Chamber	Throat	Exit	Ratio	C*	CF	Isp
6.89 (1000)	0.91%	0.63%	2.19%	0.62%	1.45%	0.14%	0.86%
5.17 (750)	0.88%	0.57%	2.15%	0.55%	0.83%	0.08%	0.84%
3.45 (500)	0.83%	0.50%	2.07%	0.48%	0.86%	0.02%	0.81%
1.72 (250)	0.76%	0.40%	1.83%	0.34%	0.87%	-0.04%	0.76%

2.3 MATLAB/Cantera Rocket Engine Model, Advanced

A new MATLAB/Cantera rocket engine model was developed with a similar solution methodology to the model discussed in the previous section. However, the new model is capable of calculating chamber pressure as a function of propellant flow rate and nozzle dimensions, specifically throat diameter. This allows the effects of varying chamber flow rate to be observed and aid in the selection of operational flow rates for the experimental rocket engine. Inputs for initial conditions are: total propellant mass flow rate, initial propellant temperature, nozzle throat diameter, and mixture ratio. To solve for chamber pressure, the equation for isentropic choked flow was employed:

$$\dot{m}^* = \frac{A^* * P_O}{\sqrt{T_O}} * \sqrt{\frac{\gamma}{R}} * \left(1 + \frac{\gamma - 1}{2}\right)^{-\frac{\gamma+1}{2(\gamma-1)}} \tag{2.15}$$

Combined with the continuity equation, chamber pressure is iterated using a bisection method. After combustion of the propellants, the flow properties found are used in determining the specific heat ratio at the throat, and the mass flow rate at the throat is calculated. Convergence is determined to be the point that the difference between the propellant mass flow and the predicted mass flow at the throat are less than a predefined tolerance:

$$abs\left(\dot{m}_{propellant} - \dot{m}^*\right) < 10^{-6} \tag{2.16}$$

The calculated chamber pressure for the inputted flow rate and initial conditions were then simulated using CEA to provide rocket performance values to compare with the results from the modified MATLAB/Cantera rocket engine model. For simulated operation of the rocket engine at sea level, five propellant flow rates were chosen to be tested, from 0.181 kg/s (0.4 lbm/s) to 0.272 kg/s (0.6 lbm/s) in 0.022 kg/s (0.05 lbm/s) increments. These were calculated for a mixture ratio of O/F=4.5 as this is the design condition for the experimental rocket.

This mixture ratio was chosen for fuel-film cooling and peak temperature concerns following previous work by Tokudome et al[33]. These run scenarios were performed to verify this method of calculating chamber pressure provided comparable results to CEA's predictions.

The advanced MATLAB/Cantera Rocket Engine Model initialization and data processing script and rocket performance calculator script can be found in Appendix D.3.1, and D.3.2 respectively. Combustion chamber pressure calculator script can be found in Appendix D.3.3.

2.3.1 Advanced MATLAB/Cantera Model Calculations

The results from the modified MATLAB/Cantera model calculating rocket performance as a function of total propellant flow rate are compared to CEA's results and tabulated in Table 2.16 and 2.17. These results are for simulated run conditions at sea level. The calculated pressure from the MATLAB/Cantera model was used to make the CEA calculations for comparison.

Table 2.16: Difference between Cantera's and CEA's temperature results for varied propellant flow rate. Calculated chamber pressure by MATLAB/Cantera model inputted into CEA as method of comparison

Propellant	Chamber			
Flow	Pressure	Temperature		
(kg/s, lbm/s)	(MPa, psi)	Chamber	Throat	Exit
0.272(0.6)	6.93(1005)	-0.64%	-1.52%	-4.20%
0.249(0.55)	6.35(921)	-0.62%	-1.51%	-4.17%
0.227(0.5)	5.76(836)	-0.60%	-1.50%	-4.15%
0.204(0.45)	5.18(752)	-0.59%	-1.26%	-4.11%
0.181(0.4)	4.60(667)	-0.39%	-1.42%	-4.09%

As with the previous version of the MATLAB/Cantera rocket engine model, the largest difference is seen with the calculated temperatures, notably the exit temperatures. The largest difference seen is a calculated exit temperature by the MATLAB/Cantera model as 4.20% less than CEA's predictions

The characteristic exhaust velocity, coefficient of thrust, and specific impulse all compare well with CEA's predictions for performance at the corresponding chamber pressure, with the maximum difference observed being the coefficient of thrust as 0.54% less than CEA's predictions. Despite the area ratio exhibiting nearly a two percent difference compared to CEA, solving for the exit ratio diameter yields a difference of less than one percent. For this reason this version of the code was used for designing the rocket engine nozzle discussed subsequently in Chapter 3.

Table 2.17: Difference between Cantera's and CEA's rocket performance results for varied propellant flow rate. Calculated chamber pressure by MATLAB/Cantera model inputted into CEA as method of comparison

Propellant	Chamber				
Flow (kg/s, lbm/s)	Pressure (MPa, psi)	Area Ratio	C*	CF	Isp
0.272(0.6)	6.93(1005)	-1.76%	0.07%	-0.45%	-0.44%
0.249(0.55)	6.35(921)	-1.84%	0.11%	-0.47%	-0.44%
0.227(0.5)	5.76(836)	-1.88%	0.19%	-0.54%	-0.42%
0.204(0.45)	5.18(752)	-1.82%	0.09%	-0.43%	-0.40%
0.181(0.4)	4.60(667)	-1.72%	0.06%	-0.36%	-0.37%

Performance calculations were made across a range of mixture ratios to develop a sense of varied rocket performance to be used in engine design. The performance calculations were made assuming perfectly expanded nozzle flow at an altitude of 1372 meters (4500ft), which is approximately the altitude of the rocket test facility. For the performance calculations, only total mass flow rate supplied to the engine and mixture ratio were varied. The developed code predicted the engine chamber pressure, ISP, and thrust output.

Various throat diameters were tried and the chamber pressure calculation checked for determining the required throat diameter that would provide the desired chamber pressure at the design condition. This design condition was 6.89MPa (1000psi) chamber pressure at a mixture ratio of approximately 4.5 that could be supplied by the constructed fuel system. A throat diameter of 8.89mm (0.35") was found to meet the design condition, and was used for all performance calculations for the plots presented. Figure 2.3 is the resultant chamber pressure plot for varied propellant flow rate.

Plots of thrust output, Figure 2.4, and specific impulse, Figure 2.5, were also produced. In addition to being used for engine design, the thrust and specific impulse plots served as checks that the MATLAB/Cantera rocket engine model provided proper performance trends.

Figures 2.3, and 2.5 showed that the thrust and specific impulse both peaked at a mixture ratio of approximately 5.2. This corresponds to a oxidizer-fuel equivalency of approximately 0.9, or slightly fuel rich. It is here that the combination of temperature and average molecular weight of the product species reaching a maximum, resulting in the peaks in the thrust and specific impulse. This trend was expected, and helped further verify that the MATLAB/Cantera model was properly predicting combustion trends.
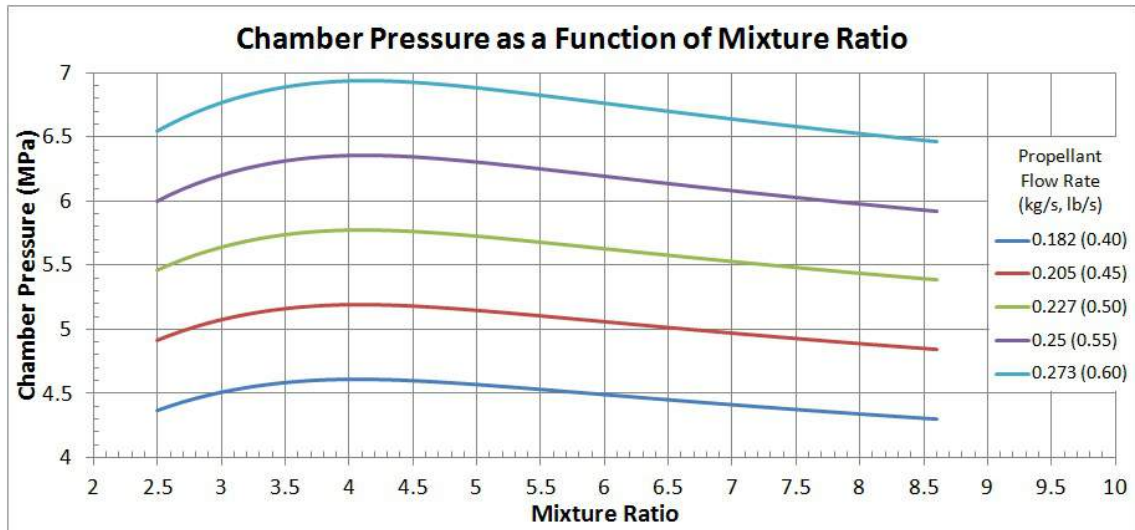
Figure 2.3: Predicted chamber pressure as a function of mixture ratio for a throat diameter of 8.89mm (0.35″) at an altitude of 1371.6 meters (4500ft).
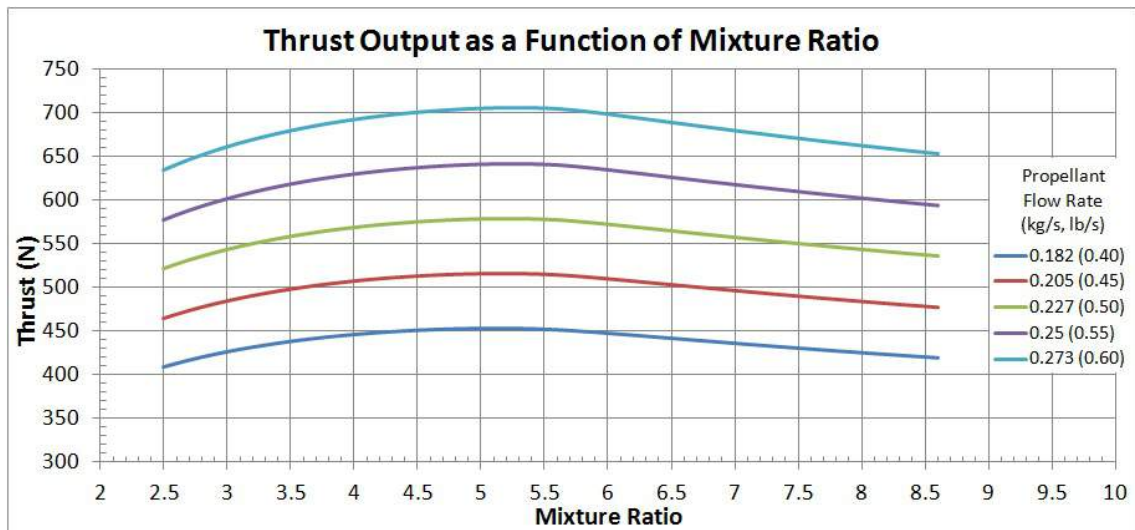
Figure 2.4: Predicted thrust output as a function of mixture ratio for a nozzle throat diameter of 8.89mm (0.35″) at an altitude of 1371.6 meters (4500ft).
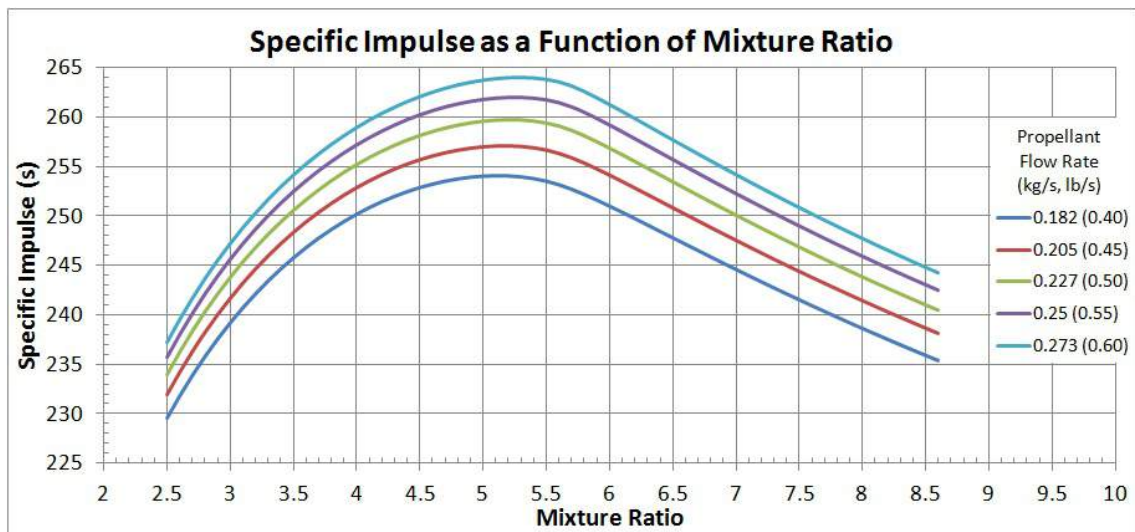
Figure 2.5: Predicted specific impulse as a function of mixture ratio for a nozzle throat diameter of 8.89mm (0.35″) at an altitude of 1371.6 meters (4500ft).

CHAPTER 3

ROCKET ENGINE DESIGN

3.1 Engine Design

While computational work is important in initial rocket engine design consideration, the majority of engine designs are based on past experimental work that had been shown to be successful [2][24][47]. The design process can vary, making some design decisions a "best guess" scenario using engineering intuition and past successful designs.

Three design principles were adhered to during the designing of the rocket engine:

1. *Modular* design to provide increased versatility and ease for future modifications and repairs.

2. *Robust* for increased safety and survivability of the engine.

3. *Simple* to decrease operational down time by using off the shelf, easily replaceable parts where possible and simple machining design for custom manufactured parts.

As a result, the designed engine and support systems were not only versatile and durable, but were capable of being easily modified for uses beyond their original design intention.

The intended use of the engine was to experimentally evaluate the performance of liquid propellant combinations. The initial propellant combination of interests was nitrous oxide and ethanol, for which the engine was designed to operate with at an approximate thrust of 667N (150lbf). Nitrous oxide and ethanol were known to be incompatible with certain materials, making material selection important.

Nitrous oxide material compatibility was important because nitrous oxide can not only degrade an incompatible material, but also combust with the material or cause an explosion. For nitrous oxide compatible material selection, the European Industrial Gas Association's (EIGA) *Code of Practice Nitrous Oxide, 2007*[39], and the Asia Industrial Gas Association's (AIGA) *Safe Practices for Handling and Storing of Nitrous Oxide, 2013*[51] were employed. These manuals provided metal and non-metal compatibilities specific for nitrous oxide. The gas

compatibility chart produced by Specialty Gas Equipment was then employed to further refining gasket selection for use with nitrous oxide[40]. Ethanol's main incompatibility was with some gasket polymers, degrading and causing them to fail. To avoid this problem, gaskets were chosen for ethanol exposure that were specifically labeled for ethanol contact.

In considering material compatibility, it was also important to ensure all machined components were properly cleaned. Oxygen cleaning was recommended by the EIGA and AIGA for all components in contact with nitrous oxide. While oxygen cleaning for components in contact with ethanol was not necessary, for simplicity and to prevent contamination, all machined components were oxygen cleaned using the procedure discussed in Chapter 4.

For cooling, the engine was designed to be passively cooled. To accomplish this, the engine body was designed with a large thermal mass to act as a heat sink for the interior walls of the engine exposed to hot combustion gases. This slowed the interior wall temperature rise, preventing burnout of the walls and allow for run-times long enough to reach steady-state operation. The large thermal mass was accomplished with the use of oxygen-free, high conductivity (OFHC) copper.

To maintain modularity of the engine, the nozzle, combustion chamber, and injector manifold were designed with flanged bolt connections. This simplified assembly and machining operations. This method of mating of components also allowed thermal expansion of the engine, minimizing the development of compressive stress in the chamber walls. The flanged connections were bolted together using 3/8″-24 grade 8 bolts and nuts. To prevent the nuts from loosening, as well as simplify assembly and dissasembly, wedge lock washers manufactured by NORD-LOCK were used. These washers utilize two halves with interlocking teeth and exterior serrations to grip against the fixture and nut, preventing loosening by vibration and impact. In addition, they are designed to be reusable. When assembled, with the force transducer mount attached, the engine is slightly over 495mm (19.5″) in length and no greater then 152mm (6″) in diameter. A rendering of the final engine design can be seen in Figure 3.1.

For sealing, non-metallic o-ring seals were used. These seals, as were all seals present on the engine, designed using the the *Parking O-ring Handbook*[52]. All o-rings used were sourced from Mcmaster-Carr. Dual o-rings were used for the flange interfaces and injector plate sealing. The dual o-rings helped promote positive sealing and also provided a back up seal in case of failure of the internal o-ring.

Propellant flow rates to the engine were controlled using cavitating venturis. For igniting the propellants injected into the combustion chamber, a small, gaseous hydrogen/oxygen torch was utilized. Figure 3.2 is a cross-sectional view of the assembled engine, and allows the dual o-rings at the flange interface, the injector plate in the injector assembly, and the igniter-engine interface and force transducer mounting assembly to be visualized.

The subsequent sections detail the design, development, and construction
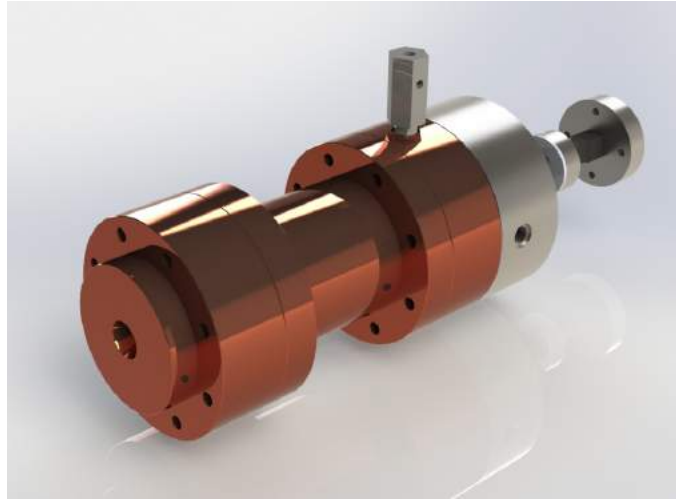
Figure 3.1: CAD render of the final rocket engine design and assembly
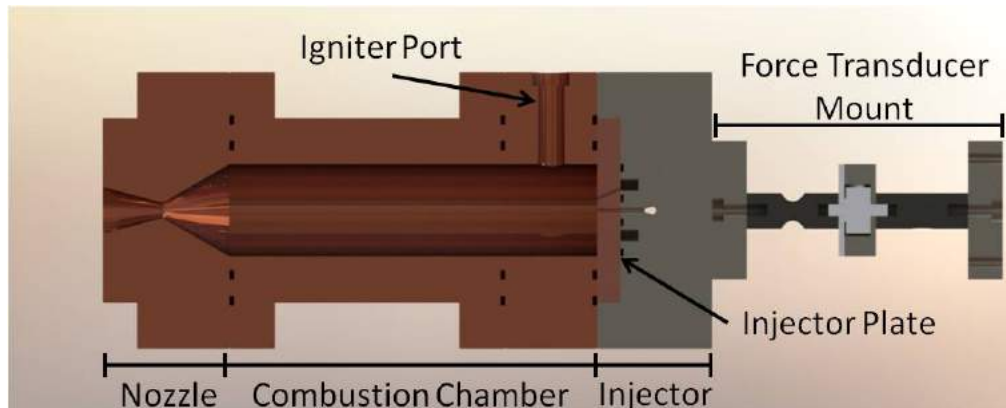
Figure 3.2: CAD render of cutaway of assembled rocket engine. Main components are labeled

of the major components of the rocket engine, to include: Propellant injector, combustion chamber, nozzle, and igniter. Machining drawings for the engine components and supporting hardware can be found in Appendix A.

3.1.1 Propellant Injector

The injector assembly for the rocket engine consisted of an injection manifold and an injector plate. The injection manifold was responsible for channeling the liquid fuel and liquid oxidizer separately to their respective ports on the injector plate. In addition, the injection manifold provided the interface with the

force transducer mount. The injector plate was responsible for directing the fuel and oxidizer propellants into the combustion chamber.

The injector plate was machined out of OFHC copper to 101.6mm (4") diameter disc with a thickness of 12.7mm (0.5"). The injector plate was an impinging jet design, with three fuel ports surrounding a single oxidizer port. The design was based on impinging jet designs described by Sutton[2] and previous engine design work [31][47]. The center port injects the nitrous oxide, and the surrounding ports inject ethanol into the nitrous oxide stream per suggestion from Mark Grubelich [31]. The propellant flow rates were governed upstream by cavitating venturis, and it was therefore important that the injection ports not further limit the flow rates. Port diameter was therefor chosen to be the smallest drill size possible that would permit the maximum flow rate of fuel and oxidizer.
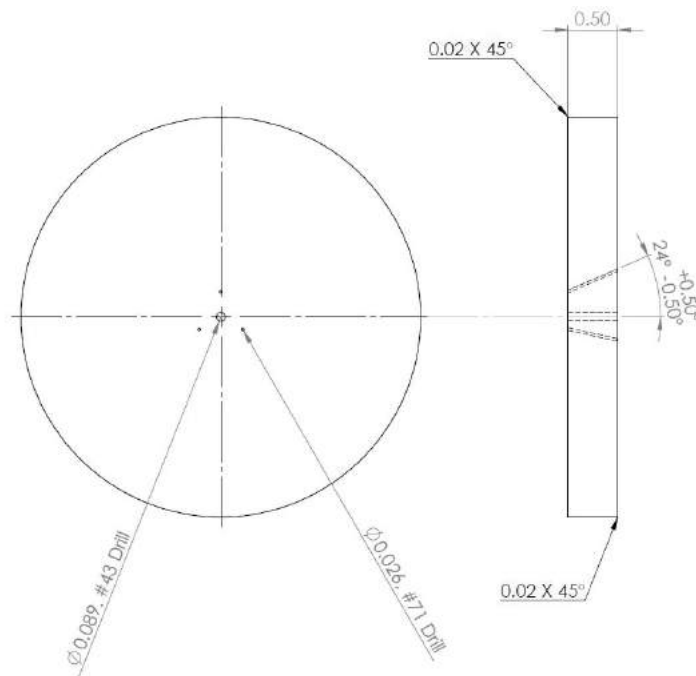
Figure 3.3: Injector plate detailing, (Note: Will add clearer image)

Figure 3.3 shows the finalized injector plate detailing for machining. A #43 drill bit, with a diameter of 2.26mm (0.089"), was selected for the single nitrous oxide port. The nitrous oxide port is drilled in line with the disc axis. A #71 drill bit, with a diameter of 0.66mm (0.026"), was selected for the three ethanol ports. The ethanol ports were drilled at $24°$ to the axis, allowing the ethanol stream to impinge into the nitrous oxide stream. This angle was chosen to create an approximately axial resultant momentum in the impingement stream, which Sutton reported often results in good performance [2]. Machining drawings for the injector plate can be found in Appendix A.1.2.

The injection manifold was machined from 6" round, 303 stainless steel, bar stock, 3" in length. 303 stainless steel alloy was chosen because it exhibited

better machinability then 304 or 316 stainless while maintaining the durability and propellant compatibility associated with stainless steel. For connection to the combustion chamber, eight 9.80mm (0.386") holes were drilled along the circumference to allow 3/8" Grade 8 steel bolts to pass through. The bolts were used for connecting the combustion chamber to the injector and were 165.1mm (6.5") long. These bolts fixtured both the portion of the combustion chamber that contained the port for the igniter, as well as the main combustion chamber section, to the injector assembly. The completed injection manifold is shown in Figure 3.4. Visible are the installed o-rings, injector plate pocket, ethanol fuel channel, nitrous oxide port, and the ethanol supply inlet port on the side of the manifold, which are discussed below. Machining drawings for the injector manifold can be found in Appendix A.1.1.
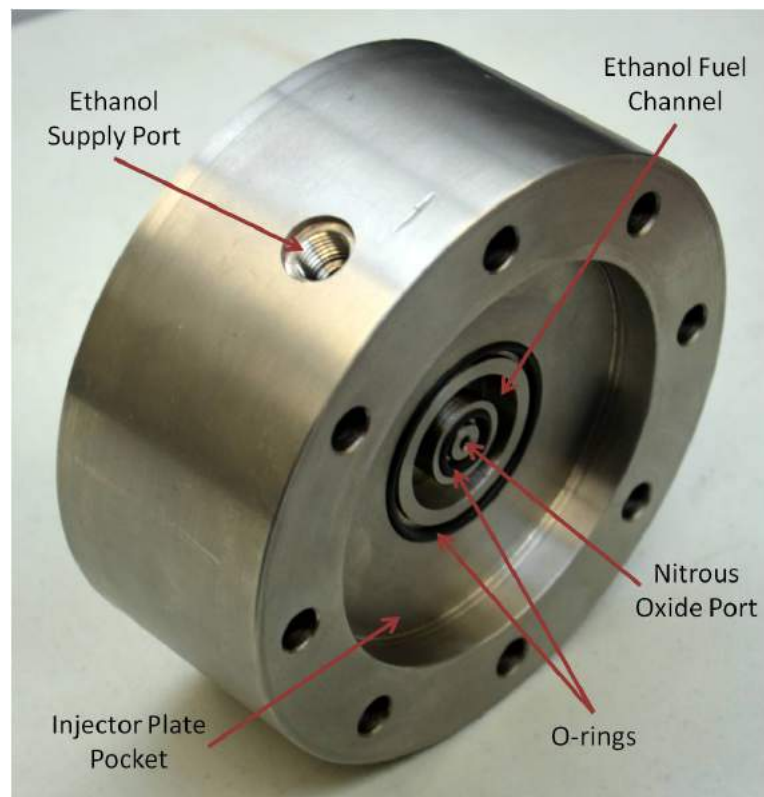
Figure 3.4: Completed injection manifold, with o-rings installed

The nitrous oxide port and ethanol fuel channel were supplied by ports perpendicular to the injection manifold face. These ports exit opposite one another on the circumference of the manifold, and terminate with 1/4" NPT threads. While these threads were effective at providing positive sealing, application of compatible thread compounds were required to seal properly and prevent galling (allowing possible future disassembly). Future designs would be better to employ straight threads for attachment of propellant supply lines and utilize o-rings for sealing.

Sealing between the injector plate and injection manifold was accomplished using Viton ETP Fluoroelastomer o-rings, which were designed for compatibility with ethanol and nitrous oxide. This was necessary due to the scale of the injector design preventing a secondary o-ring from being employed between the center nitrous oxide port and ethanol fuel channel. The o-ring therefore had to be compatible for exposure to both propellants. The inner o-ring is a #112 sized o-ring, and the outer o-ring is a #133 sized o-ring.

3.1.2 Combustion Chamber

The rocket engine combustion chamber consisted of an igniter flange and a combustion chamber main section. Both the components were machined out of a piece of 152.4mm (6") diameter OFHC copper stock. The igniter flange was 50.8mm (2") thick and was ported for attaching the igniter to the engine. The combustion chamber main section was 152.4mm (6") long with 25.4mm (1") thick flange sections on either end. The overall length of the two combustion chamber sections was 203.2mm (8"). As with the injection manifold, the igniter flange and main combustion chamber had a pattern of eight 9.80mm (0.386") holes drilled along the circumference to allow 3/8" Grade 8 steel bolts to pass through. This style of mating of the engine components and the seal design discussed subsequently in this section were inspired by communications with Mark Grubelich with regards to a similar, passively cooled rocket engine[31]. Figure 3.5 shows the completed combustion chamber main section.

Figure 3.5: Completed combustion chamber with o-rings installed

For selecting combustion chamber diameter, Sutton recommended that to avoid pressure losses, the combustion chamber diameter should be approxi-

mately twice the nozzle throat diameter[2]. While the computational work discussed in Chapter 2 supported the use of a throat diameter of 8.89mm (0.35"), the possibility existed that future nozzle designs could have a larger throat to achieve lower exit Mach numbers. Table 3.1 contains computational model predictions of exit exhaust Mach for different throat diameters. Calculations were made for the maximum designed flow rate of the system of 0.27kg/s (0.6lbm/s) at a mixture ratio of 4.5. The nozzle was assumed to have a fixed nozzle exit diameter of 25.9mm (1.02").

Table 3.1: Predicted exit Mach number for varied nozzle throat area. Predictions made for a total propellant mass flow rate of 0.27kg/s (0.6lbm/s) at a mixture ratio of 4.5. Nozzle exit diameter was fixed at 25.9mm (1.02")

Throat Diameter	Chamber Pressure	Area Ratio	Mach Number
mm (in)	MPa (psi)	-	-
8.89 (0.35)	6.93 (1005)	8.49	3.17
11.4 (0.45)	4.17 (605)	5.13	2.78
13.9 (0.55)	2.78 (403)	3.44	2.45
16.5 (0.65)	1.98 (288)	2.46	2.16
19.0 (0.75)	1.48 (215)	1.85	1.90
21.6 (0.85)	1.15 (167)	1.44	1.6544
24.1 (0.95)	0.92 (133)	1.1528	1.3761
25.4 (1)	0.83 (120)	1.0404	1.1782

Concern existed regarding the size of the spray pattern from the impinging jets. Too small of a chamber diameter could interfere with the spray pattern, resulting in unnecessary propellant being sprayed directly on to the chamber walls. Based on the predictions shown in Table 3.1, an inner diameter of 50.8mm (2") was chosen to both minimize pressure losses for nozzle throat diameters up to 25.4mm (1"), and mitigate unnecessary propellant contact with the combustion chamber walls.

Few published examples of past designs using nitrous oxide and ethanol exist. The characteristic length of a rocket engine combustion chamber, L^*, can be used to relate the volume of the combustion chamber to the area of the nozzle throat, as shown in Equation 3.1[2].

$$L^* = \frac{V_c}{A_t} \tag{3.1}$$

Here the volume of the combustion chamber V_c, can be expressed as a function of propellant mass flow rate, average specific volume of the combustion gases, and propellant stay time, which is the time the propellant gases spend in the combustion chamber. This can be seen in Equation 3.2[2].

$$V_c = \dot{m} v_{ave,gas} t_{stay} \tag{3.2}$$

For best performance, a minimum propellant stay time defines the combustion chamber volume which yields complete combustion[2]. The stay time accounts for the time necessary for vaporization, activation, and complete burning of the propellants, and is therefore usually experimentally determined[2]. As such, the characteristic length is dependent on the propellants used, the mixture ratio, and engine chamber pressure. This limits the usefulness of L^* to a particular propellant combination and a narrow range of mixture ratios and chamber pressures[2].

Tokudome et al. reported successful tests of a nitrous oxide-ethanol engine with an L^* value of approximately one meter. This value was determined for engine operation at a mixture ratio of 4.5 and 2MPa (290psi) chamber pressure [33]. The engine designed here was intended for high pressure operation of between 4.5MPa (652psi) to 7MPa (1015psi), decreasing the minimum propellant stay time t_{stay}. Therefore the required L^* would be less then what was used with Tokudome's lower pressure engine.

Too short of a combustion chamber would prevent full combustion of the propellants, and allow unburned propellant to be pushed through the nozzle. This problem was compounded by the fact that the engine was designed to run at several different flow rates as well as chamber pressures, directly effecting the rate at which the propellants would evaporate and burn. The potential also existed for different nozzles to be used that had larger throat diameters. Therefore, a total combustion chamber length of 203.2mm (8″) was chosen. Using Equation 3.1, the L^* for the engine designed here is found to be 6.6m (261″). While this value is significantly larger than Tokudome's L^* value, it was decided that it was best to ensure complete combustion of the propellants and loose some energy to heat loss due to the extra chamber length than not reach complete combustion for all test scenarios.

A dual o-ring design was used for sealing between the two sections, as shown in Figure 3.5. Specialty o-rings were required to handle the high temperatures at the chamber walls and not degrade. Metal seals would have been optimal, however the softness of the copper and the desire for multiple assemblies and disassemblies of the engine components increased the likelihood of damage to the copper sealing surface over time. As a result, PTFE based o-rings were chosen. The PTFE o-rings were designed for continual operation at temperatures of up to $260°C$ ($500°F$). While the possibility of exceeding these temperatures during operation exists, it was expected that the short duration of temperature exposures above the rated temperature would not adversely affect the o-ring or its sealing ability. After several firings of the completed engine, it was found that the o-rings did not deteriorate and maintained sealing capable for multiple firings. The inner o-ring is a #232 sized o-ring and the outer o-ring is a #241 sized o-ring.

Detailed machining drawings for the combustion chamber main section and igniter flange can be found in Appendix A.1.3 and A.1.4, respectively.

3.1.3 Nozzle

A conical nozzle was chosen for use with the developed rocket engine, and was selected for simplicity in fabrication and in performing computational modeling of the nozzle. The designed conical nozzle was based on nozzle design criteria discussed by Sutton[2]. Following Sutton's suggestions, the converging section of the nozzle was was angled 30° to the center line, and the diverging section was angled 15° to the center line.

The conical nozzle does not produce perfectly uniform, axial gas-flow [53]. The use of a conical nozzle does result in some performance loss as a result of the non-axial component of the exhaust gas velocity at the nozzle exit. This loss can be quantified with a correction factor, presented by Equation 3.3, which represents the ratio between the exit gas momentum of the conical nozzle to that of a nozzle with uniform axial gas flow.

$$\lambda = \frac{1 + \cos\alpha}{2} \qquad (3.3)$$

Here, α is the half-angle of the divergent section of the conical nozzle. For the designed nozzle with a 15° for the diverging section, the value of λ is found to be 0.982, implying a performance loss of approximately 1.7 percent using the conical nozzle. While a properly designed bell nozzle can produce near uniform, axial flow at the nozzle exit reducing losses[53], this nozzle design was not chosen. This decision was based on the fact that the small performance gains achieved using a bell nozzle did not offset the increased difficulty in machining.

Using the design criteria developed during the computational work discussed in Chapter 2, a throat diameter of 8.89mm (0.35") was selected. The computational work was also used in determining the final exit area ratio of approximately 8.5. This area ratio was selected for perfect expansion of the flow for engine operation at a mixture ratio of 4.5 at a chamber pressure of 6.89MPa (1000psi). The chosen area ratio yielded a nozzle exit diameter of 25.9mm (1.02"). Table 3.2 shows the predicted performance of the designed nozzle.

Table 3.2: Predicted nozzle performance for a chamber pressure of 6.89MPa (1000psi), mixture ratio of 4.5, throat diameter of 8.89mm (0.35"), and exit area ratio of 8.5

Mach Number	Thrust	ISP	C*
-	N (lbf)	s	m/s (ft/s)
3.1724	700 (157)	262	1614 (5295)

For designing the nozzle throat contour, Sutton suggested a radius of $0.75D_t$ for the entrance of the converging section to the nozzle throat, and a radius of $0.2D_t$ for the exit of the throat to the start of the diverging portion of the nozzle,

where D_t is the nozzle throat diameter[2]. Due to the desire to minimize the need for custom tooling and simplify machining for the EMRTC machinists, the suggested radii were averaged and a radius of $0.5D_t$ was used for the throat contour.

Figure 3.6 shows the dimensional detailing of the designed nozzle. To allow connection to the combustion chamber, eight 9.80mm (0.386") holes were drilled along the circumference to allow 3/8" Grade 8 steel bolts to pass through. Figure 3.7 shows the completed nozzle being test fitted to the rocket engine. The machining drawings can be found in Appendix A.1.5.
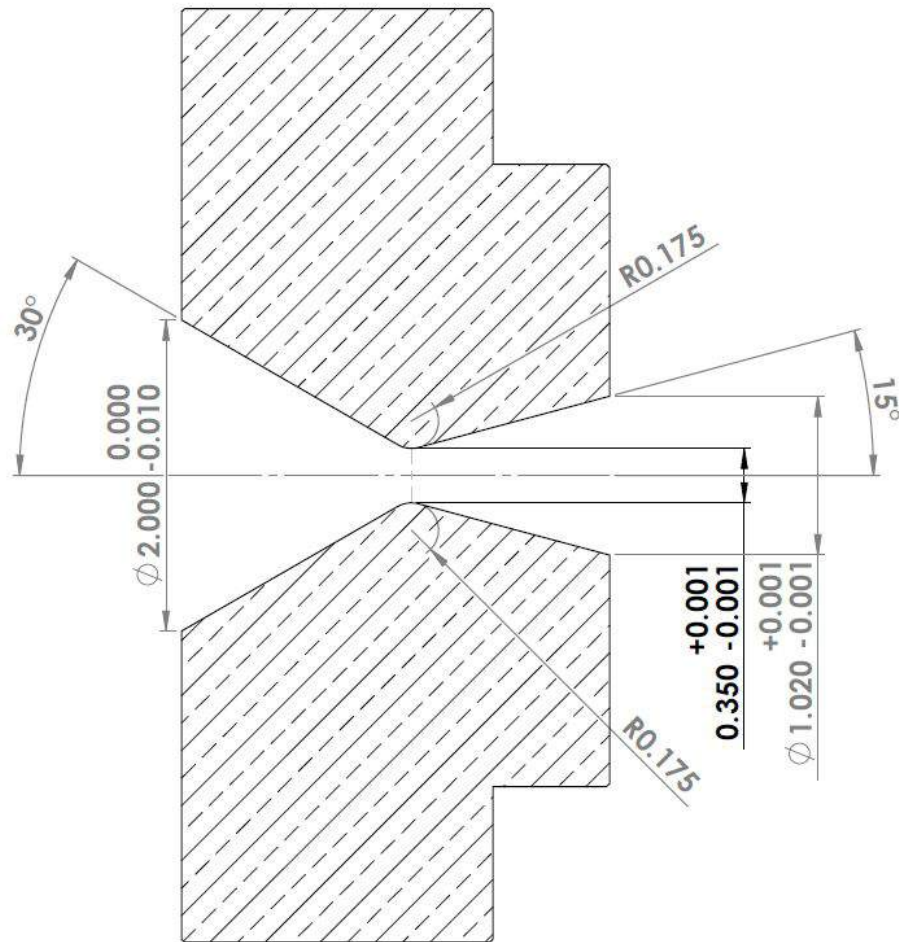
Figure 3.6: Nozzle Dimensional Detailing
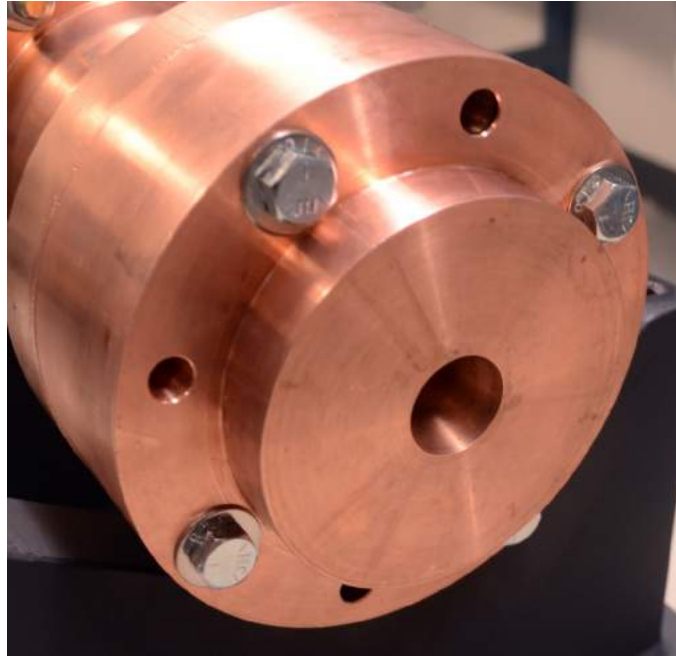
Figure 3.7: Completed Nozzle

During testing, it was discovered that the nozzle throat diameter had been undersized during machine, with an actual throat diameter of 8.48mm (0.333"). This was determined during comparison of the computational model predictions and experimental data. The effects on engine performance and methods used for determining the undersized throat condition are discussed in Chapter 5.

3.1.4   Igniter Design

The designed igniter was primarily based on a spark initiated, hydrogen/oxygen, torch igniter developed at the NASA Lewis research Center (presently the NASA Glenn Research Center) by George Repas[26]. The NASA igniter design had been reported to be successful by Repas, however research at Purdue University found that the design was problematic and inconsistent at times[28]. Because of the inconsistent operation, Purdue University performed several redesigns of the original Repas design to improve reliability[28]. While the structure and operation of the igniter remained relatively unchanged from Repas's for the Purdue igniter, the seals between igniter sections were redesigned to improve sealing and ignition hardware changes were made to improve longevity and reliability of the igniter. In developing the igniter design presented here, the Repas igniter was used for the main structural design while supporting hardware was based on the Purdue design.

Figure 3.8 shows the three main components of the igniter:

1. *The top cap* which holds the spark plug used for providing ignition.

2. *The combustion chamber* which has one gaseous H_2 inlet, one gaseous O_2 inlet, a port for taking pressure readings, and a torch ignition tube connected to its base for directing the combustion gases to the rocket engine.

3. *The igniter base* which is threaded for attachment to the rocket engine, and has one gaseous H_2 inlet for supplying hydrogen to cool the torch ignition tube as it extends to the engine.

For sealing between sections, the igniter base and top cap have o-ring grooves machined for sealing against the igniter combustion chamber.
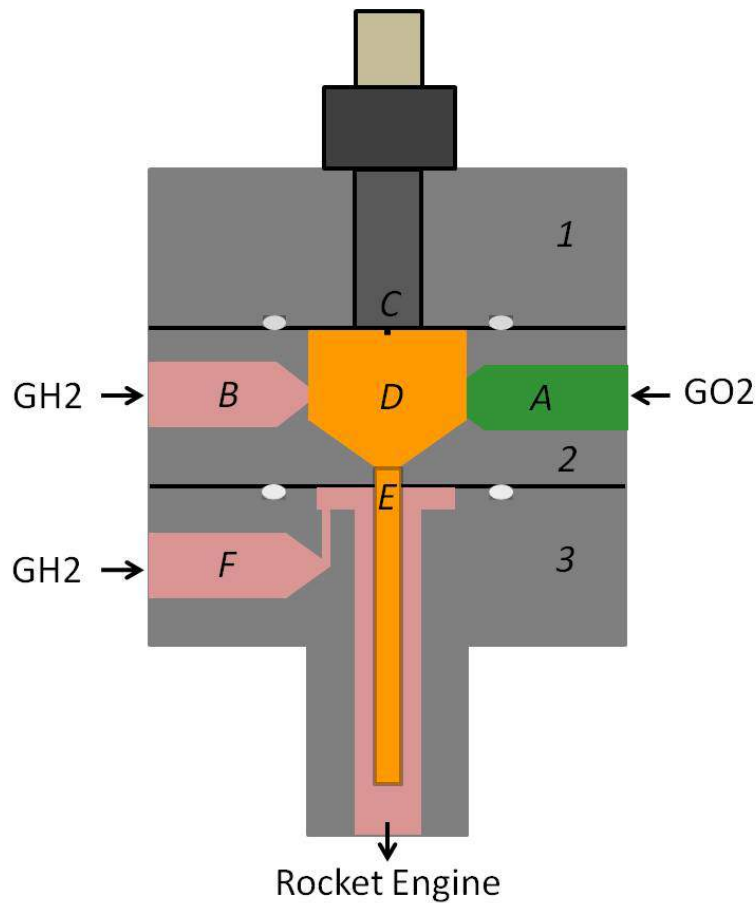
Figure 3.8: Simplified igniter schematic, labeled for operational explanation

Referencing Figure 3.8, the igniter was designed to function as outlined:

1. Gaseous O_2 is injected (A) while spark generation occurs at the spark plug (C).

2. A small core flow of gaseous H_2 is injected (B).

3. Combustion takes place in the combustion chamber (D). The flow rate is control by a choked flow orifice machined in the igniter

4. Hot Combustion gases travel down the torch ignition tube to the engine (E).

5. Gaseous H_2 is injected (F) to cool the torch ignition tube to rpolong the life of the tube.

Figure 3.9 shows the the final igniter design and over all dimensions.
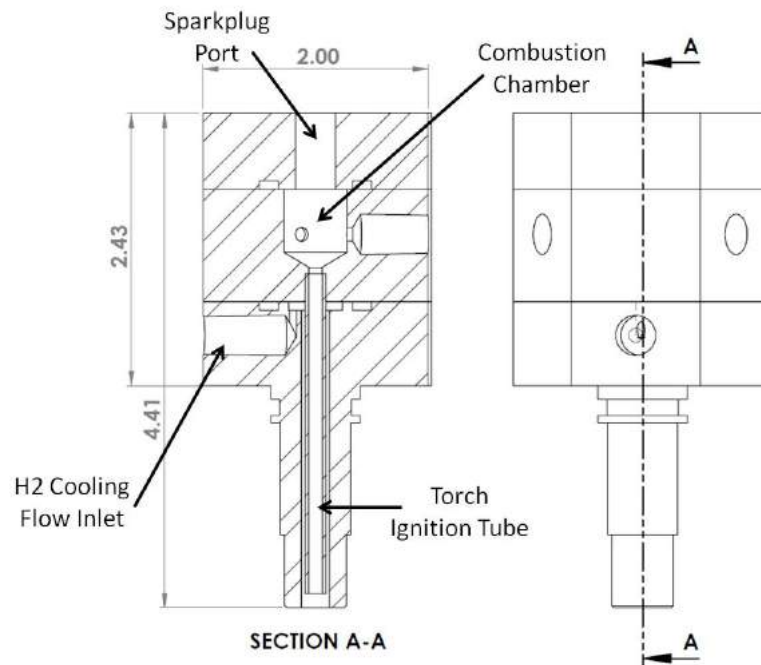
Figure 3.9: Final igniter design with overall dimensions.

Sequencing for the above operation scheme was timed in 0.25s intervals. Figure 3.10 shows the timing sequence for spark operation, gaseous oxygen flow, and gaseous hydrogen flow. The timing sequence is outlined below:

1. Gaseous O_2 is flowed for 0.25s to fill the supply line between check valve and igniter to prevent hydrogen from flowing into the oxygen supply line.

2. The spark plug is operated during the same 0.25s time frame as the gaseous O_2 flow. This is performed to start gas ionization before the gaseous H_2 is introduced into the combustion chamber.

3. H_2 flows after the above 0.25s period has passed.

4. The O_2 flow, H_2 flow, and spark are kept on for 0.75s, after which the O_2 flow and spark cease. At 0.5s, the igniter chamber pressure is checked to determine if combustion has taken place.

5. The H_2 continues to flow for another 0.25s to provide a buffer against main chamber gases entering the igniter for the duration of the test.
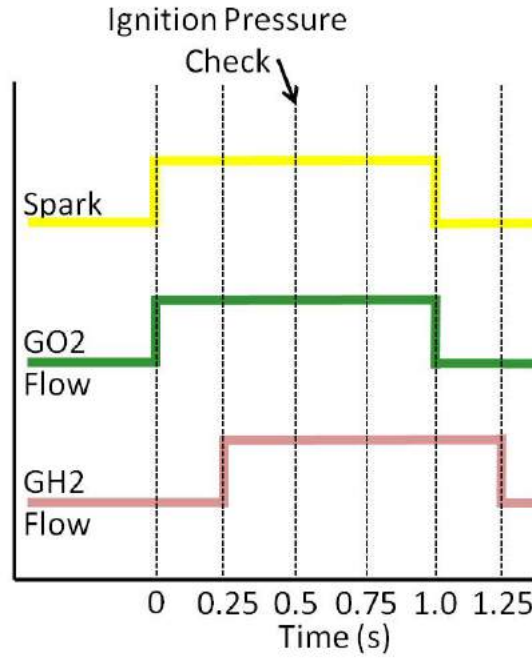
Figure 3.10: Spark, O_2 flow, and H_2 flow time sequence.

The igniter chamber pressure with only O_2 flow was determined experimentally to be approximately 0.41MPa (60psi). With the introduction of H_2, the pressure rises slowly to approximately 0.55MPa (80psi), followed by a sharp pressure rise when combustion takes place. This pressure rise was observed approximately 0.2s after H_2 flow begins. After 0.25s, the pressure rise exceeded 0.69MPa (100psi). Therefore, the control system confirms ignition by whether the igniter chamber pressure exceeds 0.69MPa (100psi). If this is confirmed, the control system initiates the rocket engine main propellant flow.

The igniter used needle valves to control the total flow rate of H_2 and O_2 supplied to the igniter, and machined a choked flow orifice for controlling the flow of H_2 into the combustion chamber. This was done with the intention of being able to adjust the igniter's performance, making it viable for use with larger rocket engines by increasing the gas flow rates and using combustion chambers with different orifice sizes. SwageLok SS-4MG-MH needles valves were used and equipped with twentieth of a turn graduated knobs, providing precision control of the flow. Coefficient of flow (Cv) values were obtained from Swagelok's part catalog, and polynomial equations were developed for expected Cv as a function of knob rotation. These equations were combined with work from AeroSmith Gases for predicting total flow rate as a function of the valve knob position[54].

Table 3.3 shows the needle valve settings and predicted total mass flow rates supplied to the igniter.

Table 3.3: Needle valve estimated flow rate

	Upstream Pressure	Metering Valve Turns	Flow Rate
Units	(Mpa, PSI)		(kg/s, lbm/s)
Total O2 Flow	7.58 (1100)	3	0.0037 (0.0082)
Total H2 Flow	4.82 (700)	2	0.0003 (0.0008)

The igniter was originally designed for a combustion chamber O/F of 30, but the completed igniter was found to have an O/F closer to 10. This was a result of mistakes in dimensioning of the machining drawings that led to the H_2 combustion chamber orifice being oversized and the H_2 cooling port being undersized. The oversized orifice resulted in the flow at the inlet to the combustion chamber failing to choke, and the undersized port resulted in choking of the H_2 cooling flow. Despite this error, the igniter still performed successfully with no appearant adverse effects to the igniter parts. Table 3.4 shows the individual desired flow rates to the igniter and the estimated actual flow rates due to the machine drawing mistakes.

Table 3.4: Desired and estimated actual flow rates

	Desired Flow Rate	Actual Flow Rate
Units	(kg/s, lbm/s)	(kg/s, lbm/s)
O2 Flow	0.0037 (0.0082)	0.0037 (0.0082)
H2 Chamber Flow	1.2e-5 (2.66e-5)	3.6e-4 (7.99e-4)
H2 Cooling Flow	2.8e-5 (7.7e-5)	3.1e-7 (6.9e-7)

A Champion aerospace surface gap spark plug was used, based on the success in use by Purdue University[28]. The spark plug was powered by a neon sign transformer, rated for 15000KV at 60ma. The neon sign transformer was chosen based on Purdue's success with using an Allison furnace transformer with their igniter system [28]. However for future testing, the neon sign transformer will be replaced with MSD automotive ignition coil and driven by a MOSFET pulsed by a 555 timer circuit. This change is due to serious electric shock hazards associated with the power capabilities of the transformer

All three components were machined out of 304 stainless steel, 50.4mm (2") wide hex bar. Stainless steel was chosen due to the harsh combustion environment the components would be exposed to. The base material was chosen to be 50.4mm (2") hex bar as it provided flat faces for machining ports and simplified fixturing for machining. The larger bar stock also helped increase thermal mass, which was employed to help decrease the operating temperature of the igniter. For sealing, high temperature PTFE O-rings were used and have shown

no degradation in sealing ability with use with the igniter. These decisions were partly based on Purdue University having reported suffering o-ring deterioration due to the high temperatures the igniter reached[28].

In the Repas igniter design, the torch ignition tube was found to be the most vulnerable part of the design[26]. In an effort to maintain the ability to order replacement parts quickly, special alloys were avoided for the torch ignition tube. Instead, the torch ignition tube was fabricated using 316 stainless steel, precision diameter tube, and was attached to the combustion chamber utilizing a shrink fit. The intention being that when the tube eventually failed, it could be faced and drilled out. A new section of tube could then be shrink fitted into the igniter combustion chamber section.

For connecting the igniter to the rocket engine, a machined 25.4mm (1") long, 5/8-18UNF threaded section was used to secure the igniter to the combustion chamber. Sealing was achieved using an axial o-ring seal. The igniter base threaded attachment and axial o-ring seal groove can be seen in Figure 3.11. The assembled and installed igniter is shown in Figure B.1. Machining drawings can be found in Appendix A.2.
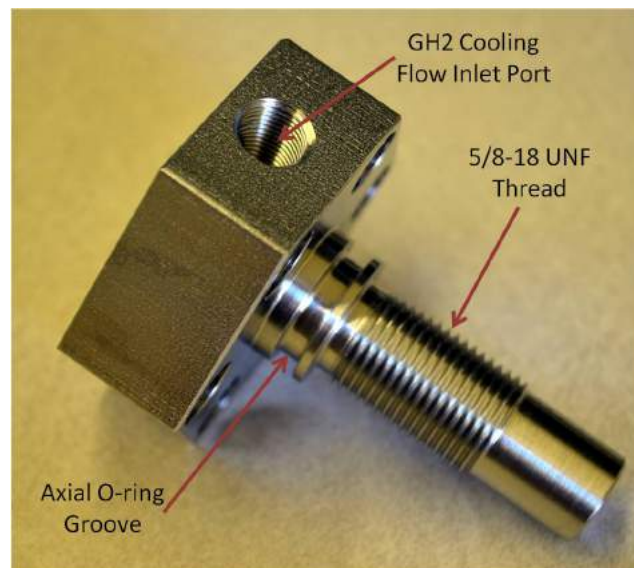
Figure 3.11: Igniter base.
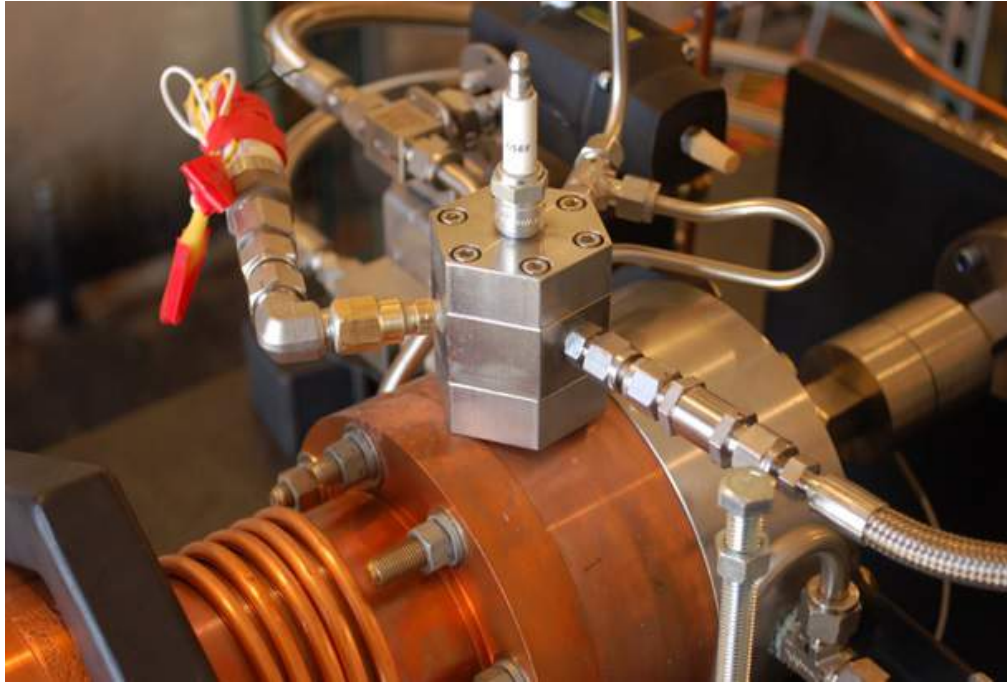
Figure 3.12: Igniter assembled in installed on rocket engine.

3.2   Supporting Hardware

3.2.1   Force Transducer Mount

A WMC-500, full-bridge, force transducer from Interface Force was used for recording the thrust output of the rocket engine. A mount was designed for connecting the transducer between the rocket engine and backstop that would protect the transducer from being overloaded and also counteract any axial misalignment, allowing a true axial thrust measurement to be recorded.

The force transducer mount used two flexure bars with the bending axis of the bars offset 90° from one another to counteract axial misalignment. A holder for the transducer was designed to displace 0.0508mm (0.002″) before further loading of the transducer was prevented. This displacement distance was selected as it was half of the total displacement of the transducer under full load. To stop the loading of the transducer, two halves were connected to either end of the force transducer that were wider than the transducer. Once the 0.0508mm (0.002″) displacement had been achieved, the two halves made contact with one another, preventing further loading of the transducer. The transducer mount design is shown in Figure 3.13. This design was ultimately found to be inadequate and failed during testing. This failure and the redesign of the transducer mount is discussed in Section 5.5.

48
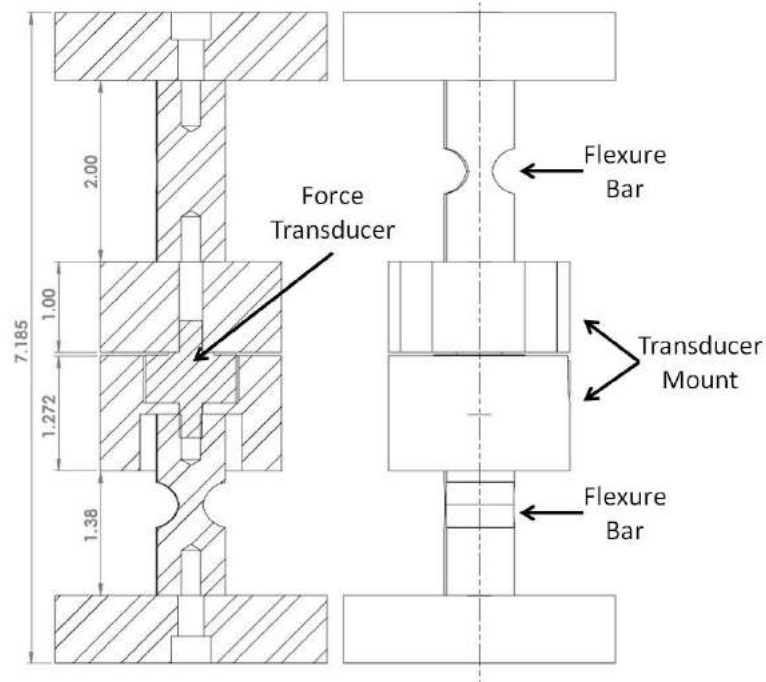
Figure 3.13: Transducer mount design

3.2.2 Cavitating Venturi

Cavitating venturi flow meters were chosen to control both the oxidizer and fuel flow rates to the engine. A cavitating venturi flow meter acts as a "hard" flow regulator, such that downstream pressure variances do not affect the flow rate, and the flow rate through the cavitating venturi is a function only of the properties of the fluid entering the meter, and the upstream absolute pressure the fluid is at[23]. This occurs due to choking at the throat. If the throat becomes unchoked, the downstream properties can affect the flow upstream.

The cavitating venturis used were manufactured and calibrated by Flow-Maxx Engineering. The design specifications provided to FlowMaxx were based on the computational calculations performed in Chapter 2.3. Using Equation 3.4, which predicts the mass flow-rate through a venturi[28], and the calibration data, graphs where generated for predicted mass flow rate as a function of upstream pressure.

$$\dot{m} = A_t * C_d \sqrt{\frac{2g\rho}{144}(P - P_v)} \tag{3.4}$$

Because the vapor pressure and density of a fluid can be assumed a function of only the fluids temperature, the mass flow rates were calculated for different propellant temperatures and plotted. Polynomial fits were used for calculating the change in vapor pressure and density as a function of the propellant temperature[22][20]. This yielded a reference guide for setting upstream supply

pressure to obtain the desired testing flow rate. Figures 3.14 and 3.15 are the resultant graphs for expected nitrous oxide flow rate and ethanol flow rate, respectively. The calibration data for the cavitating venturis and full page flow rate charts for nitrous oxide and ethanol can be found in Appendix A.4.
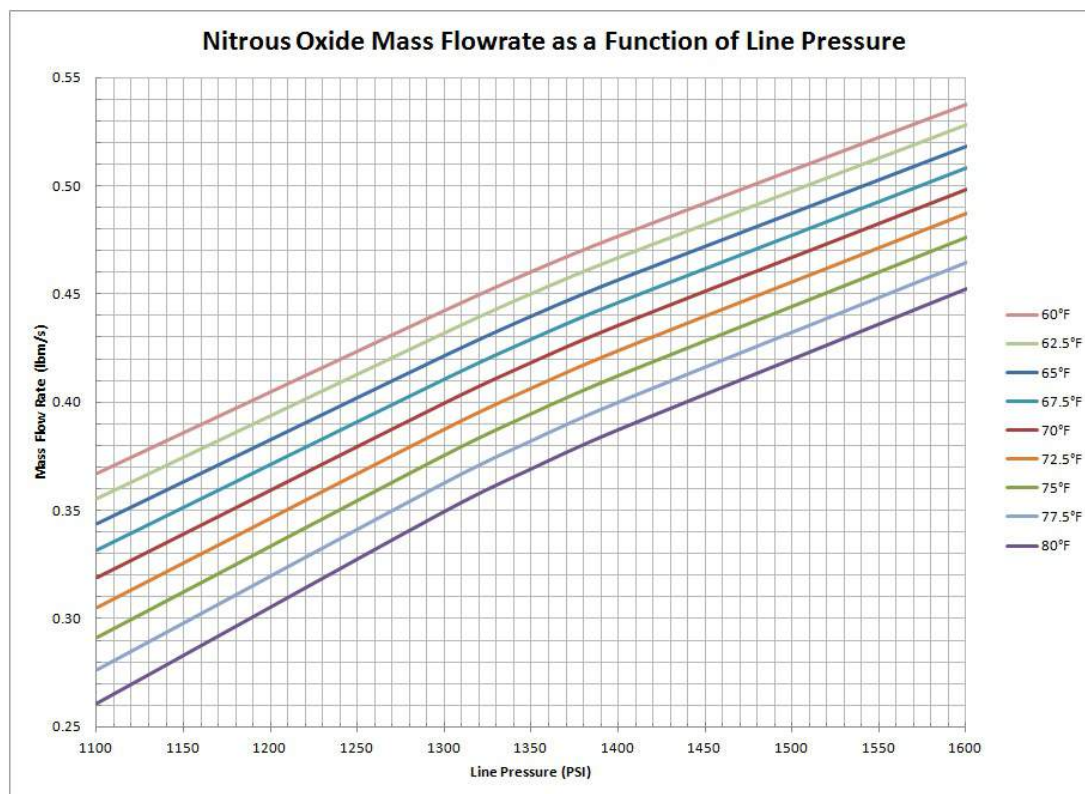
Figure 3.14: Predicted nitrous oxide flow rate as a function of upstream pressure.
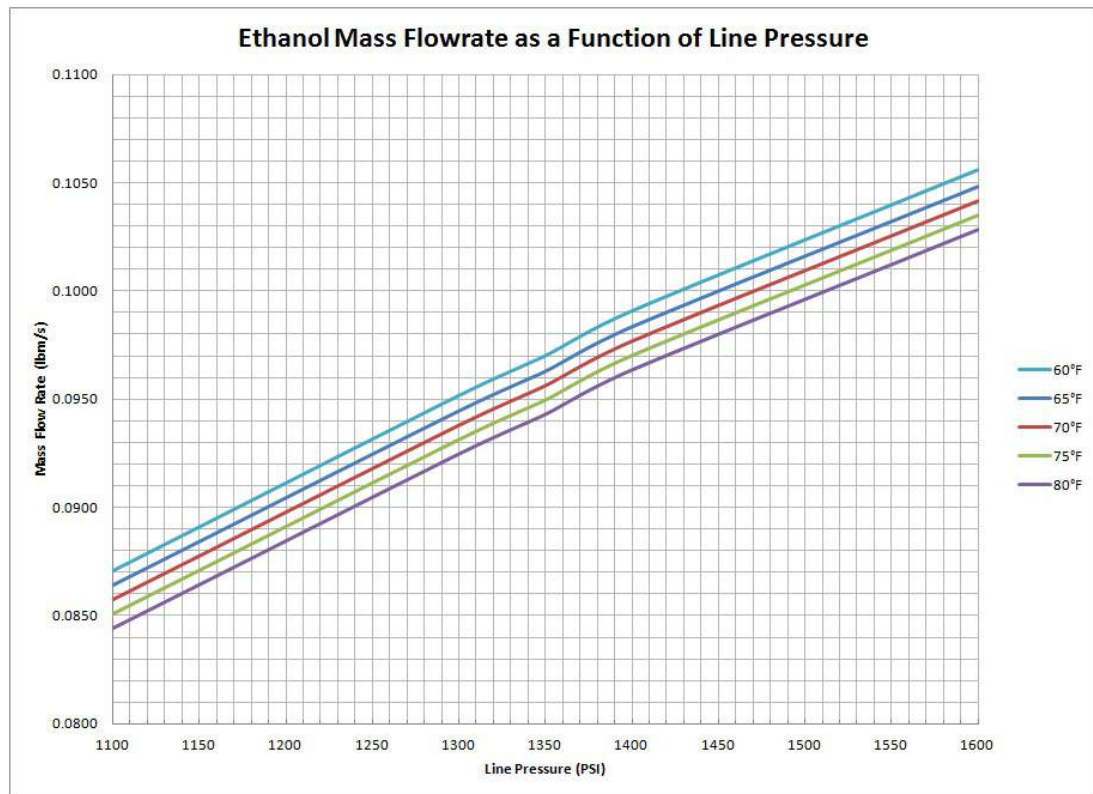
Figure 3.15: Predicted ethanol flow rate as a function of upstream pressure.

3.3 Completed Rocket Engine

Figure 3.16 shows the engine with main supply and purge valves connected prior to installation.
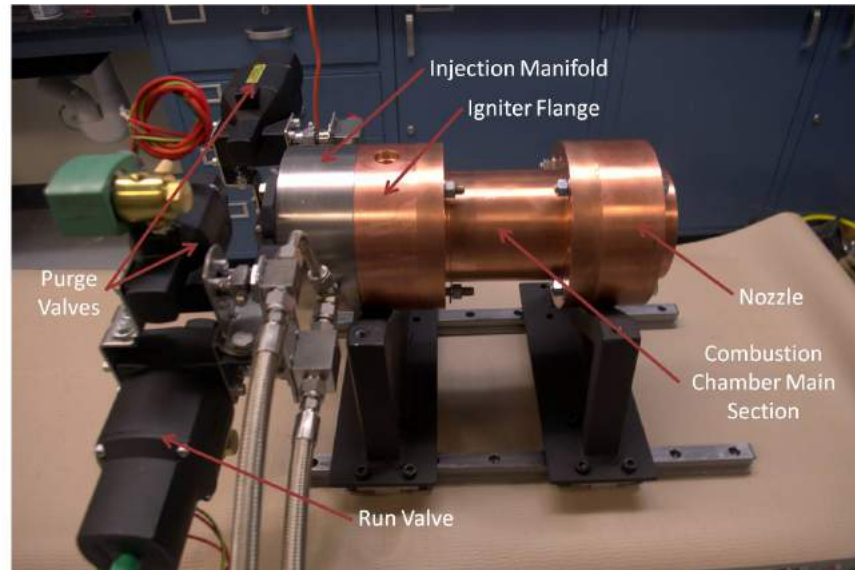
Figure 3.16: Assembled rocket engine prior to installation in test facility

CHAPTER 4

TEST FACILITY DESIGN AND CONSTRUCTION

For safe and proper operation, the rocket engine required a properly designed propellant supply system and a dedicated facility for testing. The facility serves two purposes: Provide the housing for the necessary propellant supply systems and equipment to successfully operate the rocket engine, and protect both the operators and support equipment from harm due to any sort of explosive event, whether it be an engine or propellant supply system failure. To fulfill both purposes, a hardened facility with specially designed safety features to house the rocket engine and support systems was required. From this point forward, the test facility will be referred to as the rocket engine facility (REF).

The design and construction of REF will be discussed, including:

1. Detail of the facility layout.

2. Design and construction of the propellant supply system.

3. Control and data acquisition system implementation.

4. System operation protocols.

5. Safety and explosive hazards.

6. Oxygen cleaning methods.

4.1   Facility Layout

The REF was constructed in the Torres "West Lab" bunker located on the EMRTC range. The bunker was originally designed for operations including melting and casting of TNT, and is rated to protect operators from a blast of up to 498kgs (1100lbs) of TNT. Given the small scale of the rocket engine, the explosive rating of the bunker provides a significant safety margin of protection.

The bunker floor plan allowed individual systems to be isolated from each other, preventing the failure of one system component from destroying the entire system. This made the REF ideal for testing novel propellants and engine designs when considering future research. The propellant supply system was separated

from the rocket engine test cell by placement in a storage room outside of the bunker, now referred to as the fuel galley. The final layout of the REF is shown in Figure 4.1.
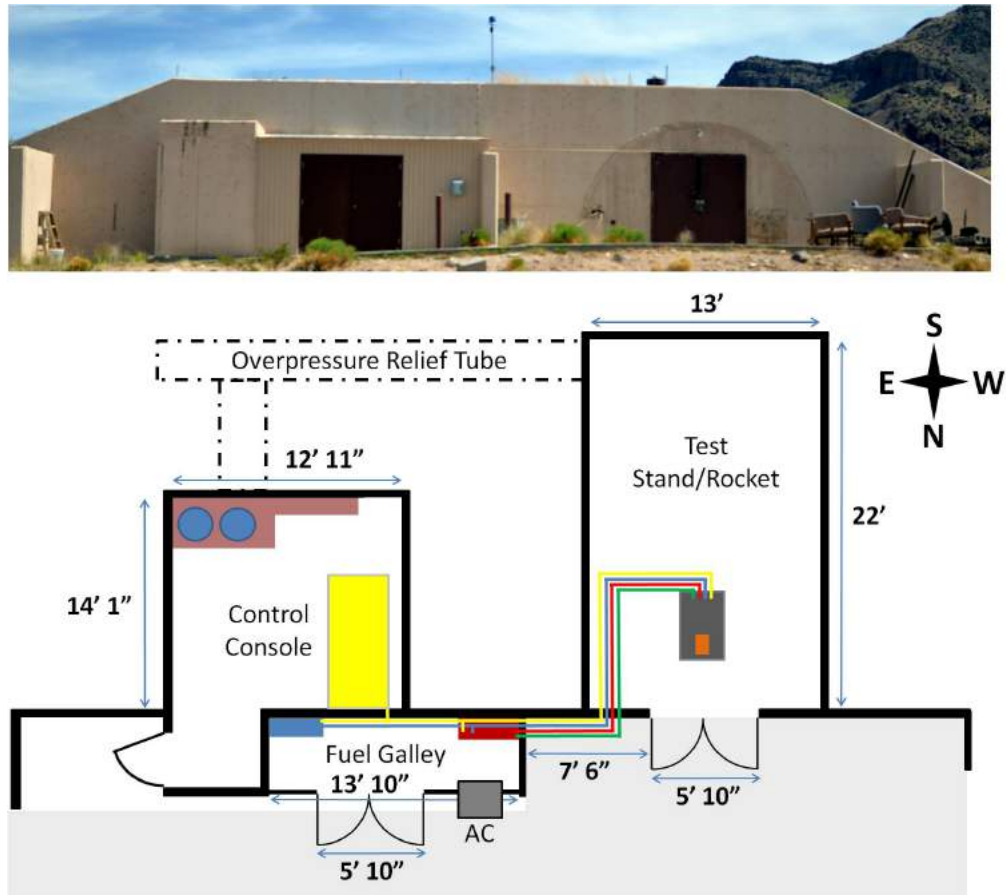
Figure 4.1: Final facility layout

The fuel galley (former storage room) was originally constructed with three reinforced concrete walls on the West, East, and South sides. The North wall is a false wall designed to fail under explosive or over-pressure loading. This allowed any explosive event inside the room to be directed away from the facility, making it ideal for housing the propellant supply system. By placing the propellant supply system components on the South concrete wall, an explosive failure would lead to the explosive energy propagating North, through the false wall, and away from the test facility. Temperature control was added to the fuel galley by installing an air conditioning (AC) unit through the false wall and insulating the room.

The rocket engine was housed in the test cell originally used for performing the TNT melt casting operations. This test cell is constructed with a false wall at the North end that was designed to fail in the case of an explosive event, directing the explosive energy away from the facility. An over pressure relief tube

was also utilized to relieve pressure at the South end of the test cell. These features were not modified during construction of the REF. For test firing the rocket engine, the steel plate double doors in the north wall are opened and secured to prevent accidental closure. The rocket engine exhaust exits the test cell through these doors.

The operator and control systems were housed in the control room. While not apparent in the floor plan, the control room was separated from the fuel galley by heavily reinforced concrete, 0.38m (15″) in thickness, providing a reasonable safety barrier. Control and system wiring were passed from the control console into the fuel galley through four 31.75mm (1.25″) holes. These holes were then sealed with fire retardant caulk to protect the operators from propellant fume infiltration into the control room and oxygen removal in the case of fire in the fuel galley.

With the REF layout planned, the propellant supply system, rocket engine test stand, and control systems were designed not only to fit within the layout but also to further enhance safety and the hardened nature of the REF.

4.2 Propellant Supply System Design

A blow-down system was designed and implemented to supply the ethanol and nitrous oxide propellants to the rocket engine. This system uses an inert gas to push propellant from a storage tank through supply lines to the rocket engine. This type of system works well for liquid propellant systems in which gravity helps to insure that pure liquid is fed to the engine by the taking of propellant from the bottom tank. Figure 4.2 depicts the basic function of this type of system. The REF facility uses high pressure nitrogen as the push gas as well as for purging the propellant supply tanks, supply lines, and rocket engine.

The the un-powered state (normally closed/normally open) of the valves selected were chosen such that the system would be naturally unable to hold pressure when shutdown. Thus, in the event of an emergency, the system would be purged and put into an inert state simply by cutting power to the valves. This is useful for required maintenance as turning off the power supply for the valves and performing a visual inspection of the valves open/close status was all that is required to ensure the system is not pressurized. This also prevents nitrous oxide from being trapped in the lines when the system is shutdown. Liquid nitrous oxide trapped in lines is a safety hazard as a pressurized line and also poses a rupture hazard as a result of increasing line temperature increasing the hydrostatic pressure. For a line volume filled with liquid nitrous oxide, AIGA reported that the hydrostatic pressure increases by $10.5 MPa/^{\circ}C (850 psi/^{\circ}F)$[51].

Figure 4.3 is a simplified schematic of the propellant supply system. For safety reasons, the system was designed such that the ethanol and nitrous oxide sides of the system were completely separate. Each side of the system has its own nitrogen supply and purge system. The schematic emphasizes the separation of
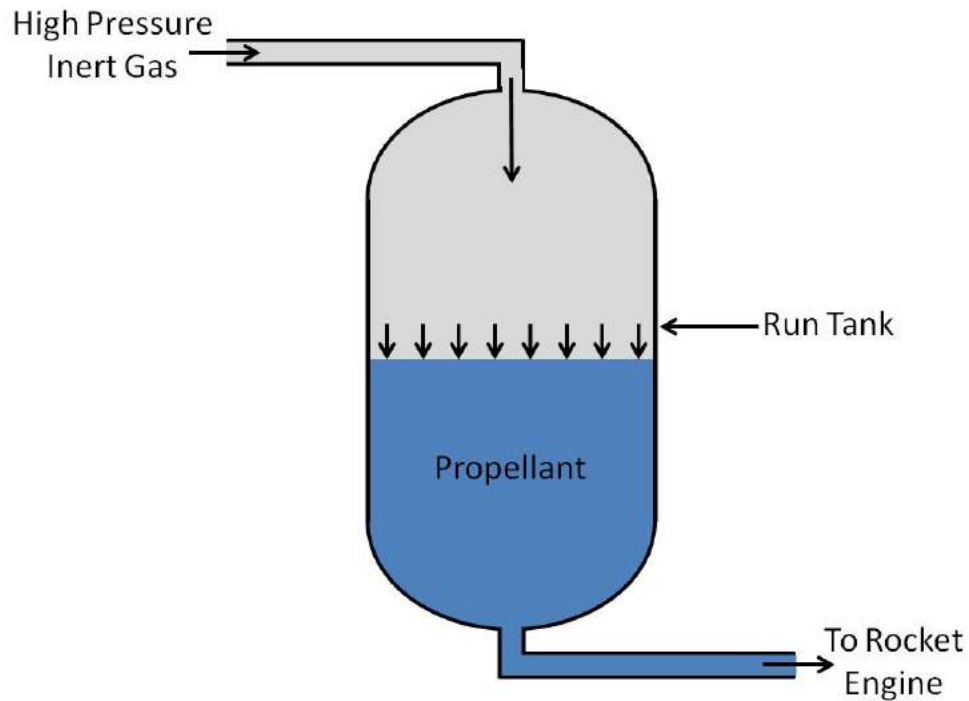
Figure 4.2: Simplified schematic of blow-down propellant supply system

the ethanol and nitrous oxide sides of the system and details the function and operation of each of the valves present on the system. Green represents supply lines in contact with nitrous oxide, red represents supply lines in contact with ethanol, and blue represents supply lines in contact with nitrogen.

Gas actuated valves were utilized due to their fast actuation rate. This was important to minimize lag time between the commanded actuation of the valve by the control system and the actual opening or closing of the valve. Three-way, electric solenoid valves were used to allow an electrical signal to control the actuation of main system valves. The three-way valves supplied gas pressure to the system valves when powered, and closed gas supply and vented the system valves when un-powered. In an effort to reduce signal noise in the measurement equipment, filtered 24VDC was used to power the three-way valves.

Supply tubing diameter selection for the system was influenced by flow velocity limitations for nitrous oxide and cost. Discussed in the nitrous oxide code of practice documents from the EIGA and AIGA, nitrous oxide flow can cause localized heating of material due to particle impact or flow friction. This is likely to occur in narrow passage tube sections, and the heating can initiate decomposition of the nitrous oxide or combustion of the heated material. There-fore, both documents recommended that the velocity limits for oxygen service be used for nitrous oxide[51][39]. From the AIGA produced *Oxygen Pipeline and Piping System* document, the maximum recommended flow velocity for oxygen
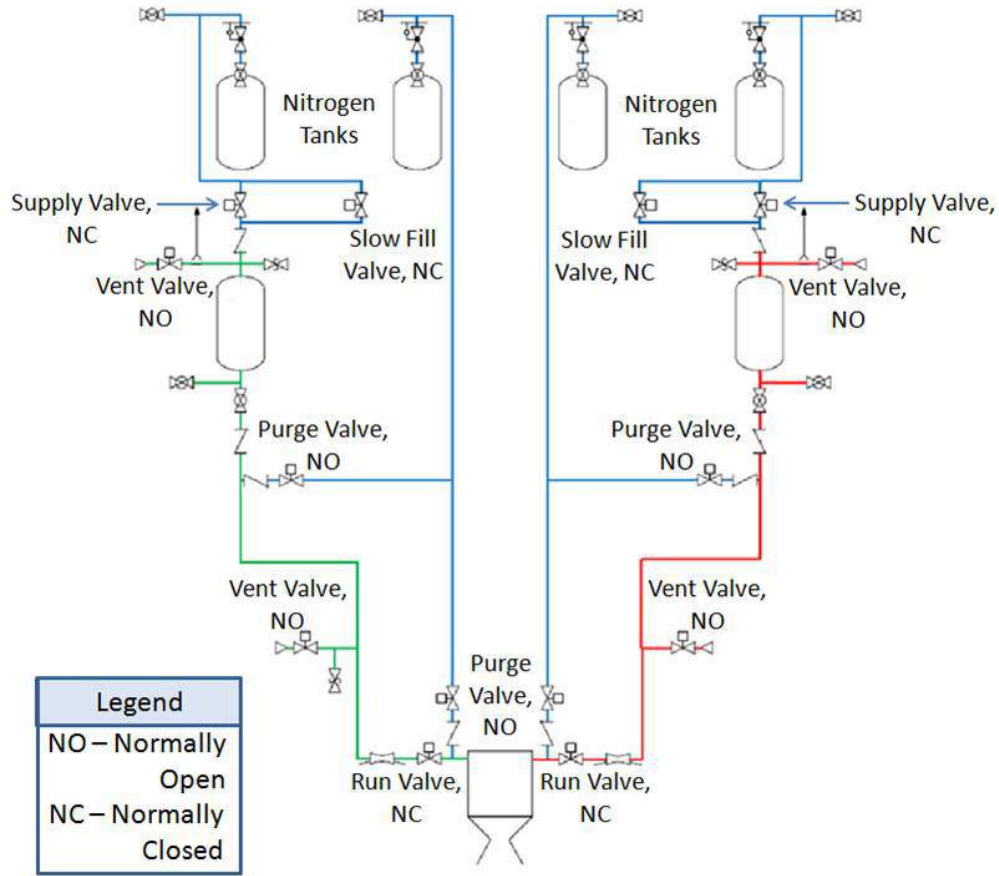
Figure 4.3: Simplified schematic of propellant supply system detailing valve function and operation

service was 8m/s (26.6 ft/s) at an operational pressure range of 10MPa (1500psi) to 20MPa (3000psi) [38].

Therefore, in sizing tubing diameter, the final selected diameter would have to meet the velocity requirements set forth by the *Oxygen Pipeline and Piping System*. The tubing diameter selection would be based on the maximum designed nitrous oxide flow rate of the REF system of 0.22kg/s (0.48lbm/s) at a temperature of 26.6 $^\circ C$ (80 $^\circ F$). This temperature was initially selected as the maximum allowable operating temperature of nitrous oxide for the facility to prevent the nitrous oxide from reaching its critical point. However, the use of this temperature limit is also supported by the EIGA and AIGA documents[**?**][39]. Flow velocity of the propellant system during normal operation was calculated using the rearranged mass flow rate equation 4.1 as recommended by the AIGA document[38].

$$V_{flow} = \frac{\dot{m}}{\rho A_{tube}} \tag{4.1}$$

It was found that for supplying the desired flow rates, the most cost effective tubing size that could be safely used was 9.525mm (0.375") outer diameter, 1.24mm (0.049") wall thickness stainless steel tubing. For this diameter, and the maximum flow rate of nitrous oxide for the facility, the calculated fluid velocity was found to be 6m/s (19.6ft/s). This was considered an upper limit as it was for an extreme operation condition. The REF in its current form cannot supply 0.22kg/s (0.48lbm/s) at 26.6 $C°$ (80 $F°$) due to the restrictions of the cavitating venturis and maximum system operating pressures.

In designing the propellant supply system, the maximum allowable pressure of the system was determined by the lowest rated component. The use of 9.525mm (0.375") outer diameter, 1.24mm (0.049") wall thickness stainless steel tubing permitted a maximum allowable working pressure (MAWP) of the system of 31MPa (4500psi). However, the lowest rated components in the system were the propellant run tanks. These tanks were double ended sample cylinders, manufactured by Swagelok. The sample cylinders were rated for a MAWP of 12.4MPa (1800psi). As a result, the MAWP of the system was rated to 12.4MPa (1800psi).

The actual system operation pressure was further limited by the safety systems incorporated. In keeping with the EIGA and AIGA design recommendations, both sample cylinders were equipped with a burst disk and a pressure relief valve for safety. The burst disks were rated to fail at a pressure of 12.4Mpa (1800psi) $\pm$0.69MPa(100psi). Because of the variance in burst pressure of $\pm$0.69MPa(100psi), the pressure relief valves connected to the system were set to open at 11.5MPa (1675psi), to prevent the burst disk from failing unless absolutely necessary. The system therefor has a maximum operating pressure of 11.5MPa (1675psi).

The propellant supply system was constructed using Swagelok components. Stainless steel swage fittings were selected for their reliability in both sealing and function as well as ability to be disassembled and reassembled. However, some components required national pipe thread (NPT) connections. These components included the pressure transducers, regulators, and run tank sample cylinders. For all connections, a oxygen complaint PTFE sealing paste called Lox-8 was used. The paste was designed for sealing of oxygen systems of up to 69MPa (10000psi) at temperatures of 60 $C°$ (140 $F°$), and was manufacture by Fluoramics Inc

Swagelok provided an oxygen cleaning service for their fittings and valves, known as SC-11. This cleaning was important for the components to be used with nitrous oxide as oxygen cleaning was mandated as a requirement by the EIGA and AIGA documents for all components in contact with nitrous oxide[51][39]. Unfortunately, Swagelok did not provide the SC-11 service for the supplied stainless steel tubing. Therefore an oxygen cleaning method was developed and used to clean the tubing and fittings whose oxygen cleaning status was questionable. The development and implementation of this procedure is discussed in Section 4.6.

The propellant supply system was divided into three main sections: The

nitrogen supply panel; the propellant run tank panel, and the rocket connection hardware. The nitrogen supply panel, propellant run tank panel, and long tubing runs were manufactured in an environmentally controlled lab space at the EMRTC main facility. The majority of the system was constructed at REF, with extreme care taken to maintain cleanliness of the system. The propellant supply system diagram shown in Figure 4.4[55] shows the final placement of system components and line routing.
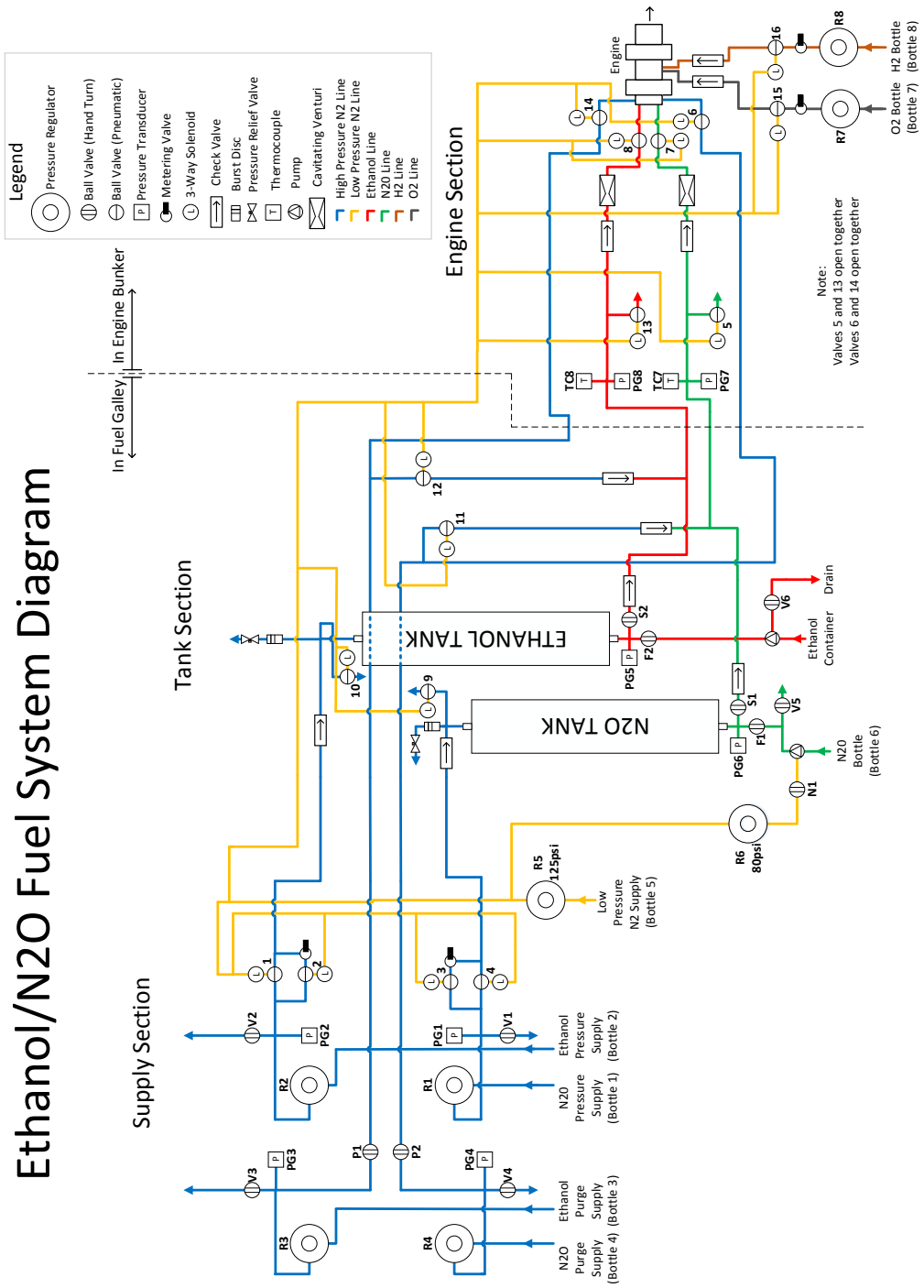
Figure 4.4: Propellant supply system schematic

4.2.1 Nitrogen Supply Panel

The nitrogen supply panel was constructed on a super strut frame and designed to supply high pressure nitrogen for both push gas use and system purging. The schematic for the nitrogen supply panel is shown in Figure 4.5. Also seen in the schematic is the low pressure nitrogen regulator (R5) for supplying nitrogen to the gas actuated valves. The completed and installed nitrogen supply panel is shown in Figure 4.6.
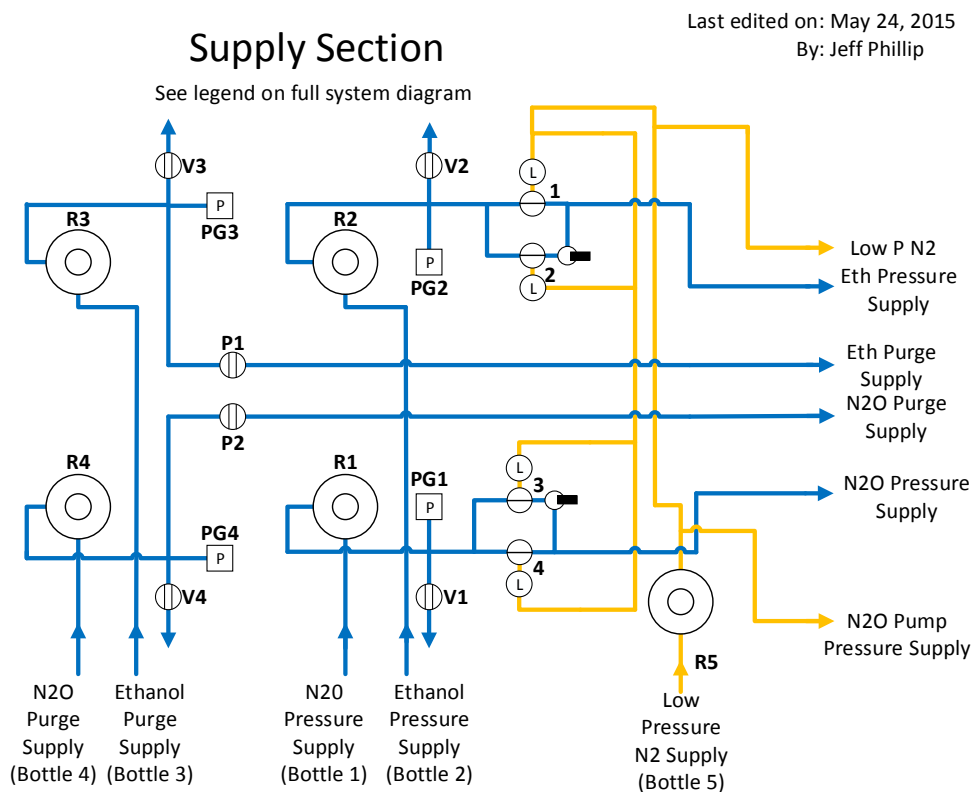
Figure 4.5: Nitrogen supply panel schematic[**?**]

The panel consists of four regulators (R1, R2, R3, R4) which allow the supply pressure and purge pressure to be individual set for the ethanol and nitrous oxide sides of the system. The panel was designed to be supplied by four 41.4MPa (6000psi), high pressure nitrogen gas cylinders. KPP series regulators were used from Swagelok as they were capable of supplying the required flow rates of nitrogen demanded by the system. Each supply line had a pressure transducer attached for monitoring static pressure (PG1, PG2, PG3, PG4).

The regulators were rated to supply up to 20.7MPa (3000psi) with 41.4MPa (6000psi) at the inlet of the regulator. This allowed operation of the propellant

system near the midrange of the regulators pressure range. Swagelok reported that at high flow rates, for optimal performance in regards to supplied pressure consistency it was best to operate the KPP regulators near their midrange. During testing, it was discovered that there was significant pressure drop during operation of the engine. It was determined that the drop was a result of the high pressure nitrogen bottles being unable to supply the necessary flow rate of nitrogen through their tanks valves. This problem will be resolved during future work, either by using high pressure nitrogen cylinders capable of supplying the necessary flow rates, or increasing the number of cylinders supplying the regulators.

The regulator outlets are connected to individual manifolds which consist of a system isolation valve (P1, P2, 1, 4), manifold vent valve (V1, V2, V3, V4), and pressure transducer. These manifolds were incorporated to allow the system to be isolated while the regulators were adjusted. This makes setting of the system pressure very quick as only a small volume is pressurized. The addition of the manifolds was a protective measure for the downstream system components. While a regulator failure was incredibly unlikely, a regulator failure allowing the full supply pressure into the system would most likely occur when the supply cylinders were first opened. In the event of failure, the use of these manifolds would isolate the high pressure nitrogen to a very small volume of the system. The manifold would allow the supply bottle valves to be closed, the manifold vented using the vent valves, supply bottle disconnected, and the regulator removed and replaced. The tubing used for assembling the manifolds had a wall thickness of 1.651mm (0.065"), providing a working pressure of 44.8MPa (6500psi) to allow the manifold to be able to handle the full supply pressure of the high pressure nitrogen cylinders.

A slow fill system was incorporated into the nitrogen supply panel. As reported by Merrill, nitrous oxide can decompose at high compression rates [36], and therefore it was best to avoid adiabatically compressing it. The slow fill system consisted of a small, gas actuated valve (2, 3) which connected the supply manifold to the run tank supply line via a needle valve. By adjusting the needle valve, the pressurization rate is controlled. The slow fill system was applied to both the nitrous oxide and ethanol sides of the system.

Figure 4.6: Installed Nitrogen Supply Panel

4.2.2 Propellant Run Tank Panel

As with the nitrogen supply panel, the propellant run tank panel was constructed on a super strut base. The run tank panel was designed to hold the propellant supply tanks and provide venting, purging, and filling capabilities of the run tanks and propellant lines. The run tank panel schematic is shown in Figure 4.7[55]. The completed and installed run tank panel is shown in Figure 4.8.

The propellant run tanks were 3.78L (1gal) double-ended sample cylinders manufactured by Swagelok. These sample cylinders were donated by the NASA White Sands Test Facility who also cleaned them for oxygen service. Because the cylinders were equipped with 1/2"NPT threaded connections on either end, tube adapters were attached to allow Swage fittings to be used with the tanks. Lox-8 sealant paste was used for sealing the NPT threads.

Each run tank was equipped with a burst disk and a pressure relief valve connected to the top of the run tank by a cross fitting. For monitoring tank pressure, pressure transducers (PG5, PG6) were attached at the base of the tanks. The temperature of the tanks was monitored using surface mount thermocouples. The monitoring of the tank pressure and temperature was most important during
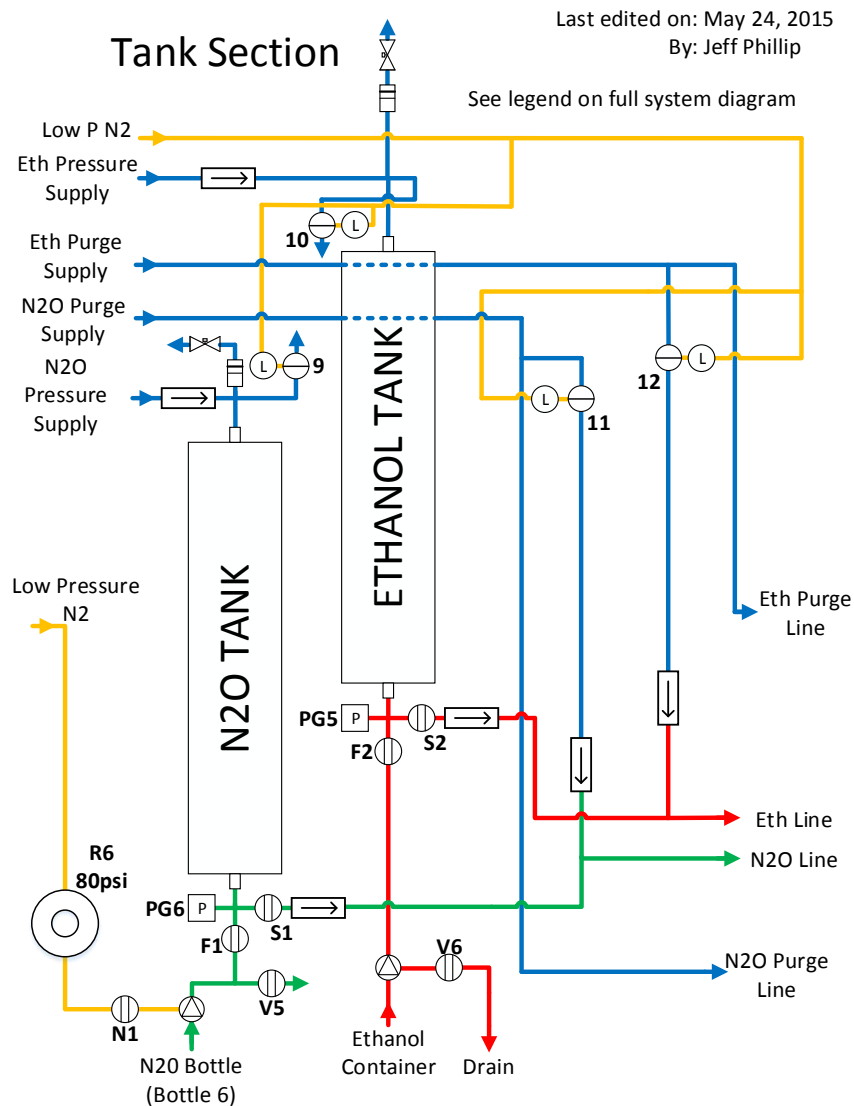
Figure 4.7: Propellant run tank panel schematic

the filling of the nitrous oxide tank to insure the nitrous oxide did not reach dangerously high pressures and temperatures that could lead to decomposition. The maximum limits were considered to be 6.89MPa (1000psi) and 32.2 $^\circ C$ (90 $^\circ F$).

Each tank was equipped with a gas actuated valve (9, 10) for manual venting. The nitrous oxide pressure relief valve, vent valve (9), and the nitrous oxide fill system vent valve (V5) were connected and plumbed outside of the fuel galley for venting. For purging the propellant lines, purge valves (11, 12) were used. Flow into the purge lines was prevented by check valves, as was the back flow

into the run tanks during line purging.

For filling the run tanks, each tank was equipped with a manually operated fill valve (F1, F2) and propellant line isolation valve (S1, S2). During the filling operation of a run tank, the isolation valves were closed to prevent the lines from being filled, and the fill valve of the tank opened to allow the propellant to be pumped into the tank. Once the fill procedure was complete, the fill valve was closed and the isolation valve opened when the test was ready to proceed. Each valve was capable of being padlocked to prevent opening, and as such the valves functioned as security lock outs for the system when the facility was not in use.

Figure 4.8: Installed propellant run tank panel

4.2.3 Rocket Engine Connections

The rocket engine propellant supply connection schematic is shown in Figure 4.9[55].
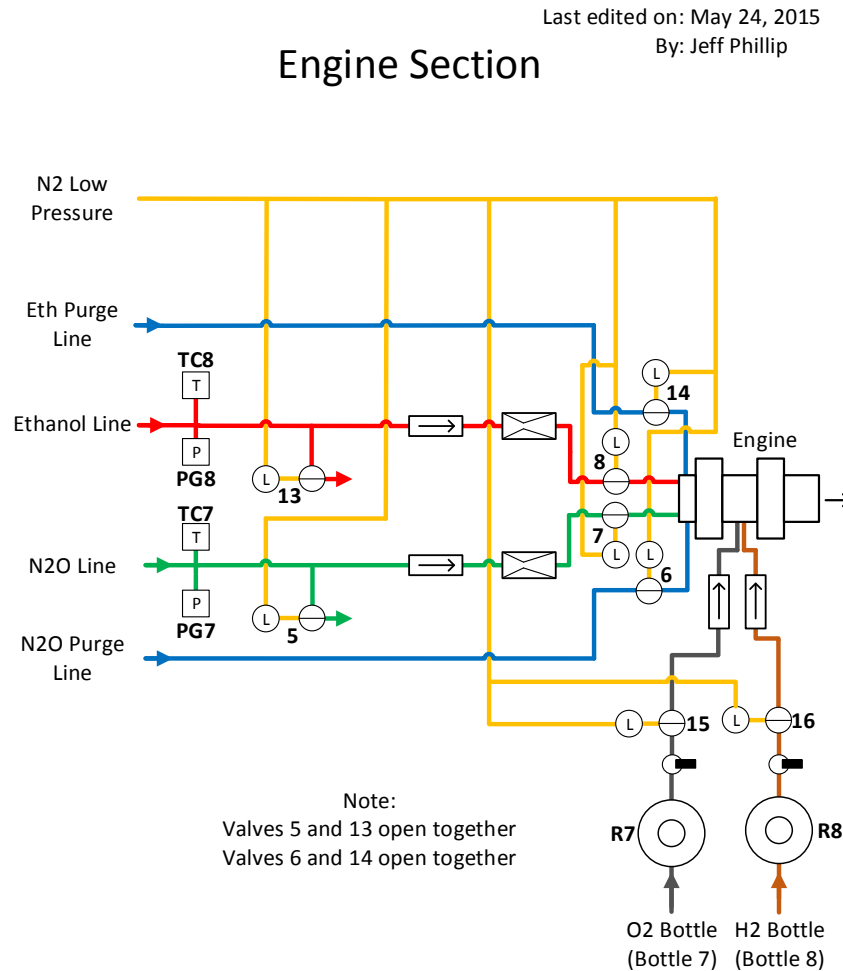
Figure 4.9: Rocket engine connection schematic

Propellant supply and purge lines were connected to the rocket engine using tee fittings. Connected to the tee fitting were the main run valves (7, 8) and engine purge valves (6, 14). The main run valves supplied the propellant while the purge valves supplied high pressure nitrogen to blow out the engine. To secure both the main run valves and purge valves, a bracket was installed that

directly supported the valves off the back of the injection manifold. The main run valves and purge valves were connected to the propellant system lines using flex lines to minimize interference with thrust measurements.

Each propellant line was equipped with a vent valve (5, 13) to allow depressurization and purging of the lines. The nitrous oxide line was vented outside of the test cell, and the ethanol line was vented to a containment vessel to recover the ethanol. To simplify operation, the purge valves (6, 14) were actuated together as were the line vent valves (5, 13).

The igniter was supplied gaseous hydrogen through regulator R8, and gaseous oxygen through regulator R7. Gas flow to the igniter was controlled by valves 15 and 16. As with the main run and purge valves, flex lines were used for connecting the igniter to the O_2 and H_2 supply lines.

The cavitating venturis were connected to the proepllant lines using AN thread fittings. To protect the venturis in the event of explosive engine failure, the venturis were installed directly behind the thrust plate to provide shielding. For making propellant mass flow rate calculations through the venturis, propellant temperature and pressure were required to be known upstream of the cavitating venturi. For measuring the state of the nitrous oxide flow, temperature was measured using thermocouple TC7 and pressure was measured using pressure transducer PG7. For measuring the state of the ethanol flow, temperature was measured using thermocouple TC8 and pressure was measured using pressure transducer PG8.

A rear view of the final propellant supply connections to the engine is shown in Figure 4.10. Visible are the hydrogen and oxygen gas cylinders for the igniter. A side view showing the final connections made to the the rocket engine is shown in Figure4.11.

Figure 4.10: Rear view of rocket engine connections

Figure 4.11: Side view of rocket engine connections

4.2.4 Propellant Handling

When designing the propellant loading system for filling the system run tanks, operator safety was of primary concern. To minimize operator risk, the loading of the propellant tanks was handled via remote operated pumps. While the operator was required to physically connect the pumps to the propellant storage vessels and operate the run tank fill valves to the,the most dangerous operation was the actual pumping of propellants into the tanks, for which the operator would command from the control room. The full operational procedure for loading propellants into the propellant supply system can be found in Appendix B.2.

For measuring the amount of propellant loaded into the system, a floor scale was utilized to measure the mass difference of the propellant storage vessels during the loading process. The scale reading was remotely observed from the control room. The nitrous oxide for the system was stored in a standard nitrous oxide gas cylinder that was inverted to allow the liquid nitrous oxide to be pulled from the cylinder. The cylinder was secured to the scale using a specially designed stand and secured in place using chains for safety, as shown in Figure 4.12.

The ethanol for the system was stored in a properly labeled 3.78L (1gal) container. This container was stored in the control room in a flammable cabinet. When the ethanol was to be loaded into the system, the operator would carry the container into the fuel galley, place on top of the nitrous oxide source cylinder, and connect the pump, as shown in Figure 4.13. The pump used for transferring the ethanol was a automotive fuel pump designed for ethanol used. After the ethanol had been loaded into the system, the container would be removed. This was done for safety to minimize the amount of fuel present in the fuel galley during system operation.

Figure 4.12: Inverted nitrous oxide source cylinder installed in fuel galley

For loading of the nitrous oxide into its respective run tank from the nitrous oxide source cylinder, a Holly compressed gas, nitrous oxide pump (P/N: 14251NOS) was used. For safety, the hoses and fittings were oxygen cleaned per the procedure discussed in Section 4.6. The pump was supplied compressed
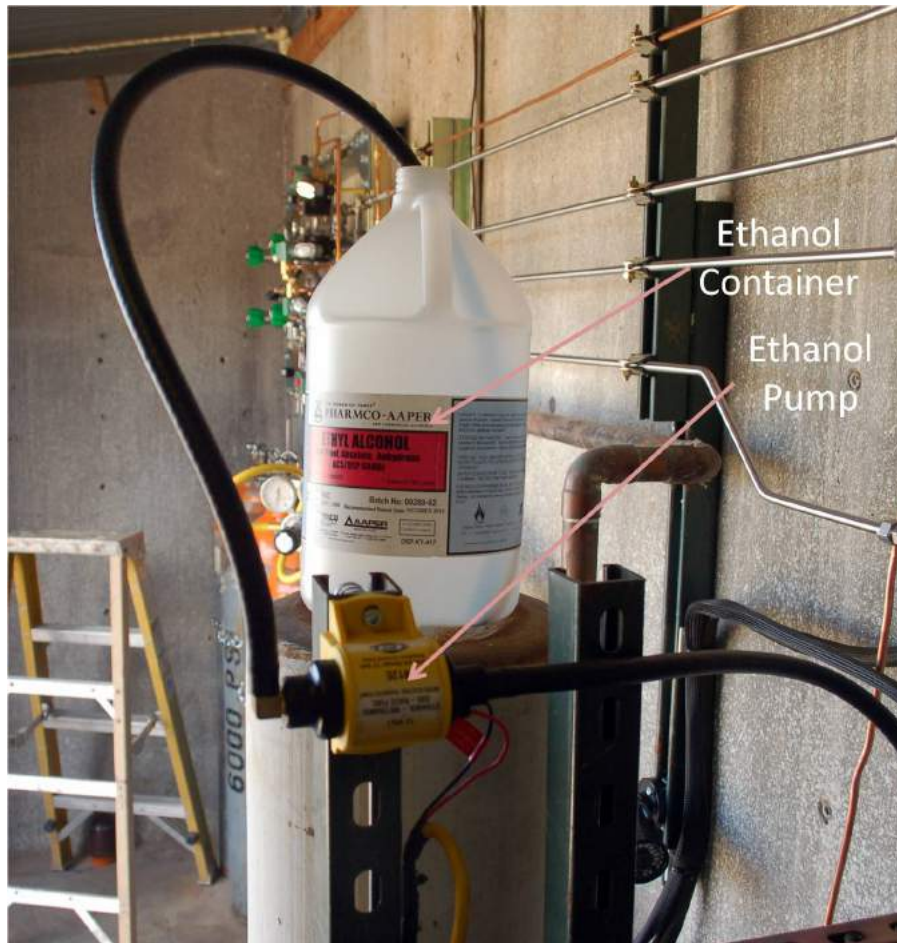
Figure 4.13: Ethanol pump connected to ethanol source container

nitrogen for operation from the low pressure nitrogen supply used by the gas actuated valves. Figure 4.14 shows the installed Holly pump.

Figure 4.14: Holley nitrous oxide pump installed

4.3 Control System Design

4.3.1 Labview Control and Data Acquisition

REF utilized a National Instruments (NI) based system for system control and data acquisition. This NI hardware system was interfaced to a computer command console using NI's Labview software. The Labview control system was designed to provide:

1. Operator control of the REF systems and operation of rocket engine.

2. Provide quick visual indication of status of system to include pressure and temperatures of propellant supply system and engine.

3. Handle data acquisition and save collected data to file.

To allow expandability for future research, a NI cDAQ-9188 Ethernet chassis was used. This chassis was capable of interfacing with up to eight data processing and control modules. For operating the rocket engine and supply system, four, four channel relay modules were used. These modules were used to power the three-way solenoids valves for controlling valve operation as well as supply power to the spark generation system for the igniter.

System pressure was monitored using Transducers Direct sourced, 20ma current pressure transducers (P/N: TD1000). These were interfaced with a NI9203 module. The NI9203 was an eight channel current sensing analog measurement module capable of up to 200,000 samples per second for a single channel. Current sensing pressure transducers were selected to minimize noise present in the data signal. All propellant supply system pressures were monitored using this module. Engine chamber pressure is currently monitor with this module, but future work will exchange the current sensing pressure transducer for a full bridge pressure transducer.

For monitoring system temperature, Type-K thermocouples were interfaced with a NI9213 module. The NI9213 module was a sixteen channel, thermocouple analog sensing module capable of up to 75 samples per second per channel. Of the the sixteen channels, four channels are used for monitoring the propellant states in the supply system, with a fifth channel used for recording rocket engine temperature data during operation. To provide for future system expansion, five additional thermocouples data lines were connected to the module for test cell temperature measurements. These lines are currently not used.

Thrust output of the engine was measured using a WMC-500 full-bridge force transducer manufactured by Interface Force. The WMC-500 was capable of measuring up to 226.8N (500lbs) of force, and was paired with a NI9237 module. The NI9237 module was a four channel full-bridge and half bridge force transducer module capable of 50,000 samples per second per channel. Table 4.1

Table 4.1: National Instruments data acquisition system overview

System	Description	Quantity
cDAQ-9188	8 slot Ethernet Module Chassis	1
NI 9203	8 Channel, Pressure Transducer 20ma Current Reader	1
NI 9213	16Cchannel, Thermocouple Reader	1
NI 9237	4 channel, Full Bridge Transducer Reader	1
NI 9482	4 channel, Relay Control	4

Figure 4.15: Installed cDAQ-9188 control and data acquisition system

summarizes the DAQ system components. The installed and wired cDAQ-9188
is shown in Figure 4.15

The Labview control interface was designed to be intuitive and system sta-
tus easily visualized. The system pressures and temperatures were displayed in
common gauge formats, and warning lights were incorporated to alert the oper-
ator of an over-pressure or unsafe temperature event in the system. In addition,

73

thrust output of the engine was displayed in real time. For added safety, certain command buttons were locked when other operations were occurring or certain commands had not been made. For example,the fire button was designed to be locked out when the system was not armed. Beyond firing the rocket engine and providing real time system status, the Labview command interface capabilities include:

1. Manual control of individual valves.

2. Automatic valve sequencing to test for function and clear lines.

3. Automated, timed propellant line fill procedures.

4. Ability to turn on or off saving of acquired data.

The Labview command interface is shown in Figure 4.16
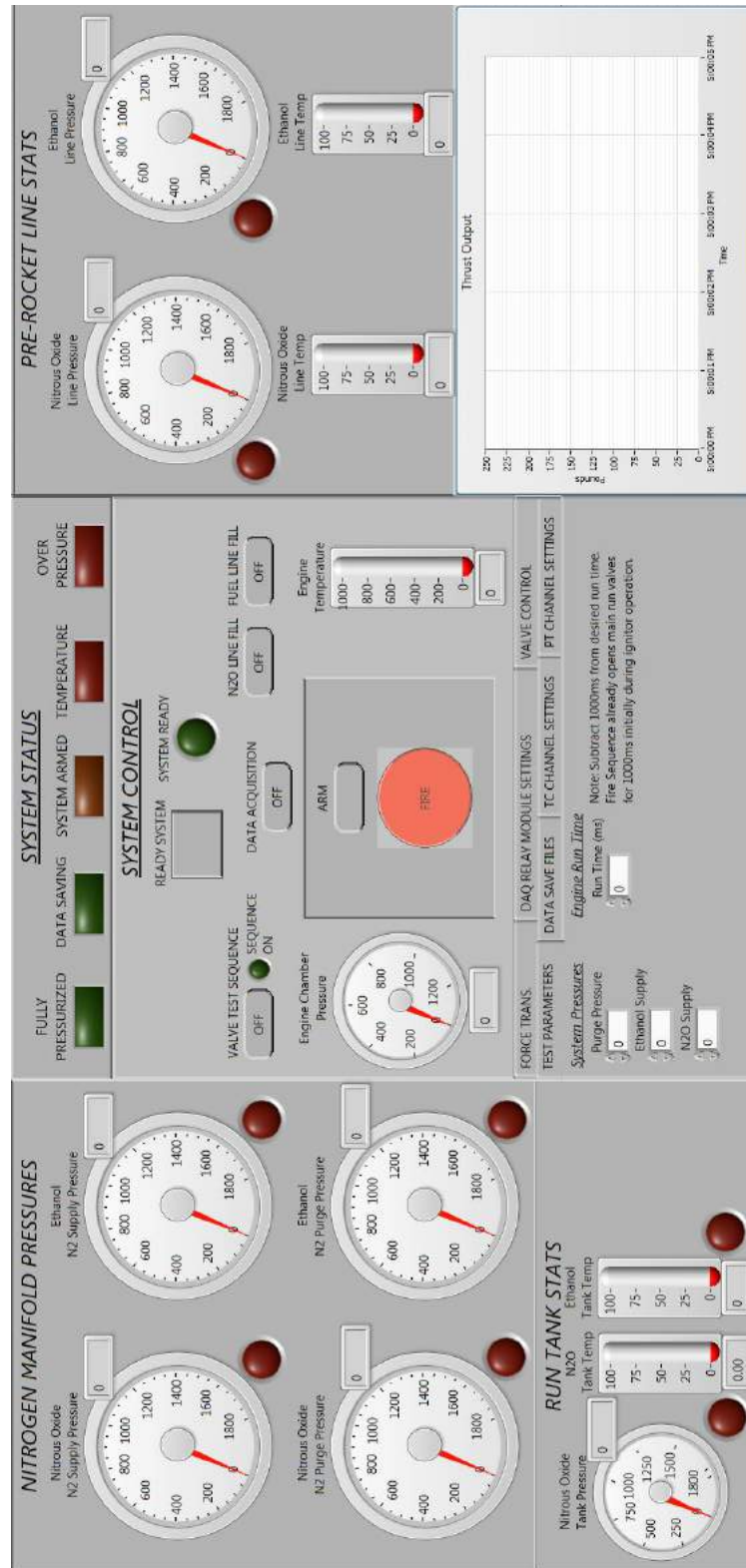
Figure 4.16: Labview computer control interface

4.3.2   Control Wiring

The control wiring installed at REF consisted of two data line bundles and one control line bundle. The data line bundles installed included an eight thermocouple line bundle and a fifteen line transducer bundle. The control line bundle installed consisted of seventeen control lines. The date bundles were shielded and grounded at the control console to minimize interference of the data signals. To protect the control and data wiring, liquid-tight metal conduit was used. Because the installation of wiring within conduit made the addition of future lines difficult, extra sensor lines and control lines were included in the installation to allow system expansion. Specifically, five extra thermocouple, three extra transducer, and one extra control line were included in the final design. Valve and sensor connections in the fuel galley and test cell were made in liquid-tight, NEMA-6 rated junction boxes, and cabling to valves and sensors was passed through liquid-tight fittings.

For making connections in the fuel galley and test cell junction boxes, DIN-rail connections blocks were used. The use of the DIN-rail blocks provided secure connections for the wiring as well as access to wire connections. To maintain accessible wire identification for troubleshooting and future modifications, all wiring was numbered. For the control wiring, the wire number directly corresponded to the number of the valve controlled. Figure 4.17 shows the structuring of the fuel galley junction box.

Figure 4.17: Fuel galley junction box

The reasons for using liquid-tight conduit and making connections in liquid-tight junction boxes was not only to protect the wiring from the elements, but also to minimize exposure of wiring to possible combustible environments. Ideally, explosion proof boxes and conduit would have been used, but these options were not budget permitted.

4.3.3 Control Room

The REF control room had a command console installed to house the facilities control and data acquisition systems as well as safety and facility observation systems. The use of the command console for housing the systems was invaluable as it provided a permanent location for which the systems could be installed and wiring organized.

Facility monitoring not handled by the NI DAQ included:

- Remote video observation. Observation included fuel galley, test cell, test pad, propellant loading scale, and a pan tilt camera for observing the area surrounding REF. The remote video observation system provided recording capability for safety during the operation of the facility..

- Fuel Galley Temperature.

- Remote weather station. The station provided wind and temperature conditions as well as barometric pressure and humidity.

- Igniter supply voltage. Used as visual safety indicator that the system is not able to be fired.

- Valve powered status indicator panel

The command console included a deadman's switch, which was a safety feature used to provide immediate termination of the test if the operator's hand was removed from the switch. It functioned by requiring the operator to depress the switch during the period the system was armed for rocket engine operation, and in the event the operator no longer depressed the switch, power was cut to the valves. This resulted in the propellant supply system purging itself and returning to an inert state. In order to arm the system by supplying power to the igniter circuits, the deadman's switch must first be pressed and held before the arm switch can be turned. The deadman's switch can be seen to the left in Figure 4.18.

A panel was constructed with a simplified system diagram for providing visual indication of power status to valves. A red light indicated a valve was in the closed position, and a green light indicated a valve was in the opened position. This indicator panel only indicates valve status by power supplied, and does not directly indicate the actually valve status via position sensors. Figure 4.19 shows the valve indicator panel.

Figure 4.18: REF control console. Visible are: Deadman's switch (#1); Fuel galley temperature monitoring (#2); Igniter supply voltage (#3); Video observation system (#4); Weather station (#5); Valve status indicator panel (#6); Propellant loading controls (#7); and system power supplies (#8)
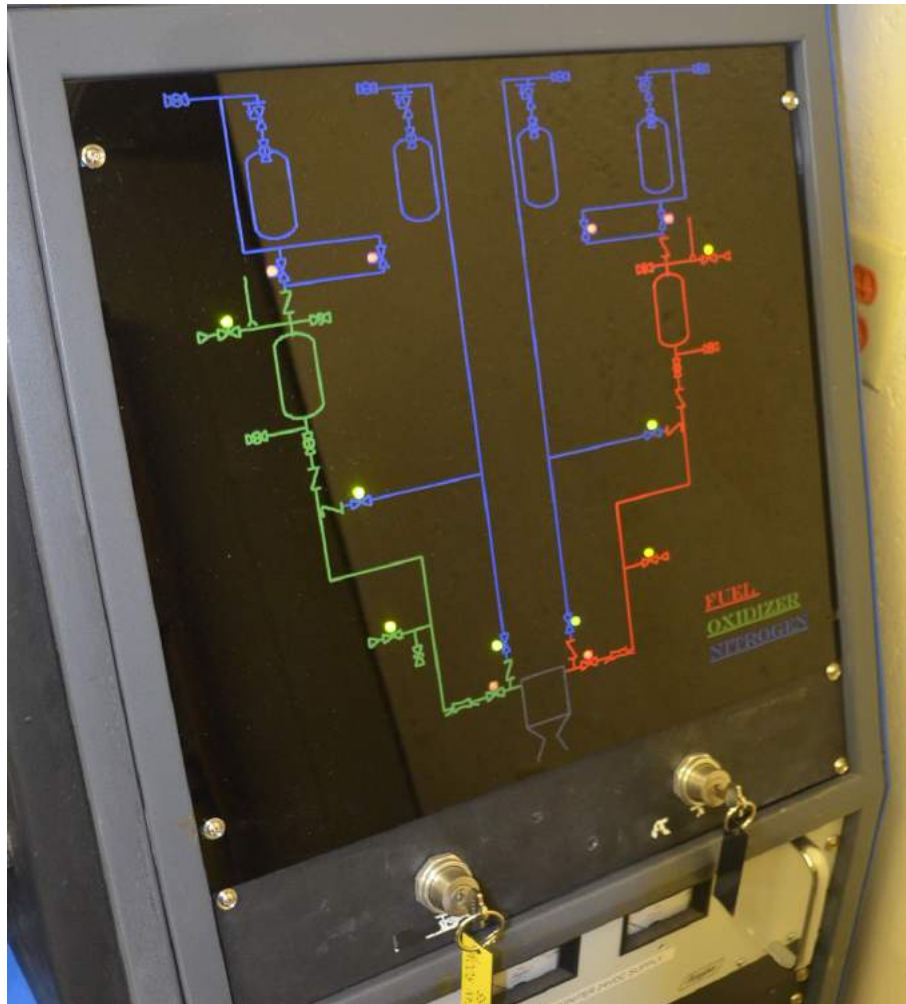
Figure 4.19: Valve status indicator panel

4.4 Safety and Explosive Hazards

For safety, the TNT equivalences of the energetic materials present on site were estimated. These values were important in establishing the required clearance distance around the facility for testing. The primary concern was for the nitrous oxide present on site, which was what was considered to be the most likely source of a major explosive event. A worst case scenario was theorized such that the decomposition event of the nitrous oxide in the run tank would lead to a chain reaction of system failures in the fuel galley. The worst case failure scenario is outlined below:

1. Decomposition of liquid nitrous oxide in a full run tank.

2. Decomposition event in run tank leads to explosive decomposition event in liquid nitrous oxide supply cylinder.

3. Decomposition event in nitrous oxide supply cylinder leads to explosive failure of the nitrogen supply tanks in the fuel galley.

While this chain of events was considered incredibly unlikely, it was used as the bases for absolute worst case scenario. In addition to the above failure scenario, a TNT equivalence was estimated for rocket engine failure due to overpressurization as well as the gas energy release from the hydrogen and oxygen cylinders.

Two forms of energy release were considered: the energy release from the compressed gas within the failing vessel; and the energy release from the reacting material contained within the vessel. For the nitrogen supply tanks, rocket engine, and hydrogen and oxygen cylinders, the primary release of energy was assumed to be from the explosive release of the contained compressed gas. For the nitrous oxide run tank and supply cylinder, the total energy release was assumed to be a combination of the energy released from the decomposing nitrous oxide as well as the stored compressed gas energy with in the cylinders.

For calculating the energy release for the stored compressed gas, the availability method described by Crowl was used [45]. The energy release was described by Equation 4.2, where V_{tank} is the volume of the storage tank.

$$E = P_{tank} * V_{tank} * \left[ln \left(\frac{P_{tank}}{P_{atm}} \right) - \left(1 - \frac{P_{atm}}{P_{tank}} \right) \right] \tag{4.2}$$

To solve for the energy released from the decomposition of nitrous oxide, it was assumed that the nitrous oxide fully decomposes irreversible:

$$N_2O \ \rightarrow \ N_2 \ + \ \frac{1}{2}O_2 + 82.05 \frac{KJ}{mol} \tag{4.3}$$
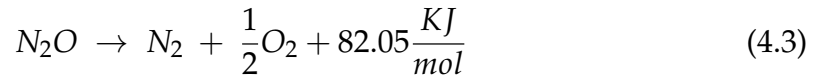
TNT equivalence was estimated by comparing the energy release of the explosive event to the energy release for 1kg (2.2lbm) of TNT. This was done using Equation 4.4 assuming $E_{TNT} = 4850KJ/Kg$ [35].

$$W_{TNT} = \frac{E_{event}}{E_{TNT}} \tag{4.4}$$

The estimated TNT equivalences for the events described above were:

1. Full nitrous oxide run tank: 2.2kg (4.85 lbm)

2. Nitrous oxide supply cylinder: 24kg (53 lbm)

3. High pressure nitrogen supply (four 41.3MPa(6000psi) tanks): 29kg (64 lbm)

4. Low pressure nitrogen supply (one 20.68MPa (3000psi) tank): 3.62kg (8 lbm)

5. Rocket engine failure (Operating at 11.72MPa (1700psi)): 0.005kg (0.012 lbm)

6. Oxygen cylinder: 3.62kg (8 lbm)

7. Hydrogen cylinder: 3.62kg (8 lbm)

The resultant TNT equivalance of all energetics on-site was found to be 146lbs of TNT, well within the TNT rating of the facility of 1100lbs.

4.5   Operation Protocols

For successful and safe operation of REF, detailed operation protocols were created to govern the operation of the facility. These protocols provided detailed operation instructions for:

- Start of day facility preparation and system checks

- Propellant Loading

- Rocket Engine Operation

- Render safe procedures for end of testing

- End of Day facility Shutdown

- Response procedures to accidents and system failure

These protocols were combined into a operating procedure list. The operating list includes a cover sheet which documents system run settings, including supply pressures, propellant masses, and environmental conditions. For each test, a new operating procedure list was used and filled out appropriately. At the end of the tests, the operating procedure list was saved as a test record in the control room. The full operating procedure list can be found in Appendix B.3.

81

4.6 Oxygen Cleaning Methods

A need for oxygen cleaning capabilities was required during the construction of REF. The goal was to produce adequate cleaning methods of parts to meet oxygen service standards. Through research, it was found that oxygen cleaning was primarily performed using ultrasonic cleaning, solvent washes, and visual inspection of the components to detect the presence of hydrocarbons and particles of unacceptable size[41].

The primary resource for developing the oxygen cleaning procedures used at REF was a service document produced by the Compressed Gas Association, Inc (CGA) titled *Cleaning Equipment for Oxygen Service*[41]. The document is now considered obsolete by the CGA. However, the methods described were compared against recommendations by the EIGA and AIGA and found that the procedures detailed by the CGA document were still applicable for providing acceptable results [38][51][39]. An oxygen cleaning procedure was developed that utilized available equipment and off the shelf solvents. The procedures involved: ultrasonic cleaning of parts in an acetone solvent bath, flushing the parts with trichloroethylene, and finishing with an acetone flush. The part was then visual inspected under bright white light and UV light to identify particles and hydrocarbons still present. The detailed cleaning procedure can be found in Appendix B.4.

CHAPTER 5

EXPERIMENTAL RESULTS

5.1 Experimental Uncertainty

When operating the rocket engine, multiple data measurements were taken that were used for both system monitoring and engine performance analysis. While the data collection was handled by a computer based control system, helping to minimize human error, each instrument had a systemic uncertainty associated with it. It was therefore important to quantify the uncertainty of the measurements to evaluate the relevance and importance of the data collected. Before the experimental data gathered from the rocket engine was processed, a brief review of the associated uncertainty of the measurements was made.

While multiple measurements were taken of the rocket engine and throughout the propellant supply system, there were six measurements that were of particular importance:

- Nitrous oxide temperature upstream of the cavitating venturi.

- Nitrous oxide pressure upstream of the cavitating venturi.

- Ethanol temperature upstream of the cavitating venturi.

- Ethanol pressure upstream of the cavitating venturi.

- Rocket engine chamber pressure.

- Rocket engine thrust output.

The measurements of the propellant states were used for calculating the mass flow rate of propellant supplied to the engine. These measurements were therefore also important in calculating specific impulse and performing comparison work using the computational model discussed in Chapter 2.

The pressure transducers, thermocouples, force transducer, and cavitating venturis all had manufacturer specified measurement uncertainties. The uncertainty of the polynomials used for calculating the ethanol properties where provided by the sources[56][20]. For the nitrous oxide polynomials, the uncertainty was estimated using Equation 5.1 and the resolution of the tabulated data provided by the source[22].

$$\Delta Q = \pm \frac{Q_{Resolution}}{2} \tag{5.1}$$

The uncertainty associated with the pressure transducers, thermocouples, force transducer, cavitating venturi and polynomial fits are presented in Table 5.1.

Table 5.1: Measurement device and estimated polynomial uncertainty

	Uncertainty	Units
Pressure Measurements (TD1000)	$\pm 0.05\ (\pm 7.5)$	$MPa\ (psi)$
Temperature (Type K Thermocouple)	$\pm 2.2\ (\pm 3.96)$	$^{\circ}C\ (^{\circ}F)$
Thrust Measurement (WMC500)	$\pm 3.33\ (\pm 0.75)$	$N\ (lbf)$
Calibrated Cd	± 0.1	$\%$
Density Polynomial, Ethanol	± 0.5	$\%$
Vapor Pressure Polynomial, Ethanol	± 1.24	$\%$
Density Polynomial, N2O	$\pm 0.05\ (\pm 0.062)$	$kg/m^3\ (lbm/ft^3)$
Vapor Pressure Polynomial, N2O	$\pm 0.0005\ (\pm 0.072)$	$MPa\ (psi)$

The mass flow rate of propellant as a function of time is calculated using Equation 3.4 and repeated here:

$$\dot{m} = A_t * C_d \sqrt{\frac{2g\rho}{144}(P - P_v)} \tag{5.2}$$

The uncertainty of an analytical equation is a function of the uncertainty associated with each independent variable present in the equation. For an arbitrary function, represented by Equation 5.3, the propagated uncertainty can be estimated using Equation 5.4.

$$Q = f(x, y, ...) \tag{5.3}$$

$$\Delta Q = \sqrt{\left(\frac{\partial f}{\partial x}\Delta x\right)^2 + \left(\frac{\partial f}{\partial y}\Delta y\right)^2 + ...} \tag{5.4}$$

Experimentally determined pressure and temperature measurements of flow states upstream of the venturi were used for calculating the vapor pressure (P_v) and density (ρ) of the propellants using the polynomial fits[22][20][56].

By inspection of Equation 5.2, the uncertainty associated with the calculations for mass flow rate through a cavitating venturi is a function of:

- Polynomial fits used for making fluid property calculations ($\Delta \rho,\ \Delta P_v$) .

- Experimental data used (ΔP)

- Coefficient of discharge (ΔC_D)

- Measurement of venturi throat diameter (ΔD_t).

This conclusion was supported by work performed by Helderman[28]. The analytical uncertainty equation for the mass flow rate through a cavitating venturi, $\Delta \dot{m}$, can be derived by combining equation 5.2 with 5.3. The estimated uncertainty for mass flow rate takes the form seen in Equation 5.5.

$$
\Delta \dot{m} = |\dot{m}| \left[\left(2\frac{\Delta D_t}{D_t} \right)^2 + \left(\frac{\Delta C_D}{C_D} \right)^2 + \left(\frac{\Delta \rho}{2\rho} \right)^2 + \left(\frac{\Delta P}{2(P-P_v)} \right)^2 + \left(\frac{-\Delta P_v}{2(P-P_v)} \right)^2 \right]^{\frac{1}{2}} \quad (5.5)
$$

The total mass flow rate and mixture ratio uncertainties are a function of the uncertainty of the mass flow rate of fuel and mass flow rate of oxidizer. Using the same solution process applied for the mass flow rate uncertainty derivation, the resultant equations are shown in Equation 5.6 and Equation 5.7, respectively:

$$
\Delta \dot{m}_{tot} = \sqrt{\Delta \dot{m}_{fuel}^2 + \Delta \dot{m}_{oxidizer}^2} \quad (5.6)
$$

$$
\Delta MR = |MR| \sqrt{ \left(\frac{\Delta \dot{m}_{fuel}}{\dot{m}_{fuel}} \right)^2 + \left(\frac{\Delta \dot{m}_{oxidizer}}{\dot{m}_{oxidizer}} \right)^2 } \quad (5.7)
$$

With the mass flow rate known and using experimental determined thrust output of the engine, specific impulse can be solved using Equation 5.8.

$$
I_{sp} = \frac{F}{\dot{m}_{total} g} \quad (5.8)
$$

The uncertainty equation for ISP was derived using the same method and is shown in Equation 5.9. The derivations for Equations 5.5, 5.6, 5.7, and 5.9 can be found in Appendix C.1.

$$
\Delta ISP = |ISP| \sqrt{ \left(\frac{\Delta F}{F} \right)^2 + \left(\frac{\Delta \dot{m}}{\dot{m}} \right)^2 } \quad (5.9)
$$

The uncertainty for calculated mass flow rate, mixture ratio, and specific impulse for experimental testing was estimated as the uncertainty associated

with the predicted engine design condition of 0.22kg/s (0.5lbs/s) total propellant flow rate and a mixture ratio of 4.5. These uncertainties will be applied to the tests discussed in the following section. This decision was based on the rocket engine operation during the tests being near the design condition. Table 5.2 shows the design condition assumptions for initial conditions used for calculating the uncertainties. Table 5.3 shows the calculated uncertainties that will be applied to the experimental test results.

Table 5.2: Initial design condition test parameters and predicted engine performance for calculating uncertainties

Test Parameter	Value	Units
N2O Line Temperature	21.1 (70)	$°C$ $(°F)$
N2O Line Pressure	9.17 (1330)	MPa (psi)
Ethanol Line Temperature	21.1 (70)	$°C$ $(°F)$
Ethanol Line Pressure	8.34 (1210)	MPa (psi)
Desired Mass Flow Rate	0.22 (0.5)	kg/s (lbm/s)
Desired Mixture Ratio	4.5	-
Model Predicted Thrust	583 (131)	N (lbf)
Model Predicted ISP	261	s

Table 5.3: Calculated uncertainties and reported uncertainties for mass flow rates, mixture ratio, ISP, and experimental measurements

Test Parameter	Calculated	Reported	Units
Calculated Mass Flow			
Nitrous oxide	0.0029 (0.0065)	±0.003 (±0.007)	$kg/s(lbm/s)$
Ethanol	0.00149 (0.0033)	±0.002 (±0.004)	$kg/s(lbm/s)$
Total	0.0033 (0.0073)	±0.004 (±0.008)	$kg/s(lbm/s)$
Calculated Mixture Ratio	0.1818	±0.2	-
Calculated ISP	4.11	5	s
Experimental Measurement	Manuf. Specified	Reported	
Pressure	±0.05 (±7.5)	±0.06 (±8)	MPa (psi)
Thrust	±3.33 (±0.75)	±4 (±0.8)	N (lbf)

    For comparison purposes, the maximum known uncertainty was applied to each value and the mass flow rate, mixture ratio, and ISP are calculated. The results were checked to see if they fell within the bounds calculated via error propagation. The calculated results for maximum uncertainty are presented in Table 5.4. The derived uncertainty with values presented in Table 5.3 was applied to the test case and the results presented in table 5.5.

Table 5.4: Calculated maximum uncertainties for mass flow rates, mixture ratio, and ISP

Test Parameter	Max	Min	Units
Calculated Mass Flow			
Nitrous oxide	0.192 (0.424)	0.182 (0.401)	$kg/s(lbm/s)$
Ethanol	0.043 (0.095)	0.039 (0.086)	$kg/s(lbm/s)$
Total	0.235 (0.518)	0.221 (0.487)	$kg/s(lbm/s)$
Calculated Mixture Ratio	4.67	4.49	-
Calculated ISP	267	254	s

Table 5.5: Calculated values with derived uncertainties for mass flow rates, mixture ratio, and ISP

Test Parameter	Max	Min	Units
Calculated Mass Flow			
Nitrous oxide	0.188 (0.416)	0.182 (0.402)	$kg/s(lbm/s)$
Ethanol	0.043 (0.095)	0.039 (0.087)	$kg/s(lbm/s)$
Total	0.230 (0.508)	0.223 (0.492)	$kg/s(lbm/s)$
Calculated Mixture Ratio	4.7	4.3	-
Calculated ISP	266	256	s

By inspection of the results shown in Tables 5.2 and Table 5.3, it can be observed that not all values using the maximum uncertainty method are within the bounds of the calculated uncertainty using the error propagation method. However, the values are either contained or just slightly out of the the bounds of error propagation. This is not surprising as the application of carrying the maximum uncertainty should yield a "worse" case scenario, and supports the use of the uncertainties calculated using error propagation as appropriate.

5.2 Testing Summary

The first successful test fire of the rocket engine at REF took place on March 25, 2015. In total, seven test firings of the engine have been conducted using liquid nitrous oxide and ethanol as propellant. Operational parameters for the seven tests were chosen to be near the design condition of a total propellant flow rate of 0.22kg/s (0.5lb/s) at a mixture ratio of 4.5. For all but one test firing, 99.9% pure ethanol was used. 95.5% pure ethanol was used for a single test due to the unavailability of 99.9% pure ethanol at the time.

Figure 5.1 shows the operation of the rocket engine during a test. This image was taken during steady state operation of the engine, approximately eight seconds after ignition had occurred.
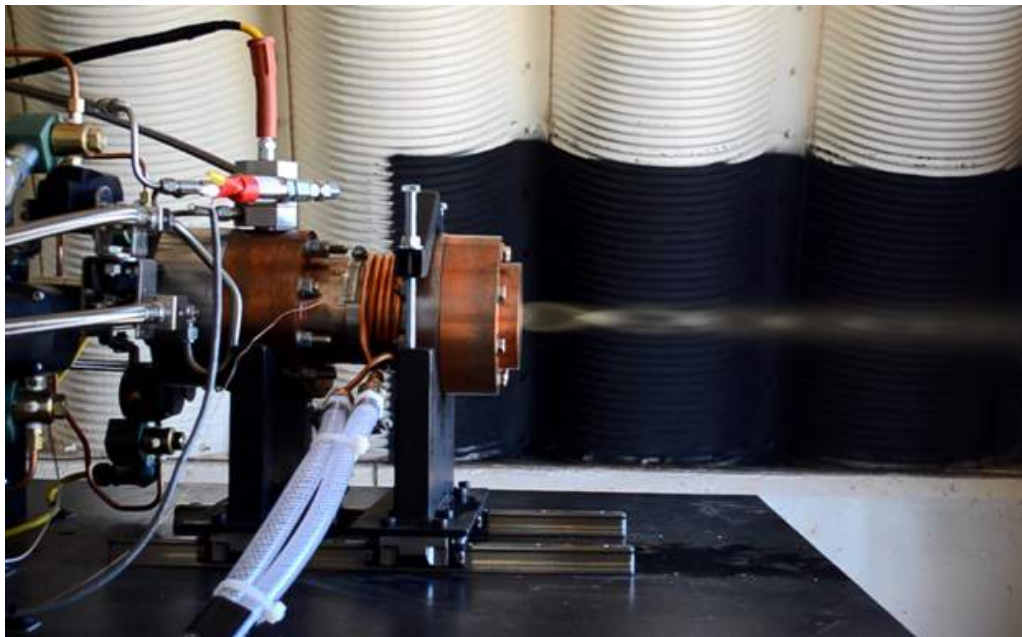
Figure 5.1: Steady state rocket engine operation during Test 5/29

Prior to the March 25th test, a cold-flow test was performed to verify proper system function. The cold-flow test conducted involved the operation of the rocket engine without ignition. For safety reasons, nitrous oxide and water were used as propellants with the nozzle unattached for the test. The cold-flow test demonstrated successful operation of the system, and test firing of the engine proceeded. The operating parameters for the cold-flow test and seven test firings are tabulated in Table 5.6.

The tabulated pressures in Table 5.6 were the desired operating pressures for the system upstream of the cavitating venturi. The desired supply pressure varied between tests due to propellant temperature conditions at the time of testing affecting the propellant density. This directly affected the predicted mass flow rate, and the supply pressures were changed accordingly to compensate.

Table 5.6: Experimental rocket engine initial test parameters

Test	Oxidizer	Fuel	Oxidizer Pressure	Fuel Pressure	Desired Flow Rate	Desired MR
			Mpa (psi)	Mpa (psi)	kg/s (lbm/s)	
3/18	N2O	H2O	1350	1350	-	-
3/25	N2O	Eth.	1365	1350	0.23 (0.52)	4.4
4/1	N2O	95% Eth.	1580	1400	0.245 (0.54)	4.2
5/21	N2O	Eth.	1345	1365	0.25 (0.55)	4.7
5/27	N2O	Eth.	1320	1300	0.24 (0.53)	4.7
5/29	N2O	Eth.	1240	1310	0.22 (0.5)	4.5
6/2 (#1)	N2O	Eth.	1360	1310	0.22 (0.5)	4.5
6/2 (#2)	N2O	Eth.	1390	1320	0.22 (0.5)	4.5

Of these seven tests, five test were found to have suffered technical failures. Despite the rocket engine actually firing for these tests, the experimental results were invalidated due to the failures. Given the new nature of of the system, technical failures were expected. These failures were used in refining the system to prevent further issue. The five tests and the associated failures are detailed in Table 5.7.

Table 5.7: Technical failures resulting in invalidation of test data

Test	Technical Failure
3/25	Data acquisition failed to record pressure and temperature data
4/1	Data acquisition failed to record pressure and temperature data
5/21	Ethanol supply line leak due to NPT fitting
5/27	Nitrous oxide supply line leak due to Swage connection
6/02 (#2)	Hard start

All failures have been resolved except for the the hard start experienced during the 6/2 (#2) test, which has prevented any further testing while repairs and revisions to the system are made (discussed in Section 5.5). A hard start refers to an over pressure condition of a rocket engine during start up. The over pressure condition is a result of too much propellant having entered the combustion chamber prior to ignition. Hard starts are not desirable as they can cause serious damage and even destroy the engine due to the rapid pressure rise.

While the propellant supply system was successful in supplying propellant to the rocket engine, it was discovered during testing that the system experienced a pressure drop during engine operation. The supply line pressure was observed to drop from the initially set pressure, resulting in a deviation from the desired propellant flow rate. This directly affected the desired operation of the

engine, making it difficult to achieve engine operation as set by the initial test parameters. Supply line pressure upstream of the cavitating venturi, for Test 5/27 is shown in Figure 5.2.
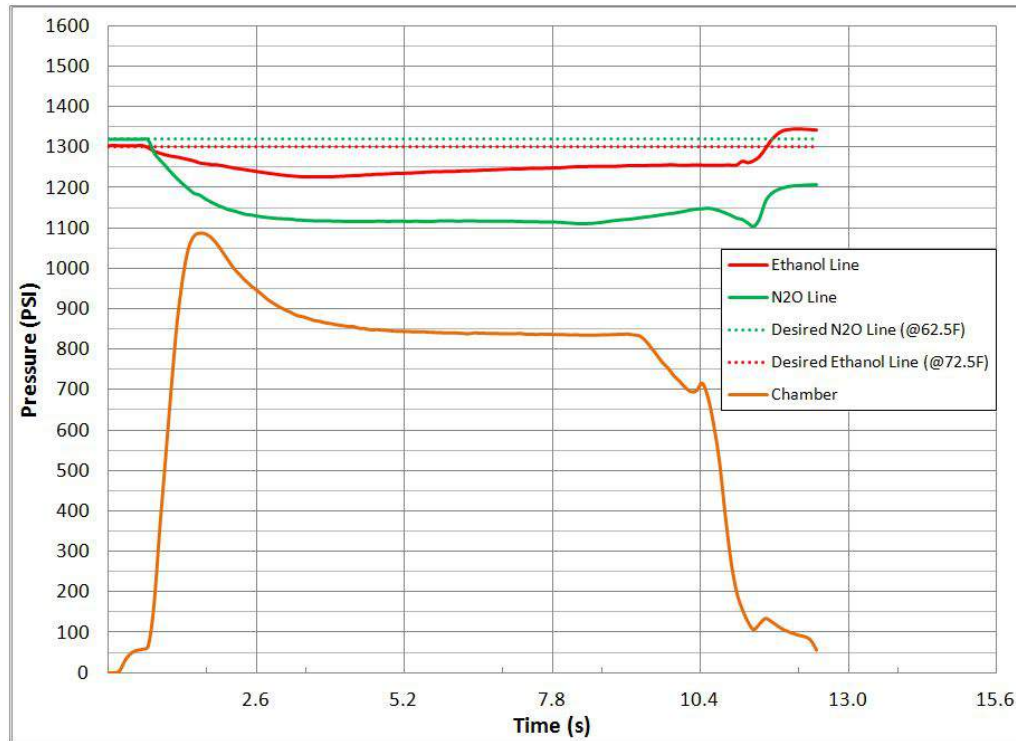
Figure 5.2: Plotted propellant supply line pressures and rocket engine chamber pressure for Test 5/27

Nitrous oxide and ethanol supply line pressures are plotted as green and red lines, respectively. The pressures to achieve the nitrous oxide and ethanol flow rates necessary for desired engine operation are plotted as green and red dashed lines, respectively. Figure 5.2 shows the pressure drop effect and the resultant supply line pressure deviation from the set pressure for achieving the desired engine performance. The deviation in supply line pressure, and consequently propellant flow rate to the engine, resulted in an initial spike in chamber pressure when the line pressure, and therefore propellant flow rate, was highest. The engine pressure spike was followed by a decrease to steady state over several seconds as the line pressure dropped and steadied, as shown by the chamber pressure trace in orange. The cause of the pressure drop was determined to be a result of the nitrogen supply bottles having a restricted flow rate at the tank valve.

To mitigate the pressure drop and obtain the desired run conditions, the supply line pressures were increased such that the supply pressure would settle near the desired pressure during engine operation. Figure 5.3 shows recorded supply and chamber pressure for Test 6/2 (#1). The desired nitrous oxide and

ethanol supply line pressures are displayed as green and red dashed lines, respectively.
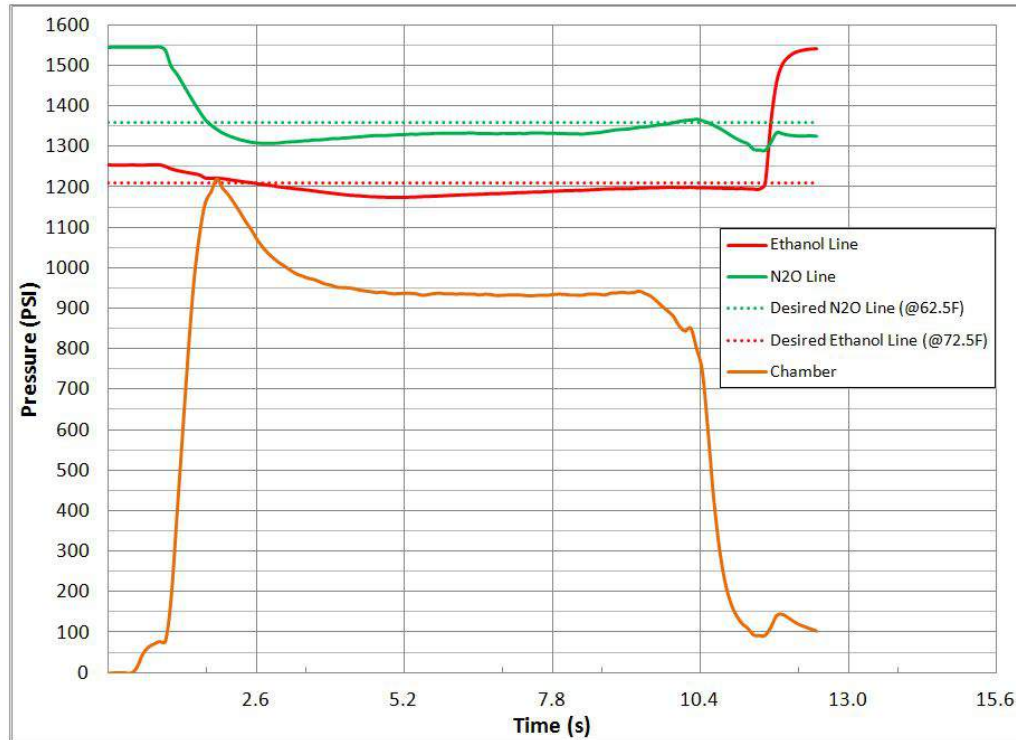
Figure 5.3: Plotted propellant supply line pressures and rocket engine chamber pressure for Test 6/2

It can be seen that that desired operating line pressures were achieved to a reasonable degree by using pressure drop estimation. For tests before Test 5/29, the recorded supply pressures in Table 5.6 were the supply pressures pre-engine operation, and did not account for the resultant pressure drop. For Test 5/29 and later, the tabulated supply pressures were the desired pressure after compensation for the pressure drop.

A consequence of this operation methodology was high chamber pressures during start up, as seen by the chamber pressure trace in Figures 5.2 and 5.3. While experimental data was able to be collected successfully, this method of operation over stresses the engine hardware and increase the possibility for a hard-start and ignition stabilization problems.

5.3 Experimental Results

For analysis, three parameters were used for evaluating the engine and propellant performance. These parameters were: thrust output, specific impulse,

and chamber pressure. These parameters were used in evaluation of the performance of the engine, propellants, and validation of computational models. While exhaust temperature would also be useful, collection of this data was not part of the data acquisition system.

An initial unsteady region of the data existed at start up of the engine, which over time would transition to steady state. The transition to steady state operation was determined by identifying a region of engine operation, at least 0.5s in length, for which the variance in chamber pressure, thrust output, and upstream propellant line temperature and pressure were less then the measurement uncertainty defined in Section 5.1.

The engine function is outlined below in Figure 5.4:
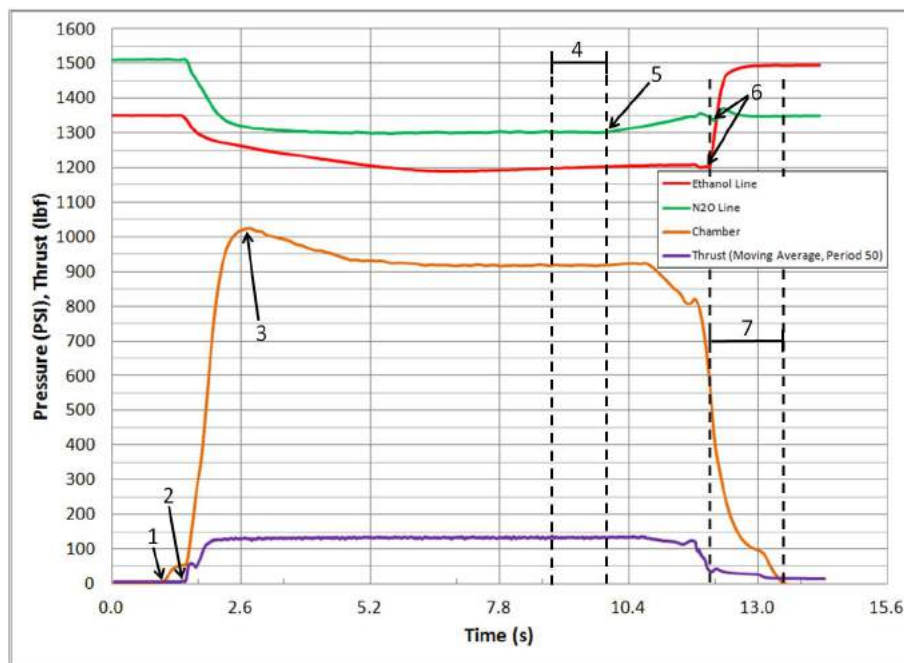
Figure 5.4: Test 5/29 rocket engine operation with plotted chamber pressure, supply line pressure, and thrust. Labeled events and regions include: Igniter initiation (#1); Propellant supply valves open, starting propellant flow to engine (#2); Chamber over-pressurization. Max chamber pressure reached indicated (#3); Steady state region of operation (#4); Liquid nitrous oxide exhuasted upstream of cavitating venturi and nitrogen flow begins through venturi (#5); Propellant supply valves close (#6); Engine shutdown period (#7).

The liquid Nitrous oxide upstream of the cavitating venturi being exhausted was an unintended operation of Test 5/29. The loss was a result of both underestimation of nitrous oxide mass lost during vent operations, and higher initial flow rates during start up as a result of the pressure drop compensation.

For comparative analysis, a portion of data from a test's identified steady state region was selected and averaged over that region's time period. For Tests 3/25 and 4/1, where pressure and temperature data were unavailable, the steady state region was approximated by thrust output only. A moving average was applied to the thrust data for all tests with a period of 50, (N), using Equation 5.10.

$$F_{t+1} = \frac{1}{N} \sum_{j=1}^{N} A_{t-j+1} \tag{5.10}$$

A represents the actual data value at time j, and F is the calculated forecasted value. The moving average was applied to help smooth the thrust data for better identification of thrust output and steady state operation.

Table 5.8 shows the averaged steady state region results for the seven tests. For tests that suffered a technical failure, data that was collected is included and data that was not is marked by a dash.

Table 5.8: Experimental engine performance results summary

Test	Calculated Flow Rate	MR	Chamber Pressure	Thrust	ISP
Units	kg/s (lbm/s)		MPa (psi)	N (lbf)	s
Uncertainty	±0.004 (±0.008)	±0.2	±0.06 (±8)	±4 (±0.8)	±5
3/25	-	-	-	536 (120.5)	-
4/1	-	-	-	524 (117.9)	-
5/21	0.210 (0.465)	4.11	5.74 (833)	525 (118.0)	255
5/27	0.203 (0.449)	3.91	5.76 (835)	514 (115.6)	259
5/29	0.230 (0.508)	4.71	6.32 (917)	592 (133.2)	262
6/2 (#1)	0.241 (0.532)	4.97	6.44 (935)	590 (132.6)	251
6/2 (#2)	0.213 (0.470)	4.36	6.47 (938)	-	-

Tests 5/29 and 6/2 (#1) were determined to be the best representative tests of engine operation based on no technical failures experienced and similar operating conditions and recorded performance. The mixture ratio and specific impulse were plotted alongside chamber pressure and measured thrust output of the rocket engine to visualize the rocket engine's performance. The experimental data sets recorded over the length of engine operation for Tests 5/29 and 6/2 (#1) are presented below in Figures 5.5 and 5.6.

Figure 5.5 shows the performance of the rocket engine for Test 5/29 operating at an average, steady-state flow rate of 0.040kg/s (0.089lbm/s) of ethanol and 0.190kgs/ (0.419lbm/s) of nitrous oxide. The average mixture ratio for this region was 4.71 ± 0.2. For these operating conditions, average thrust output of the engine was found to be $592 \pm 4N(133.2 \pm 0.8lbf)$ with an average ISP of $262 \pm 5s$.

The recorded performance for Test 6/2 (#1) is shown in Figure 5.6. The engine was found to operate at an average steady-state propellant flow rate of
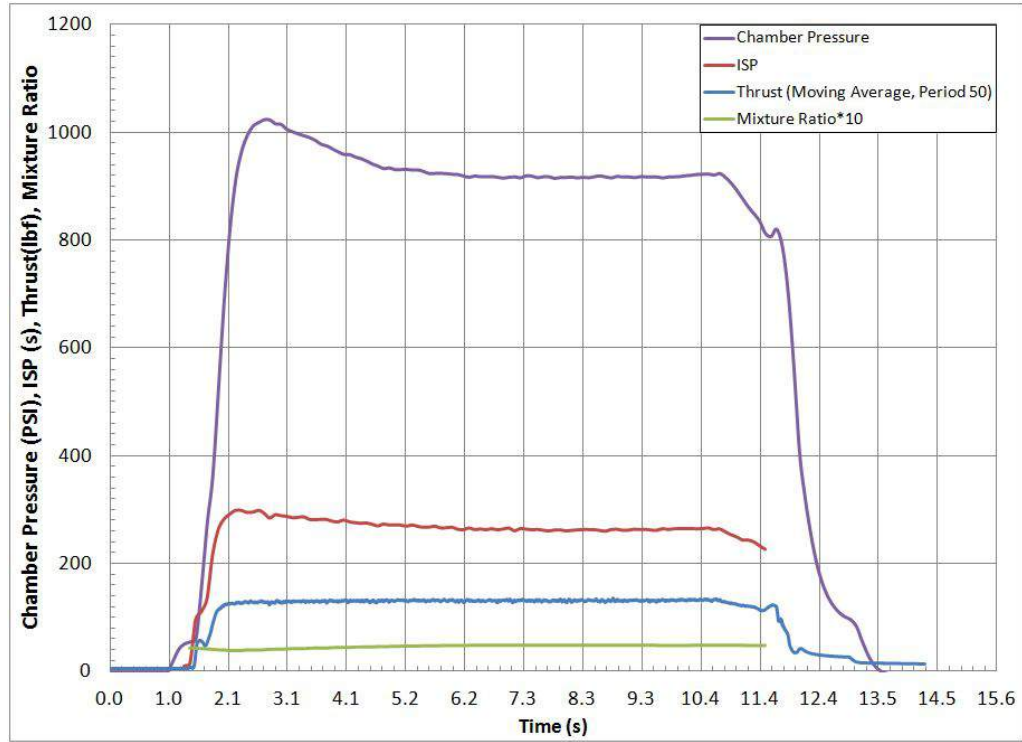
Figure 5.5: Plotted rocket engine performance for Test 5/29. Chamber pressure, ISP, thrust, and mixture ratio are plotted as a function of time. Average steady-state flow rates were 0.190kgs/ (0.419lbm/s) of nitrous oxide and 0.040kg/s (0.089lbm/s) of ethanol. The average mixture ratio for this region was 4.71 ± 0.2

0.200kgs/ (0.442lbm/s) of nitrous oxide and 0.04kg/s (0.089lbm/s) of ethanol. The average mixture ratio was 4.97 ± 0.2. For these operating conditions, average thrust output of the engine was found to be $590 \pm 4N(132.6 \pm 0.8lbf)$ with an average ISP of $251 \pm 5s$.

While the resultant experimental values were different due to differences in testing conditions, the operational characteristics for both tests followed the same trends. The determined specific impulses for Tests 5/29 and 6/2 (#1) were comparable to propellant combinations used in other engine designs, such as RP-1 and LO_2 used in and A-1 Stage Engine with a specific impulse of 262.4s for sea-level operation[47].

Tests 5/29 and 6/2 (#1) therefore demonstrated promising performance of nitrous oxide and ethanol as well as consistency in engine operation and the ability for the engine to reach steady state.

5.4 Computational Comparison

Comparison of computational predictions to experimental data were made for Tests 5/29 and 6/2 (#1), as they were considered the most representative data sets of engine operation. The averaged steady state calculated mass flow rate for each test was inputted into the MATLAB/Cantera model, and the predicted chamber pressure, thrust, and ISP were compared to the experimental values. Initial comparison of the computational predictions and experimental data produced concerning results as shown in Table 5.9. An experimental value less then the predicted computational model is indicated by negative signage.

With the ideal assumptions made in the computational model (as discussed in Chapter 2), a higher chamber pressure should have been predicted than what was recorded experimentally. This was because the model did not account for processes such as heat transfer from the combustion gas flow to the engine walls and nozzle, nor real world combustion effects such as propellant droplet vaporization and chemical kinetics. These phenomenon reduce the performance of the real engine, and therefore the model should predict higher performance
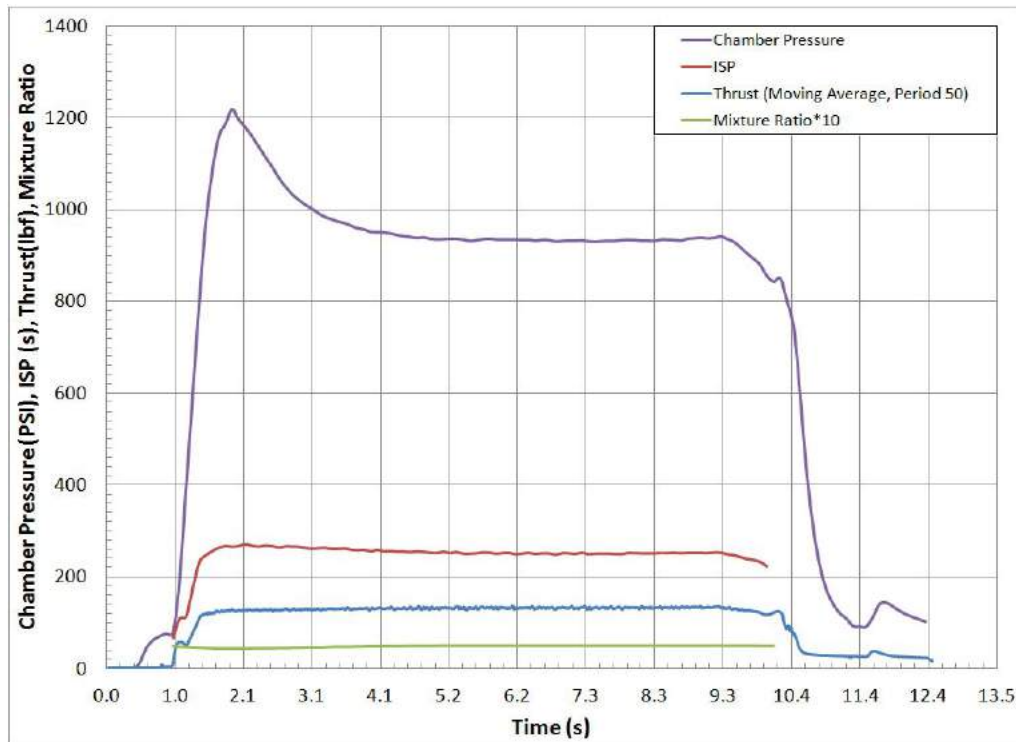
Figure 5.6: Plotted rocket engine performance for Test 6/2 (#1). Chamber pressure, ISP, thrust, and mixture ratio are plotted as a function of time. Average steady state flow rates were 0.200kgs/ (0.442lbm/s) of nitrous oxide and 0.04kg/s (0.089lbm/s) of ethanol. The average mixture ratio was 4.97 ± 0.2

Table 5.9: Initial comparative results of computational predictions and experimental engine performance

	Chamber Pressure	Thrust	ISP
Units	Mpa (psi)	N (lbf)	s
Test 5/29			
Experimental	6.32 (917)	592 (133.2)	262
Computational	5.85 (848)	593 (133.4)	262
Difference (%)	8.14	-0.60	0
Test 6/2 (#1)			
Experimental	6.44(935)	590 (132.6)	251
Computational	6.10 (885)	621.6 (139.7)	262
Difference (%)	5.65	-5.08	-4.20

then what is seen experimentally because the model is not accounting for these effects. Even when taking into account the associated uncertainty of the pressure measurements of $\pm 0.06 MPa$ ($\pm 8psi$), these result were contradictory to how the model should have performed. With the computational model's performance results supported by CEA, it was thought that the lower predictions made were related to a difference in operational conditions between the model and engine.

The MATLAB/Cantera model used the choked flow mass flow rate equation for predicting chamber pressure, shown in Equation 2.15 and repeated here 5.11. For the iteration method and the mass flow rate equation used, calculated pressure was strongly dependent on the total propellant mass flow rate and nozzle throat area. Therefore, the propellant mass flow rates and nozzle dimensions were investigated.

$$\dot{m}^* = \frac{A^* * P_O}{\sqrt{T_O}} * \sqrt{\frac{\gamma}{R}} * \left(1 + \frac{\gamma - 1}{2}\right)^{-\frac{\gamma+1}{2(\gamma-1)}} \qquad (5.11)$$

While the predicted chamber pressure deviation could have been influenced by the uncertainties of the estimated mass flow rates through the venturis, it appeared unlikely that such a large deviation could be explained by these uncertainties given their relatively small scale. It was therefore theorized that the lower chamber pressure predicted by the model was related to a difference in the throat diameter used by the model from the actual throat diameter of the rocket engine nozzle. The nozzle throat diameter had been reported to be within tolerance of the designed 8.89mm (0.35") diameter after machining, and this value was what had been used by the computational model for calculating the throat area for use in Equation 5.11.

The nozzle diameter was varied in the computational model for a single

set of experimental mass flow rates and compared to the experimental performance recorded. The computational results are shown in Table 5.10 with the actual experimental data tabulated at the bottom.

Table 5.10: Chamber Pressure comparison of nozzle throat diameters for a fixed exit diameter of 25.9mm (1.02inch), MR of 4.71, and total propellant flow rate of 0.023kg/s (0.508lbm/s). Experimental results for these conditions tabulated at bottom

Throat Diameter	Area Ratio	Mach Number	Chamber Pressure
mm (in)	-	-	Mpa (psi)
9.4 (0.37)	7.60	3.05	5.22 (757)
9.14 (0.36)	8.03	3.1	5.51 (800)
8.89 (0.35)	8.49	3.14	5.84 (857)
8.63 (0.34)	9	3.19	6.19 (898)
8.38 (0.33)	9.55	3.23	6.58 (954)
Experimental	-	-	6.32 (917)

From the results, it was determined that the nozzle throat diameter was likely between 8.38mm (0.33") and 8.63mm (0.34"). The nozzle throat was plug gauged, and found to be 8.45mm (0.333") in diameter. The computational model was updated with the corrected nozzle throat diameter and the predictions for engine performance recalculated. With the nozzle throat updated, the area ratio of the nozzle was now 9.38 instead of the 8.5 area ratio that was originally designed.

Despite the determined difference in throat diameter, the experimental results presented in the previous section are unaffected in regards to error in recording. In addition, the computational work presented in Chapter 2 is still accurate for a nozzle throat diameter of 8.89mm (0.35"). The only inaccurate data presented is in Table 5.9 for discussion purposes.

Comparison of the corrected computational predictions to experimental data for Tests 5/29 and 6/2 (#1) are reported in Tables 5.11 and 5.12. Because of concern that the ethanol used experimentally could have absorbed moisture from the air, decreasing its concentration, the ethanol was tested at EMRTC using a portable Raman spectrometer. It was found that the ethanol tested contained no more than 0.1% water, and was still within the original manufacturing specifications of 99.9% alcohol[50]. Further analysis was to be performed using a Gas Chromatography-Mass Spectrometer (GC-MS), however at the time the available GC-MS was down for repairs. Because the ethanol was found to still be approximatly 99.9%, the computational calculations were made assuming 100% ethanol as fuel based on the results from Chapter 2.

It was found that the computational model predictions compared well to the experimental data. The averaged steady state calculated mass flow rate for each test was inputted into the MATLAB/Cantera model, and the predicted chamber pressure, thrust, and ISP were compared to the averaged steady state experimental values. The model was found to predict a higher chamber pressure then experimentally found, as expected.

Table 5.11: Computational predictions compared to experimental data for a mixture ratio of 4.71, total mass flow rate of 0.230kg/s (0.508lbm/s), a nozzle throat diameter of 8.45mm (0.333"), and an area ratio of 9.38

	Chamber Pressure	Thrust	ISP
Units	Mpa (psi)	N (lbf)	s
Experimental	6.32 (917)	592 (133.2)	262
Computational	6.46 (937)	600 (134.9)	265
% Difference	-2.13	-1.26	-1.13

Table 5.12: Computational predictions compared to experimental data for a mixture ratio of 4.97, total mass flow rate of 0.241kg/s (0.532lbm/s), a nozzle throat diameter of 8.45mm (0.333") and an area ratio of 9.38

	Chamber Pressure	Thrust	ISP
	Mpa (psi)	N (lbf)	s
Experimental	6.44 (935)	590 (132.6)	251
Computational	6.74 (978)	629 (141.4)	265
% Difference	-4.70%	-5.80%	-5.28%

These results demonstrated that the developed MATLAB/Cantera model was capable of making predictions of engine performance that were comparable to real operational performance. The process and results above demonstrated that the computational model was capable of not only being used for predicting the expected performance of the rocket engine, but analyzing why the rocket engine did not perform as expected. This showed that the developed MATLAB/-Cantera model was valuable not only in design but also in trouble shooting engine operation.

5.5 System Revisions

. The hard start experienced during Test 6/2 (#2) was the result of a delayed ignition. The delayed ignition was attributed to the igniter and a failed spark plug. The rocket engine and facility were found to be undamaged except for the force transducer mount, and the engine was still able to continue operation during Test 6/2 (#2) after the hard start occurred, as seen in Figure 5.7.

Figure 5.7: Engine operation after hard start

The green hue to the exhaust had been noticed in previous test during initial start up of the engine. The green color is a result of copper from the interior of the engine combustion chamber and nozzle burning off during initial start up, and was not related to the hard start in this test.

The resultant hard start damaged the force transducer mount requiring redesign and replacement of the mount. In addition, procedure and hardware changes were made with regards to the igniter.

5.5.1 Igniter

The igniter was taken apart after the 6/02 (#2) test to determine the cause of the delayed ignition. It was found that the spark plug had failed and a portion of the ceramic insulator had fallen into the igniter combustion chamber. It was theorized that the insulator debris plugged the torch igniter tube based on debris observed in the igniter tube. This prevented the hot combustion gases from reaching the rocket engine combustion chamber at initial start up.

As a result, the igniter combustion chamber pressure rose. Once a high enough pressure was reached, the debris was forced through the torch igniter tube, igniting the propellant in the engine. The resultant delay of approximately

0.75s had allowed the rocket engine combustion chamber to fill with propellant and a plume of propellant to form outside of the engine. The combustion of the excess propellant accumulated in the chamber resulted in an over pressure of the combustion chamber and consequently the resultant thrust output overloaded the force transducer mount.

While the insulator damage could have resulted from a variety of factors, it was believed that the thermal loading on the insulator resulted in failure. It has been theorized that the neon sign transformer may have played a role in the thermal loading failure, as the power discharged through the spark plug was well beyond what the plug was designed to operate with. As a response to the spark plug failure, it was made standard operating procedure to inspect the spark plug before every test firing. The timing of propellant injection was also increased 0.1s past the igniter combustion check to help minimize the amount of propellant that could flow during a delayed ignition. For future testing, the neon sign transformer will be replaced with a MSD automotive ignition coil and driven by a MOSFET pulsed by a 555 timer circuit. This change was driven both by the spark plug failure as well as the serious electric shock hazards associated with the power capabilities of the transformer.

5.5.2 Force Transducer Mount

While the force transducer mount performed its function to protect the force transducer from overloading, the flexure bars permanently yielded under the load as did some of the fixturing hardware. The hardware that yielded was a result of the flexure bars being too rigid, directing significant force to the connection hardware. A new transducer mount was designed which used a less rigid, one piece flexure bar with flexure points machined 90° to one another.

The single bar design was chosen to ensure the flexures were exactly at a 90° offset from one another. The flexure bar was designed to be machined from 19.05mm (0.75") bar stock, with the strong bending axis 19.05mm (0.75") thick. The thickness at the weak axis of the flexure was selected as the minimum thickness that would not permanently yield under the maximum force the transducer was rated for, or 2224N (500lbf). This thickness was found to be 2.032mm (0.08") thick, yielding at 2668N (600lbs) of force. Figure 5.8 shows the new transducer mount design.

The same transducer holder was utilized from the previous design as it had been successful in preventing the transducer from being overloaded. To protect the flexure bars from yielding, a hard stop was incorporated in the form of a sleeve that slid over the entire assembly. Allowable displacement due to the thrust load from the rocket can be adjusted using 0.0254mm (0.001") shims. The new transducer mount is currently under construction, and will be used for future testing. Machining drawings can be found in Appendix A.3.

!h
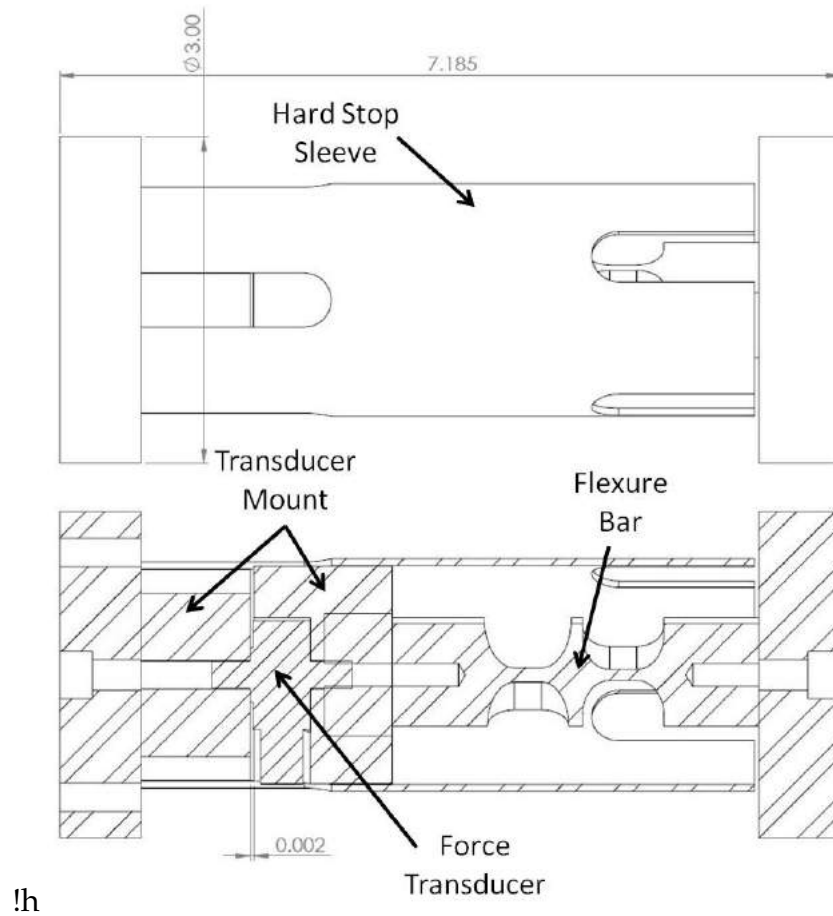
Figure 5.8: New transducer mount design

CHAPTER 6

CONCLUSIONS

6.1 Conclusions

The work discussed here has provided new computational methods for modeling of rocket engine performance as well as a test facility designed for the evaluation of novel propellant combinations and rocket engine designs. The developed test facility has not only provided research capabilities for evaluating nitrous oxide and ethanol as rocket engine propellants, but also brought renewed space propulsion research to the New Mexico institute of Mining and Technology.

The computational methods discussed here have demonstrated Cantera as an acceptable alternative to NASA CEA, and successfully shown the capabilities of the MATLAB/Cantera rocket engine model to predict experimental rocket engine performance. The use of Cantera by integration with the MATLAB computational environment provided the opportunity to develop a rocket engine model that was could be expanded beyond NASA CEA's capability for predicting rocket engine performance. The development of the model to predict performance as a function of specific nozzle design and supplied propellant flow rates provided an improved evaluation of engine performance based on actual test parameters. This allows the developed model to not only be useful in preliminary design work but also in predicting engine performance for a specific test case before actual testing.

In validating the MATLAB/Cantera model, the opportunity was demonstrated to use the model for evaluation of unexpected engine performance, as was the case of higher then expected rocket engine chamber pressures. The use of the model in successfully predicting that the nozzle throat was undersized from the original design further expanded the models usefulness in evaluating unexpected engine performance. The use of MATLAB and Cantera also provides further opportunity to expand modeling efforts to potentially account for real world phenomenon such as heat transfer or chemical kinetics. This can further improve a computational models ability to provide better predictions of experimental performance.

The experimental data collected from the two successful tests showed nitrous oxide and ethanol to provide good performance when compared to the computational predicted performance, and helped in validating the MATLAB/-Cantera rocket engine model. For the two successful tests, thrust output was

observed slightly over 578N (130lbf), with values of specific impulse in the range of 250 to 260 seconds. These preliminary results of nitrous oxide and ethanol performance support further testing of the propellant combination to evaluate its performance.

The developed rocket engine and supporting test facility demonstrated successful design methodology for the development of a functional rocket engine test facility. The methods established provide safe and successful means for designing rocket engine components, propellant supply system, and supporting hardware. These procedures are valuable to those looking to develop or expand their own rocket engine test capabilities, such academic and private institutions. The test facility not only demonstrated the successful use of nitrous oxide and ethanol as rocket engine propellants, but provides the opportunity for further research in evaluating this rocket propellant combination. In doing so, the repeatability of the performance of the propellant combination can be established as well as evaluation of optimal operating conditions.

The present research has demonstrated the means for successful construction of a small-scale rocket engine test facility and computational methods for modeling the rocket engine tested. The development of this facility provides an invaluable teaching tool for propulsion engineers and New Mexico Tech as an institution. This facility also provides a test bed for development of new rocket propulsion technologies as well as diagnostic techniques, to include flow visualization and plume analysis. New computational methods for rocket engine performance modeling have been established for modeling rocket engines using direct test parameters, such as propellant mass flow rate and nozzle dimensions. This work also established Cantera as an acceptable alternative to NASA CEA for equilibrium calculations, as well as Cantera's applicability in rocket engine modeling. Overall, the present research has provided substantial testing capabilities for evaluation of not only nitrous oxide and ethanol as rocket propellants, but other novel propellant combinations and engine designs.

6.2   Best Practices

In conducting this research, certain practices were employed which were necessary for safe and reliable operation of the system. These include the use of cavitating venturis, proper fuel system design, and system wiring management. These procedures will be briefly outlined in this section.

The application of cavitating venturis for controlling the propellant flow rate provides reliable and safe operation of a rocket engine. Caviating venturis allow the propellant flow rate to the engine to be a function of only the upstream pressure as a result of the flow through the venturi throat being choked. Controlling the flow rate via upstream pressure simplifies operation of the propellant supply system. This function also allows steady flow of the propellants to the engine during operation, and is important during start up of the engine as it prevents high initial flow rates due to the lower pressure in the engine combustion

chamber. The venturi also prevents flow feedback to the upstream lines and supply tank. This includes pressure fluctuations as a result of engine operation as well as the prevention of combustion products from traveling back upstream in the event of an over pressure event of the rocket engine.

While a cavitating venturi can provide safe and reliable operation, a pressure differential is required across the venturi to prevent the throat from unchoking. Cavitating venturis can reliably operate with a downstream pressure of 85% to 90% of the upstream pressure[23]. Once this pressure limit is exceeded, the throat can unchoke and the flow rate through the venturi will become a function of the pressure differential across the venturi. This can allow fluctuations in flow rate as well as upstream flow feedback to the propellant supply tanks, which can have catastrophic results.

When designing a fuel system, certain safety features and practices are necessary for safe and reliable operation of the system. Pressure relief valves are necessary to relieve pressure in the event of an over pressurization of the system. A burst disk is also required as a worst case scenario safety device in the event the pressure relief valve can not relieve the system pressure fast enough to reach safe pressures, or fails all together. Proper line identification is a priority, as it not only provides quick visual identification of parts of the system, but mitigates the risk of misidentifying lines for both experienced and new users of the system.

To prevent isolation of propellants in the supply lines after system shutdown, valve and check valve locations are crucial in preventing propellant from being isolated in a line. While the prevention of propellant isolation is important for safety during system maintenance, it is crucial when using propellants that have a high vapor pressure, such as nitrous oxide. With small rises in temperature, high pressure increases can result as the propellant attempts to expand in the sealed line. This can result in system damage or even explosive failure of the system.

When selecting fittings for make system connections, thought must be paid to the location and orientation of the fitting to be installed. Swagelok manufactured swage and VCO fittings provide reliable sealing and allow significant freedom in attaching and orienting fittings. While NPT is a common fitting of choice for pressure systems, NPT can be difficult to install and orient properly on precision systems. More importantly, NPT fittings can prove to be hard to achieve positive sealing with. In general, the avoidance of NPT will help provide trouble-free system operation. For applications where high pressure and/or hazardous materials are being used with the system, avoidance of NPT fittings is in the operators absolute best interest with regards to operation and system safety.

While systems can be built with minimal wiring management, properly designed wire management for a system provides safer operation and simplifies repairs. The use of liquid tight conduit and fittings not only provides wire management but protects control and data lines from damage. For systems exposed to the elements or locations with rodent and insect presence, liquid tight conduit protects the control and data acquisition systems from intrusion of animals and the environment, preventing internal damage. Care must be taken during design

of the system to consider future expansions, as once the wiring and management systems are installed, future expansion can prove challenging.

While other favorable design practices exist, the proper implementation of the practices described in this section will provide significant benefit in yielding a safe and reliable system.

CHAPTER 7

RECOMMENDATIONS FOR FUTURE RESEARCH

Significant room for future research exists to improve propellant and rocket engine performance evaluation methods. This also includes research to improve the test facility operation and capabilities. Continuing testing for the evaluation of the performance of nitrous oxide and ethanol will allow the repeatability of the propellant performance to be evaluated. This testing can also be utilized in optimizing the desired operating conditions for best performance.

Currently, the primary focus of future work should be in making the necessary revisions to the test facility to resume testing. This will include completing the redesigned force transducer mount and installing on the test bed. Following this, the installation of a new power supply for the igniter will take place as the neon sign transformer has been retired from the facility. The completion of the transducer mount repairs and igniter power supply replacement will allow testing to resume.

To improve the operation of the facility, the supply line pressure drop experienced during testing needs to be corrected. While the testing at the facility can be performed despite the pressure drop, the methods used to achieve desired operation are potentially damaging to the engine long term. This is a result of the potential for a hard start and the over stressing the engine components due to the high starting engine pressures. The most promising solution is adding additional supply bottles to the inlet of the supply regulators. The additional bottles should allow the necessary flow rate to be supplied. This may be a temporary solution however, as the facility long term would be best to move away from individual bottles to a multi-bottle manifold to improve reliability and safety. For longer engine operation times, active cooling will be required, and likely will involve the use of a water jacket and heat exchanger or open loop cooling system.

For improving the capabilities of rocket engine performance evaluation, expansion of the data acquisition system would prove invaluable. This would include capabilities for exhaust temperature measurements as well as temperature measurements along the engine to quantify heat flux from the combustion gases to the chamber and nozzle walls. High speed optical analysis of the exhaust plume could also be used to provide evaluation of the nozzle performance and characterize the exiting exhaust plume.

With regards to the computational modeling work, significant future expansion exists. While the model has been designed to predict performance as a

function of test parameters, future work would best look to expand on the modeling of the combustion environment within the engine. This would include chemical kinetics, heat transfer, and propellant droplet vaporization. Accounting for these effects would improve the predictions made by the model. This would improve future engine design work and analysis of the rocket engine performance and system energy losses. Accounting for these effects will also provide methods for determining L^* computational rather then experimentally.

APPENDIX A

ROCKET ENGINE

A.1 Rocket Engine CAD

A.1.1 Injector Manifold

Technical drawing annotations:

ϕ 6.000 $^{0.000}_{-0.010}$

ϕ 4.000 $^{+0.010}_{0.000}$

R2.500 $^{+0.001}_{-0.001}$

ϕ 0.386 THRU

FINISH:		DEBUR AND BREAK SHARP EDGES	CONTACT: **STEWART YOUNGBLOOD, PH# 505-470-7551**	
			Notes: 1)Hole Size For Hole Pattern = 0.386", W Drill Size	
UNLESS OTHERWISE SPECIFIED: DIMENSIONS ARE IN INCHES SURFACE FINISH: TOLERANCES: LINEAR: ANGULAR:			TITLE: MANIFOLD FACE AND BOLT PATTERN	
MATERIAL: 303 Stainless			DWG NO. MANIFOLD_1	A4
	WEIGHT:		SCALE:1:1	SHEET 1 OF 1

Groove Depth 0.075", +0.005/-0.000

$\varnothing 2.005$ +0.005/-0.000

0.170 +0.010/-0.000

$\varnothing 1.35$ +0.005/-0.005

0.250 +0.001/-0.001

Groove Depth 0.4", +0.001/-0.001

Groove Depth 0.075", +0.005/-0.000

0.170 +0.010/-0.000

$\varnothing 0.688$

FINISH:		DEBUR AND BREAK SHARP EDGES	CONTACT: **STEWART YOUNGBLOOD, PH# 505-470-7551**		
			Notes:		
UNLESS OTHERWISE SPECIFIED: DIMENSIONS ARE IN INCHES SURFACE FINISH: TOLERANCES: LINEAR: ANGULAR:			TITLE: Manifold Seal Design		
MATERIAL: 303 Stainless			DWG NO. Manifold_2		A4
WEIGHT:		SCALE:1:2		SHEET 1 OF 1	

111

R1.125 +0.001 -0.001

22.50°   22.50°

4 x ⌀ 0.21 ▽ 0.68
1/4-28 UNF ▽ 0.50

R2.500 +0.001 -0.001

⌀ 0.386 THRU

FINISH:		DEBUR AND BREAK SHARP EDGES	CONTACT: **STEWART YOUNGBLOOD, PH# 505-470-7551**		
			Notes: 1)Hole Size For Hole Pattern = 0.386", W Drill Size		
UNLESS OTHERWISE SPECIFIED: DIMENSIONS ARE IN INCHES SURFACE FINISH: TOLERANCES: LINEAR: ANGULAR:			TITLE: Manifold Rear		
MATERIAL: 303 Stainless			DWG NO. Manifold_3		A4
WEIGHT:			SCALE:1:2	SHEET 1 OF 1	

112

0.100" Deep, +/-0.01

$\varnothing$ 0.75 ②

$\varnothing$ 0.328, 21/64 Drill

0.02 X 45°

1/4 NPT, Q Drill

0.000
2.575 -0.005

0.02 X 45°

+0.010
1.100 -0.010

①

$\varnothing$ 0.125, 0.730 Deep

0.000
3.063 -0.005

+0.010
1.100 -0.010

0.02 X 45°

1/4 NPT, Q Drill

SECTION A-A
SCALE 1 : 1

$\varnothing$ 0.75

$\varnothing$ 0.328, 21/64 Drill

0.100" Deep, +/-0.01

FINISH:		DEBUR AND BREAK SHARP EDGES	CONTACT: **STEWART YOUNGBLOOD, PH# 505-470-7551**
			Notes: 1) Port is 0.125", 0.73" deep +0.002/-0.000. 1/8" Drill or End Mill 2) 0.75" Diam, 0.1" Deep Cuts can be 3/4" End Mill
UNLESS OTHERWISE SPECIFIED: DIMENSIONS ARE IN INCHES SURFACE FINISH: TOLERANCES: LINEAR: ANGULAR:			TITLE: Manifold Propellant Ports
MATERIAL: 303 Stainless			DWG NO. Manifold_4 · A4
	WEIGHT:	SCALE:1:2	SHEET 1 OF 1

22.50°   22.50°

114

A.1.2 Injector Plate

0.50

0.02 X 45°

24° +0.50° -0.50°

0.02 X 45°

⌀0.089, #43 Drill

⌀0.026, #71 Drill

A.1.3 Combustion Chamber

0.000
$\varnothing$ 6.000 -0.010

0.02 X 45°

0.02 X 45°

0.02 X 45°

0.02 X 45°

$\varnothing$ 4.00 +0.02 / 0.00

6.000 +0.020 / -0.020

0.960 +0.020 / 0.000

0.96 +0.02 / 0.00

FINISH:		CONTACT: STEWART YOUNGBLOOD, PH# 505-470-7551		
	DEBUR AND BREAK SHARP EDGES			
UNLESS OTHERWISE SPECIFIED: DIMENSIONS ARE IN INCHES TOLERANCES: +0.020/-0.020 LINEAR: ANGULAR:		TITLE: Chamber Exterior Dimensions		
MATERIAL: OFHC, 6" Round		DWG NO. Chamber_1		A4
	WEIGHT:	SCALE:1:1	SHEET 1 OF 1	

Chamber ID. Bore Through

Bolt Hole, Bore Through Flange

$\phi 2.000 \begin{smallmatrix} 0.000 \\ -0.010 \end{smallmatrix}$

R2.500 +0.005 -0.005

$\phi 0.386$

$0.210 \begin{smallmatrix} +0.010 \\ 0.000 \end{smallmatrix}$

$0.210 \begin{smallmatrix} +0.010 \\ 0.000 \end{smallmatrix}$

$\phi 3.007 \begin{smallmatrix} +0.005 \\ 0.000 \end{smallmatrix}$

$\phi 4.132 \begin{smallmatrix} +0.005 \\ 0.000 \end{smallmatrix}$

Groove Depth 0.107", +0.005/-0.000

Groove Depth 0.107", +0.005/-0.000

FINISH:		DEBUR AND BREAK SHARP EDGES	DO NOT SCALE DRAWING	
			Notes: 1)Hole Size For Hole Pattern = 0.386", W Drill Size 2)Dimensions/Design Same For Both Faces	
UNLESS OTHERWISE SPECIFIED: DIMENSIONS ARE IN INCHES SURFACE FINISH: **S, RMS values** TOLERANCES: LINEAR: ANGULAR:			TITLE: Chamber Faces, Oring Grooves Bolt Pattern	
MATERIAL: OFHC, 6" Round			DWG NO. Chamber_2	A4
	WEIGHT:	SCALE:1:5	SHEET 1 OF 1	

A.1.4 Igniter Flange

0.02 X 45°

0.02 X 45°

⌀ 0.58 THROUGH
5/8-18 UNF ▽ 1.25

⌀0.80

22.50°   22.50°

⌀0.386 THRU

R2.500 +0.001 -0.001

0.300 +0.010 0.000

FINISH:			
	DEBUR AND BREAK SHARP EDGES	CONTACT: **STEWART YOUNGBLOOD, PH# 505-470-7551**	
		Notes: 1) 0.386" Hole Pattern, W Drill	
UNLESS OTHERWISE SPECIFIED: DIMENSIONS ARE IN INCHES SURFACE FINISH: TOLERANCES: LINEAR: ANGULAR:		TITLE: Ignitor Port Dimensions	
MATERIAL: MATERIAL		DWG NO. Ignitor_1	A4
WEIGHT:		SCALE:1:2	SHEET 1 OF 1

Bore Through, Match
Chamber ID by +0.001/-0.000

0.000
-0.010
$\varnothing$2.000

$\varnothing$0.386 THRU

R2.500 +0.005 -0.005

+0.010
0.000
0.210

$\varnothing$4.132 +0.005 -0.000

0.210 +0.010 0.000

+0.005
0.000
$\varnothing$3.007

Groove Depth 0.107", +0.005/-0.000

Groove Depth 0.107", +0.005/-0.000

FINISH:		DEBUR AND BREAK SHARP EDGES	DO NOT SCALE DRAWING		
			Notes: 1)Hole Size For Hole Pattern = 0.386", W Drill Size		
UNLESS OTHERWISE SPECIFIED: DIMENSIONS ARE IN INCHES SURFACE FINISH: **S, RMS values** TOLERANCES: LINEAR: ANGULAR:			TITLE: Ignitor Face, Oring Grooves Bolt Pattern		
MATERIAL: OFHC, 6" Round			DWG NO. Ignitor_2		A4
WEIGHT:		SCALE:1:5		SHEET 1 OF 1	

A.1.5 Nozzle

FINISH:

DEBUR AND BREAK SHARP EDGES

DO NOT SCALE DRAWING

Notes: 1)Hole Size For Hole Pattern = 0.386", W Drill Size

UNLESS OTHERWISE SPECIFIED:
DIMENSIONS ARE IN INCHES
SURFACE FINISH:
TOLERANCES:
  LINEAR:
  ANGULAR:

TITLE:

Nozzle Front, Bolt Pattern

MATERIAL:
OFHC, 6" Round

DWG NO.
Nozzle_1

A4

WEIGHT:

SCALE:1:2

SHEET 1 OF 1

+0.020
2.000 -0.020

0.02 X 45°

0.02 X 45°

0.02 X 45°

No Chamfer,
Want Sharp Edge

R0.175

30°

15°

Need to Match
Chamber ID by
+0.001/-0.000

0.0000
Ø 2.000 -0.010

+0.001
0.350 -0.001

+0.001
Ø 1.020 -0.001

R0.175

SECTION C-C
SCALE 1 : 1

+0.020
0.980 -0.002

+0.001
2.749 -0.001

121

Need to Match
Chamber ID by
+0.001/-0.000

$\varnothing 2.000 \begin{smallmatrix} 0.000 \\ -0.010 \end{smallmatrix}$

122

A.2 Igniter CAD

FINISH:

DEBUR AND
BREAK SHARP
EDGES

CONTACT: **STEWART YOUNGBLOOD, PH# 505-470-7551**

Notes: NOTES

UNLESS OTHERWISE SPECIFIED:
DIMENSIONS ARE IN INCHES
SURFACE FINISH:
TOLERANCES:
  LINEAR:
  ANGULAR:

TITLE:

Ignitor Assembled

MATERIAL:
  MATERIAL

DWG NO.

Ignitor_4

A4

WEIGHT:

SCALE:1:1

SHEET 1 OF 1

4.41

R0.850 +0.002 -0.002

∅ 0.35 THRU ALL
M10x1.0 - 6H THRU ALL

6 x ∅ 0.22 THRU ALL
⌴ ∅ 0.38 ↧ 0.19

0.680 +0.005 -0.005

∅ 1.000 +0.005 0.000

0.000 -0.010

∅ 0.660 -0.010

0.075" deep +0.005/-0.000
#117 Oring Groove

FINISH:		DEBUR AND BREAK SHARP EDGES	CONTACT: **STEWART YOUNGBLOOD, PH# 505-470-7551**	
			Notes: M10X1.0 Thread for spark plug. Thread Through	
UNLESS OTHERWISE SPECIFIED: DIMENSIONS ARE IN INCHES SURFACE FINISH: TOLERANCES: LINEAR: ANGULAR:			TITLE: Ignitor Top	
MATERIAL: SS 306			DWG NO. Ignitor_1	A4
WEIGHT:		SCALE:1:1	SHEET 1 OF 1	

∅ 0.563 ▽ 0.56

R0.850 +0.002 / -0.002

6 x ∅ 0.159 ▽ 0.47
10-32 UNF ▽ 0.38

∅ 0.36 ▽ 0.60
1/8-27 NPSM ▽ 0.79

1.000 +0.005 / -0.005

∅0.125

∅0.097 ▽ 0.30 +0.005 / -0.005

0.01" X 45 Deg Chamfer

∅0.250

∅0.185 ▽ 0.30 0.000 / -0.002

∅0.125

6 x ∅ 0.16 ▽ 0.47
10-32 UNF ▽ 0.38

FINISH:			
	DEBUR AND BREAK SHARP EDGES	CONTACT: **STEWART YOUNGBLOOD, PH# 505-470-7551**	
		Notes:	
UNLESS OTHERWISE SPECIFIED: DIMENSIONS ARE IN INCHES SURFACE FINISH: TOLERANCES: +0.01/-0.01 LINEAR: ANGULAR:		TITLE: Ignitor Combustion Chamber	
MATERIAL: SS 306		DWG NO. Ignitor_2	A4
WEIGHT:		SCALE:1:1	SHEET 1 OF 1

6 x ⌀ 0.159 ⤵ 0.47
10-32 UNF ⤵ 0.38

⌀ 0.563 ⤵ 0.56

R0.850 +0.002 -0.002

FINISH:

DEBUR AND
BREAK SHARP
EDGES

CONTACT: **STEWART YOUNGBLOOD, PH# 505-470-7551**

Notes: NOTES

UNLESS OTHERWISE SPECIFIED:
DIMENSIONS ARE IN INCHES
SURFACE FINISH:
TOLERANCES: +0.01/-0.01
  LINEAR:
  ANGULAR:

TITLE:

Igniter_Comb_1

MATERIAL:
304 SS

DWG NO.
1A

A4

WEIGHT:

SCALE:2.5:1

SHEET 1 OF 1

6 x ∅ 0.159 ⤵ 0.47
10-32 UNF ⤵ 0.38

∅ 0.12 ⤵ 0.29
        +0.001
⌴ ∅ 0.185 -0.001 ⤵ 0.240

R0.850 +0.002
        -0.002

FINISH:		CONTACT: **STEWART YOUNGBLOOD, PH# 505-470-7551**		
	DEBUR AND BREAK SHARP EDGES	Notes: Overview		
UNLESS OTHERWISE SPECIFIED: DIMENSIONS ARE IN INCHES SURFACE FINISH: TOLERANCES: +0.01/-0.01 LINEAR: ANGULAR:		TITLE: Igniter_Comb_2		
MATERIAL: 304 SS		DWG NO. 1A		A4
	WEIGHT:	SCALE:2.5:1	SHEET 1 OF 1	

Ø0.480 ▽ 0.075

0.075" +0.005/-0.000
#117 Oring Groove

+0.005
Ø0.660 0.000

0.000
Ø1.000 -0.010

+0.002
Ø 0.070 -0.002 ▽ 0.320

+0.005
0.800 0.000

+0.005
0.750 0.000

+0.005
0.120 0.000

+0.010
0.146 0.000

+0.001
Ø0.798 -0.001

Ø 0.36 ▽ 0.73
1/8-27 NPSM ▽ 0.79

0.000
Ø0.637 -0.004

Ø 5/8 - 18 UNF X 1.0"

+0.005
1.000 - 0.005

0.000
2.729 -0.005

Ø0.55

Ø0.25 THRU

+0.005
0.630 -0.005

0.02" X 45 deg
Chamfer

+0.002
R0.850 -0.002

6 x Ø 0.22 THRU ALL
⌴ Ø 0.38 ▽ 0.19

FINISH:		DEBUR AND BREAK SHARP EDGES	CONTACT: **STEWART YOUNGBLOOD, PH# 505-470-7551**		
			Notes: NOTES		
UNLESS OTHERWISE SPECIFIED: DIMENSIONS ARE IN INCHES SURFACE FINISH: TOLERANCES: LINEAR: ANGULAR:			TITLE: Ignitor Base		
MATERIAL: SS 306			DWG NO. Ignitor_3		A4
WEIGHT:		SCALE:1:1		SHEET 1 OF 1	

129

⌀0.480 ⫧ 0.075

0.075" +0.005/-0.000
#117 Oring Groove

⌀0.660 +0.005 / 0.000

⌀1.000 0.000 / -0.010

⌀ 0.070 +0.002/-0.002 ⫧ 0.320

0.800 +0.005 / 0.000

⌀0.25 THRU

R0.850 +0.002/-0.002

6 x ⌀ 0.22 THRU ALL
⌴ ⌀ 0.38 ⫧ 0.19

FINISH:		DEBUR AND BREAK SHARP EDGES	CONTACT: **STEWART YOUNGBLOOD, PH# 505-470-7551**		
			Notes: NOTES		
UNLESS OTHERWISE SPECIFIED: DIMENSIONS ARE IN INCHES SURFACE FINISH: TOLERANCES: LINEAR: ANGULAR:			TITLE: Ignitor Base		
MATERIAL: SS 306			DWG NO. Ignitor_3		A4
WEIGHT:			SCALE:1:1	SHEET 1 OF 1	

$\varnothing\,0.358 \downarrow 0.73$
1/8-27 NPSM $\downarrow 0.79$

$\varnothing\,0.798 \begin{smallmatrix}+0.001\\-0.001\end{smallmatrix}$

$\varnothing\,0.637 \begin{smallmatrix}0.000\\-0.004\end{smallmatrix}$

$0.750 \begin{smallmatrix}+0.005\\0.000\end{smallmatrix}$

$0.146 \begin{smallmatrix}+0.010\\0.000\end{smallmatrix}$

$0.120 \begin{smallmatrix}+0.05\\0.00\end{smallmatrix}$

0.063

5/8 - 18 UNF X 1.0"

$1.000 \begin{smallmatrix}0.000\\-0.010\end{smallmatrix}$

$0.630 \begin{smallmatrix}+0.050\\-0.050\end{smallmatrix}$

$\varnothing\,0.550 \begin{smallmatrix}0.000\\-0.010\end{smallmatrix}$

$\varnothing\,0.625$

FINISH:		CONTACT: **STEWART YOUNGBLOOD, PH# 505-470-7551**		
	DEBUR AND BREAK SHARP EDGES	Notes: NOTES		
UNLESS OTHERWISE SPECIFIED: DIMENSIONS ARE IN INCHES SURFACE FINISH: TOLERANCES:+/-0.01 LINEAR: ANGULAR:		TITLE: Ignitor Base 2		
MATERIAL: 304 SS		DWG NO. Ignitor_3A		A4
WEIGHT:		SCALE:1:1	SHEET 1 OF 1	

131

A.3 Force Transducer Mount

SECTION A-A
SCALE 1 : 2

A

A

FINISH:		DEBUR AND BREAK SHARP EDGES	CONTACT: **STEWART YOUNGBLOOD, PH# 505-470-7551**
			Notes: NOTES
UNLESS OTHERWISE SPECIFIED: DIMENSIONS ARE IN INCHES SURFACE FINISH: TOLERANCES: LINEAR: ANGULAR:			TITLE: Final Assembly
MATERIAL: MATERIAL			DWG NO. DRAWING 5

WEIGHT: SCALE:1:1 SHEET 1 OF 1

A4

0.375

$\emptyset$ 0.21 ⍿ 0.61
1/4-28 UNF ⍿ 0.50

0.080

0.375

0.250

2.125

1.250

0.250

3.375 $^{+0.001}_{-0.001}$

0.080

0.335

0.625 $^{+0.001}_{-0.001}$

$\varnothing$ 1.120 $^{0.000}_{-0.002}$

$\varnothing$ 0.21 THRU ALL
1/4-28 UNF THRU ALL

R1.068

R1.005 +0.002 / 0.000

0.500

1.500

1.250

5.645 +0.002 / 0.000

⌀ 0.213 THRU ALL
1/4-28 UNF THRU ALL

Centered

1.000

⌀ 2.000

UNLESS OTHERWISE SPECIFIED:
DIMENSIONS ARE IN INCHES
SURFACE FINISH:
TOLERANCES: +/-0.01
  LINEAR:
  ANGULAR:

TITLE:
Transducer Mount Upper

MATERIAL:
304 SS

DWG NO.
DRAWING 4

A4

WEIGHT:

SCALE:1:1

SHEET 1 OF 1

1.125 ±0.002

1.125 ±0.002

⌀ 0.261 THRU
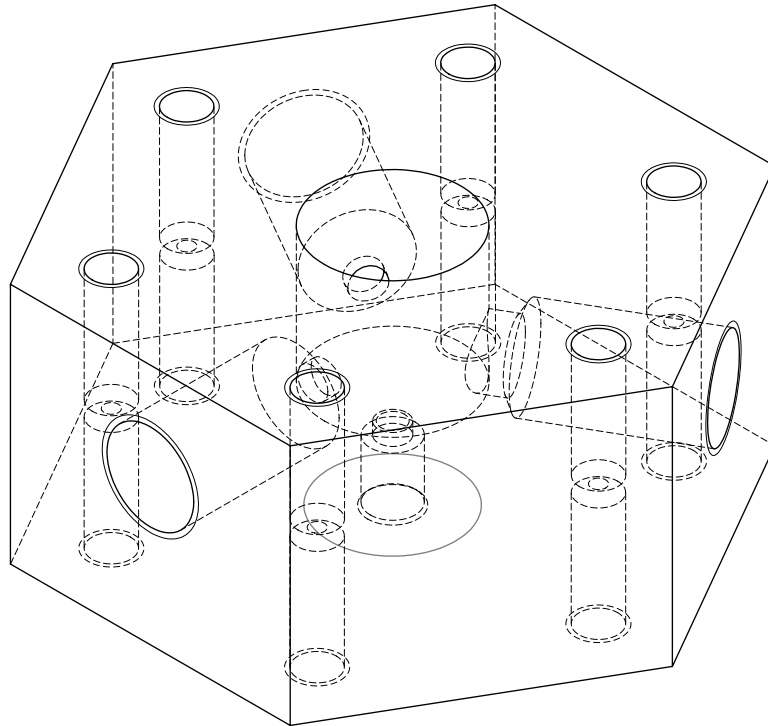
⌀ 0.281 THRU ALL
⌴ ⌀ 0.44 ▼ 0.30

⌀ 3.000

0.750

FINISH:		DEBUR AND BREAK SHARP EDGES	CONTACT: **STEWART YOUNGBLOOD, PH# 505-470-7551**		
			Notes: Need 2 machined		
UNLESS OTHERWISE SPECIFIED: DIMENSIONS ARE IN INCHES SURFACE FINISH: TOLERANCES: +/- 0.01 LINEAR: ANGULAR:			TITLE: Main Plate		
MATERIAL: 304 SS			DWG NO. DRAWING 1		A4
WEIGHT:		SCALE:1:1		SHEET 1 OF 1	

R1.000

R0.525

0.5" Radius flush with
recess bottom.
Cut with 0.5" Endmill

⌀0.257

+0.001
0.522 0.000

0.125

0.625

SECTION A-A
SCALE 2 : 1

⌀1.125

A

A

138

Centered

⌀ 0.213 THRU ALL
1/4-28 UNF THRU ALL

1.000

⌀ 2.000

FINISH:		CONTACT: **STEWART YOUNGBLOOD, PH# 505-470-7551**		
	DEBUR AND BREAK SHARP EDGES	Notes: NOTES		
UNLESS OTHERWISE SPECIFIED: DIMENSIONS ARE IN INCHES SURFACE FINISH: TOLERANCES: +/-0.01 LINEAR: ANGULAR:		TITLE: Transducer Mount Upper		
MATERIAL: 304 SS		DWG NO. DRAWING 4		A4
WEIGHT:		SCALE:1:1	SHEET 1 OF 1	

A.4 Cavitating Venturi Specifications
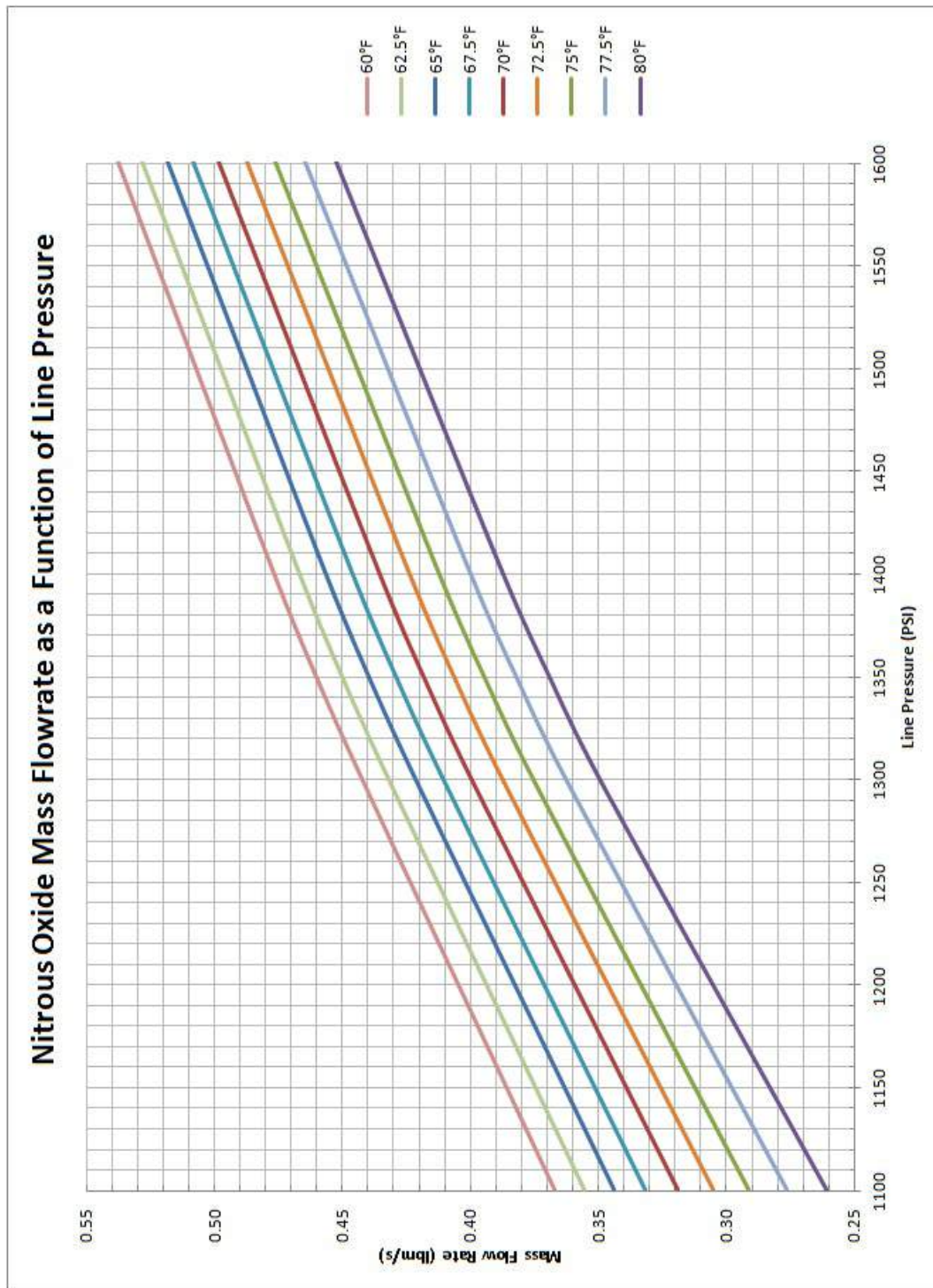
Figure A.1: Predicted nitrous oxide flow-rate as a function of upstream pressure.
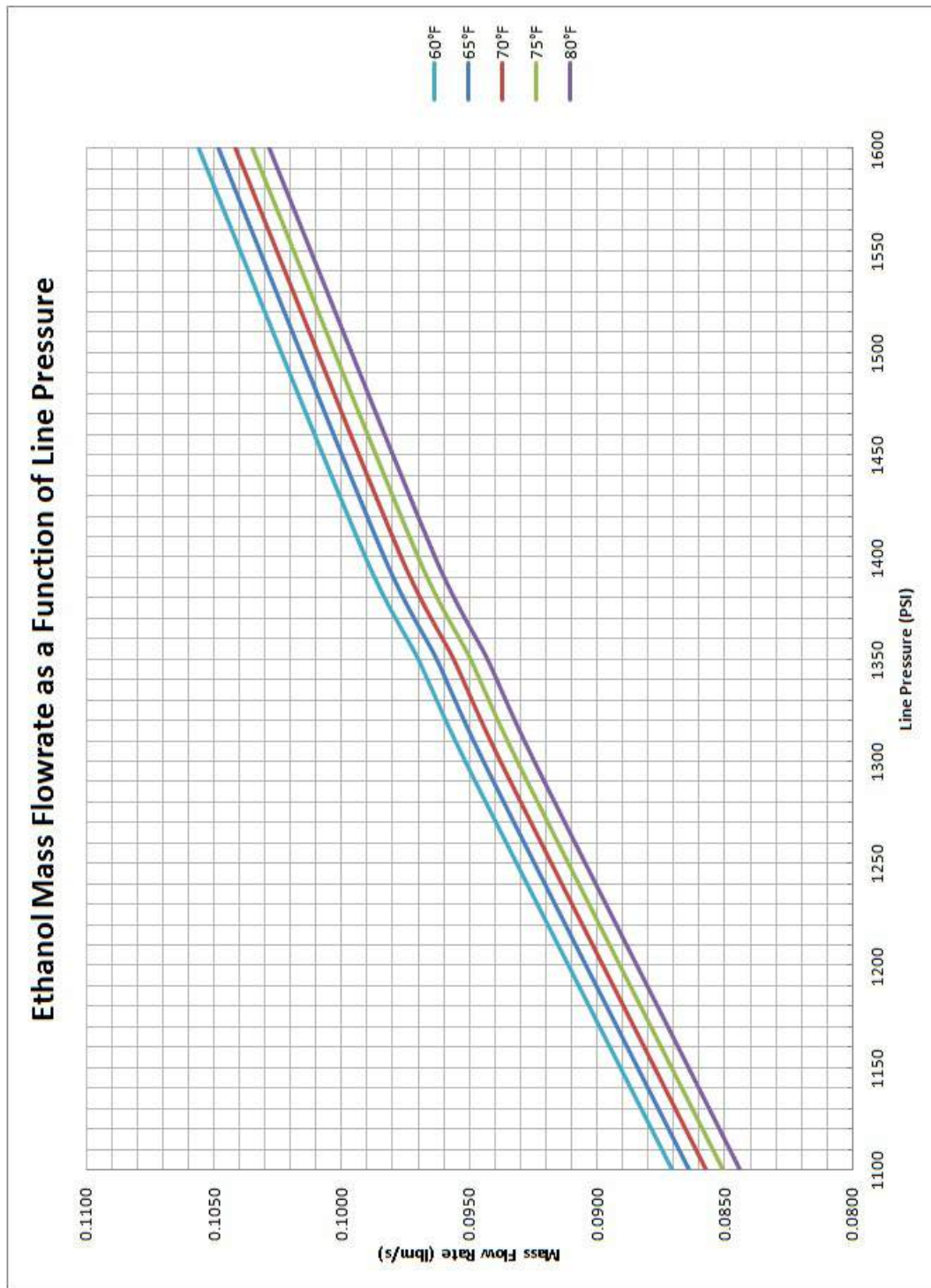
Figure A.2: Predicted ethanol flow-rate as a function of upstream pressure.

APPENDIX B

TEST FACILITY

B.1 Propellant Supply System Diagrams

B.2 Propellant Loading Procedures

1. PROPELLANT LOADING PROCEDURE

Tools Needed: Compressed air can, wrench to attach N2O fitting

1.1. Start Video Recording

1.2. Nitrous Oxide Supply Bottle Install (If required):

    1.2.1.   All personnel except 2 people needed to mount N2O bottle must be in Control Room cell with door closed.

    1.2.2.   Turn scale on

    1.2.3.   Attach cylinder stand to N2O source bottle by threading on to cylinder cap threads. Check that the fill port is not in line with any of the supports when the bottle is securely threaded. Back off ¼ turn if necessary.

    1.2.4.   With a minimum of two people, tip the bottle on its side onto the stand, then tip vertically so bottle is inverted. Move to scale, and secure in rack.

    1.2.5.   Use compressed air to blow out N2O attachment port and fitting

    1.2.6.   Connect inverted N2O cylinder to N2O fill pump via bottle CGA fitting.

1.3. Nitrous Oxide Fill (Referencing Holly Manual):

    1.3.1.   Remove all personnel to the personnel shelter/Control Room

    1.3.2.   Vent the run tank by opening valve #9 using manual Labview control. Then close Valve 9.

    1.3.3.   Obtain clearance from the Test Manager that the area is clear, personnel accounted for, and that the fill process is ready to proceed.

    1.3.4.   Record the initial mass on the scale (N2O tank weight) below and fill out the remainder of the table below for the desired values:
N2O flow rates are given in the appendix for reference

Desired Mass of N2O:_____ Actual mass N2O: _____

Initial scale reading:_____

Desired final scale reading:_____ Actual final mass: ____
_____

    1.3.5.   1 person exits the Control Room to complete the following steps.

1.3.6.	Open the valve on run tank fill line (F2).

1.3.7.	Confirm regulator (R6) is set at 80psi, and open the transfer pump supply safety valve, N1.

1.3.8.	Slowly open the valve on the N2O source cylinder. N2O will briefly flow as pressure between source bottle and run tank equalize

1.3.9.	Return to control cell, close control cell door.

1.3.10.	Arm Fill Control with key switch.

1.3.11.	Using the Propellant Fill camera, engage N2O transfer pump until designated weight decrease displayed by the scale is observed. Monitor temperature and run tank pressure via LabVIEW. If run tank pressure reaches 1000psig or temperature exceeds 90F, stop fill and wait for temperature to return to drop below 82 F and pressure to drop below 900psig.

1.3.12.	Disarm Fill Control. Wait for run tank to return to a pressure below 1000psi and to ambient temperature or below 82 degrees Fahrenheit.

1.3.13.	1 person leaves cell to complete final steps

1.3.14.	Close transfer pump safety valve (N1)

1.3.15.	Close N2O run tank fill valve (F2)

1.3.16.	Close N2O source cylinder.

1.3.17.	Slowly open the transfer pump system vent V5. Once fill system has vented, close valve.

1.3.18.	Return to control cell

1.4. Ethanol fill (As required):

1.4.1.	Open the ethanol run tank vent valve #10 using Labview Manual Control and keep open during fill procedure.

1.4.2.	1 person leaves the cell for the following steps

1.4.3.	Visually confirm Valve 10 is open

1.4.4.	Place ethanol supply bottle in holder.

1.4.5.	Attach pump hose to bottle.

1.4.6.   Open ethanol run tank fill valve (F1)

1.4.7.   Return to the control cell and close the Control Room door.

1.4.8.   Record the initial mass on the scale (fuel bottle weight) below and fill out
the remainder of the table below for the desired values:
Ethanol fuel flow rates are given in the appendix for reference

Desired Mass of fuel:_____   Actual mass
fuel: _____

Initial scale reading:_____

Desired final scale reading:_____   Actual final mass: ____
_____

1.4.9.   Obtain clearance from the Test Manager that the area is clear, personnel
accounted for, and the fill process is ready to proceed.

1.4.10.   Arm Fill Control. Using Propellant Fill camera, engage ethanol transfer
pump until designated weight decrease displayed by the scale is observed.

1.4.11.   Disarm Fill Control.

1.4.12.   End fill sequence, close vent valve #10 using Labview Manual Control

1.4.13.   1 person leaves cell for the following steps

1.4.14.   Visually check valve 10 is closed

1.4.15.   Close ethanol run tank fill valve (F1)

1.4.16.   Disconnect supply bottle from fill hose. Cap bottle and remove from Fuel
Galley.

1.4.17.   Store ethanol bottle in East Lab or onsite in flammable cabinet in Test
Cell.

B.3 REF Testing Procedures

NEW MEXICO TECH
SCIENCE • ENGINEERING • RESEARCH UNIVERSITY
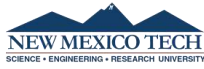
1. START OF DAY PRETEST PROCEDURE
(If already completed and start of new test, go to 2)

1.1. System Operating Conditions:

1.1.1.   Test Manager: _____

1.1.2.   Personnel present: _____

Total persons present: _____

1.1.3.   Check that the two gates at the Butler Building are closed with bunker contact info signs attached and that Z-sign is on road to West Lab/REF.

1.1.4.   Note date/time: _____

1.1.5.   Check forecast for next 2 hours.

1.1.6.   Barometric pressure (inHg): _____

1.1.7.   Outside temperature: _____

1.1.8.   Desired N2O mass flowrate (lbm/s): _____

1.1.9.   N2O Mass: _____   N2O Pressure: _____
N2O Pressure Desired, After Pressure Drop: _____

1.1.10.   Desired ethanol mass flowrate (lbm/s): _____

1.1.11.   Ethanol Mass: _____   Ethanol Pressure: _____
Ethanol Pressure Desired, After Pressure Drop: _____

1.1.12.   Purge pressure: _____

1.1.13.   Engine operation period (s): _____

1.1.14.   Check fuel galley temperature monitor to ensure fuel galley temperature does not exceed 80 degrees Fahrenheit. Activate air conditioner if necessary to control temperature and close galley doors.

1.1.15.   Review current wildfire conditions. If "extreme" conditions exist, priority of testing should be reviewed with the safety office.

1.1.16.   Review wind conditions. If winds greater than 15 mph are present, testing shall not commence.

1.2. Support Systems (control cell):

    1.2.1.   Inspect all control equipment for proper power up.

    1.2.2.   Insure Labview and NI DAQ connect properly. Review proper interfacing with DAQ modules and control and data ports.

    1.2.3.   Ensure laptops are plugged in, set to not sleep.

    1.2.4.   Lock out 24VDC ignition system supply.

    1.2.5.   Lock out fill control.

    1.2.6.   Close all powered valves using LabView: 1-16

    1.2.7.   Input test parameters into LabVIEW and Test Document
        Mass of fuel entered in Section 2
        Operating pressure entered in Section 3

1.3. Visual Inspection, Fuel Galley:

  Ensure gas cylinders are properly secured.

    1.3.1.   Ensure gas cylinders are properly closed.

    1.3.2.   Ensure all hand valves on supply panels and run tank are in the closed position.
        Supply Panel: V1, V2, V3, V4, P1, P2
        Run Tank Panel: S1, S2, F1, F2, V5, N1 (Unlock if needed)

    1.3.3.   Check exposed wiring for damage.

    1.3.4.   Turn on scale for measuring N2O/fuel mass

    1.3.5.   Remove vent covers and inspect ports for blockages.
        4 vents on N2 panel, 1 N2O vent outside fuel galley, 1 N2O vent outside test cell

1.4. Visual Inspection, Test Cell:

  Ensure gas cylinders are properly secured.

    1.4.1.   Ensure gas cylinders are properly closed.

    1.4.2.   Ensure propellant lines and rocket engine grounding hardware connections are secure.

    1.4.3.   Check exposed wiring for damage.

    1.4.4.   Check that Test Cell doors are open and secured in the open position.

1.4.5.   Remove and inspect igniter spark plug for damage.

1.5. Clear Test Site and Safety Equipment:

1.5.1.   Remove all non-essential personnel to personnel shelter/Control Room

1.5.2.   Essential personnel should wear safety glasses and ear protection from this point forward.

1.6. Valve N2 Supply Pressurization (Fuel galley):

1.6.1.   Open N2 valve supply cylinder 5 and check regulator is at 125psig.
Regulator: R5

1.6.2.   Inspect system for leaks by listening for gas escaping and using proper leak checking fluid if necessary. Check in both fuel galley and test cell for leaks.

1.7. Propellant System Pressurization:

1.7.1.   Check that all regulators are closed (dial completely out)
Regulators: R1, R2, R3, R4

1.7.2.   Open all four N2 supply bottles for propellant system.
Bottles: 1, 2, 3, 4

1.7.3.   Check that the pressure in each bottle 1-4 is greater than **2000 psi**
Bottle 1: _____   Bottle 3: _____
Bottle 2: _____   Bottle 4: _____

1.7.4.   Set all four regulators to 150psig.
Regulators: R1, R2, R3, R4

1.7.5.   Open propellant system supply hand valves.
Supply Panel: P1, P2
Run Tank Panel: S1, S2

1.7.6.   Inspect system for leaks by listening for gas escaping. If any gas leak is detected, close propellant supply hand valves and close system using the End of Day checklist. Check in both the fuel galley and test cell for leaks.

1.7.7.   Sequence through valves using Manual Control in LabView. Two personnel required. One operates the LabView system, other observes valves for proper actuation and checks off each valve on checklist. Insure Labview operation ceases after check. Close all valves after check
Supply Panel: 1, 2, 3, 4
Run Tank Panel: 9, 10, 11, 12
Test Cell: 5/13, 6/14, 7, 8

1.7.8.   Close propellant system supply hand valves.
Supply Panel: P1, P2

Run Tank Panel: S1, S2

2. PROPELLANT LOADING PROCEDURE

Tools Needed: Compressed air can, wrench to attach N2O fitting

2.1. Start Video Recording

2.2. Nitrous Oxide Supply Bottle Install (If required):

2.2.1.   All personnel except 2 people needed to mount N2O bottle must be in Control Room cell with door closed.

2.2.2.   Turn scale on

2.2.3.   Attach cylinder stand to N2O source bottle by threading on to cylinder cap threads. Check that the fill port is not in line with any of the supports when the bottle is securely threaded. Back off ¼ turn if necessary.

2.2.4.   With a minimum of two people, tip the bottle on its side onto the stand, then tip vertically so bottle is inverted. Move to scale, and secure in rack.

2.2.5.   Use compressed air to blow out N2O attachment port and fitting

2.2.6.   Connect inverted N2O cylinder to N2O fill pump via bottle CGA fitting.

2.3. Nitrous Oxide Fill (Referencing Holly Manual):

2.3.1.   Remove all personnel to the personnel shelter/Control Room

2.3.2.   Vent the run tank by opening valve #9 using manual Labview control. Then close Valve 9.

2.3.3.   Obtain clearance from the Test Manager that the area is clear, personnel accounted for, and that the fill process is ready to proceed.

2.3.4.   Record the initial mass on the scale (N2O tank weight) below and fill out the remainder of the table below for the desired values:
N2O flow rates are given in the appendix for reference

Desired Mass of N2O:_____   Actual mass N2O: _____

Initial scale reading:_____

Desired final scale reading:_____   Actual final mass: _____

2.3.5.   1 person exits the Control Room to complete the following steps.

2.3.6.   Open the valve on run tank fill line (F2).

2.3.7.   Confirm regulator (R6) is set at 80psi, and open the transfer pump supply safety valve, N1.

2.3.8.   Slowly open the valve on the N2O source cylinder. N2O will briefly flow as pressure between source bottle and run tank equalize

2.3.9.   Return to control cell, close control cell door.

2.3.10.   Arm Fill Control with key switch.

2.3.11.   Using the Propellant Fill camera, engage N2O transfer pump until designated weight decrease displayed by the scale is observed. Monitor temperature and run tank pressure via LabVIEW. If run tank pressure reaches 1000psig or temperature exceeds 90F, stop fill and wait for temperature to return to drop below 82 F and pressure to drop below 900psig.

2.3.12.   Disarm Fill Control. Wait for run tank to return to a pressure below 1000psi and to ambient temperature or below 82 degrees Fahrenheit.

2.3.13.   1 person leaves cell to complete final steps

2.3.14.   Close transfer pump safety valve (N1)

2.3.15.   Close N2O run tank fill valve (F2)

2.3.16.   Close N2O source cylinder.

2.3.17.   Slowly open the transfer pump system vent V5. Once fill system has vented, close valve.

2.3.18.   Return to control cell

2.4. Ethanol fill (As required):
2.4.1.   Open the ethanol run tank vent valve #10 using Labview Manual Control and keep open during fill procedure.

2.4.2.   1 person leaves the cell for the following steps

2.4.3.   Visually confirm Valve 10 is open

2.4.4.   Place ethanol supply bottle in holder.

2.4.5.   Attach pump hose to bottle.

2.4.6.   Open ethanol run tank fill valve (F1)

2.4.7.   Return to the control cell and close the Control Room door.

2.4.8.   Record the initial mass on the scale (fuel bottle weight) below and fill out
the remainder of the table below for the desired values:
Ethanol fuel flow rates are given in the appendix for reference

Desired Mass of fuel:_____   Actual mass fuel: _____

Initial scale reading:_____

Desired final scale reading:_____   Actual final mass: _____

2.4.9.   Obtain clearance from the Test Manager that the area is clear, personnel
accounted for, and the fill process is ready to proceed.

2.4.10.   Arm Fill Control. Using Propellant Fill camera, engage ethanol transfer
pump until designated weight decrease displayed by the scale is observed.

2.4.11.   Disarm Fill Control.

2.4.12.   End fill sequence, close vent valve #10 using Labview Manual Control

2.4.13.   1 person leaves cell for the following steps

2.4.14.   Visually check valve 10 is closed

2.4.15.   Close ethanol run tank fill valve (F1)

2.4.16.   Disconnect supply bottle from fill hose. Cap bottle and remove from Fuel
Galley.

2.4.17.   Store ethanol bottle in East Lab or onsite in flammable cabinet in Test
Cell.

3. ROCKET TEST PROCEDURE

3.1. System Pressurization/Igniter Connection:

3.1.1.   Conduct a no voltage check on igniter firing line using voltmeter in Control Room.

3.1.2.   Obtain clearance from the Test Manager that the area is clear, personnel accounted for, and that igniter connection/system pressurization is ready to proceed.

3.1.3.   One person leaves cell for the following steps

3.1.4.   Plug in ignition transformer in Test Cell

3.1.5.   Connect the ignition wire to the spark plug on the igniter in Test Cell.

3.1.6.   Open O2 and H2 bottles.

3.1.7.   Set O2 regulator in test Cell to 1100psi.

3.1.8.   Set H2 regulator in Test Cell to 700psi.

3.1.9.   Open valves H1 and H2.

3.1.10.   Ensure rocket engine is ready to fire by inspecting region around rocket engine exit nozzle. Ensure nozzle cover has been removed. Perform a final visual check of area. This is the last step in the test cell before firing.

3.1.11.   Walk to Fuel Galley

3.1.12.   Open propellant system supply hand valves (S1, S2)

3.1.13.   Set N2 purge regulators to predetermined test pressure (R3, R4)
Set Pressure:＿＿＿＿＿＿＿＿

3.1.14.   Set N2 supply regulators to predetermined test pressure (R1, R2)
Set Pressure:＿＿＿＿＿＿＿＿
Purge pressure must be greater than supply pressure

3.1.15.   Open purge supply valve slowly to pressurize system (P1, P2)

3.1.16.   Perform a final visual check of the fuel galley, this is the last step in the fuel galley before firing.

3.1.17.   Remove all personnel to the personnel shelter/Control Room and close Control Room door.

3.2. Line Fill Procedure:

3.2.1.   Obtain clearance from the Test Manager that the area is clear using exterior cameras and monitor. Confirm all personnel are accounted for. Confirm the line fill procedure is ready to proceed.

3.2.2.   Ensure data acquisition is operational.

3.2.3.   Ensure video recording is active.

3.2.4.   Activate Labview control system by depressing "Ready System" button.

3.2.5.   Performing Line Fill procedure through Labview Manual Control:

3.2.5.1.   Turn on Labview Manual Control.

3.2.5.2.   Slow pressurize N2O by opening Valve 3, keep open until pressure in N2O run tank equals pressure in N2 push gas. Close Valve 3.

3.2.5.3.   Ensure temperature in N2O run bottle is below 85 F.

3.2.5.4.   Open Valve 4.

3.2.5.5.   Close Valve 4.

3.2.5.6.   Slow pressurize ethanol by opening Valve 2 until pressure in ethanol run tank is within 200 psi of the N2 push gas. Close Valve 2.

3.2.5.7.   Open Valve 1.

3.2.5.8.   Close Valve 1. Turn off Labview Manual Control.

3.2.5.9.   Activate N2O Line Fill using LabView control. Repeat operation until N2O is observed exiting rocket engine.

3.2.5.10.   Activate Ethanol Line Fill using LabView control. Repeat operation until ethanol is observed exiting rocket engine.

3.3. Rocket Engine Firing:

3.3.1.   Obtain final clearance from the Test Engineer that all personnel are accounted for, are a go, and the test is ready to proceed.

3.3.2.   Read all steps in this sequence up to the test manager resuming control out loud to everyone before proceeding, then read them out loud during sequencing.

3.3.3.   Operator takes control for next steps.

3.3.4.   Turn on "Data Acquisition Save to File" operation.

3.3.5.   Depress deadman's switch and arm the ignition system with the key switch. The deadman's switch must be depressed to prevent full system shutdown. In emergency, release deadman's switch.

3.3.6.   Arm Labview control system firing procedure.

3.3.7.   Operator announce intent to fire rocket, then depress red fire button in LabView when ready.

3.3.8.   Depress red fire button in Labview

3.3.9.   Disarm Labview firing procedure.

3.3.10.   Disarm the ignition system and remove hand from deadman's switch.

3.3.11.   Test manager resumes control.

3.3.12.   Turn off data acquisition.

3.3.13.   If additional test are to be performed, purge N2O propellant tank and line:
If not, move to step 3.3.14

3.3.13.1.   Turn on Labview Manual Control.

3.3.13.2.   Open valve 3 until N2O tank pressure is equal to supply pressure. Close Valve 3.

3.3.13.3.   Open Valve 4.

3.3.13.4.   Purge N2O propellant system by opening Valve 5/13 until observed clear through video observation system.

3.3.13.5.   Close Valve 4.

3.3.13.6.   Open Valve 5/13 until N2O tank and line pressure is equal to zero.

155

3.3.13.7.   Open valve 10 to relieve ethanol tank pressure.

3.3.14.   If no additional tests are to be performed, purge system of propellant:
If additional tests to be performed, move to 3.3.14

3.3.14.1.   Open valve 3 until N2O tank pressure is equal to supply pressure.

3.3.14.2.   Open Valve 4.

3.3.14.3.   Pulse Valves 5/13 until observed clear through video observation. (N2O line purge).

3.3.14.4.   Close Valve 4.

3.3.14.5.   Open Valves 5/13.

3.3.14.6.   Open valve 12 then close valve 12 (Ethanol line purge).

3.3.14.7.   Close valve 5/13

3.3.15.   When the area is safe and cleared by the Test Engineer by visual inspection using the camera observation system, personnel may exit the personnel shelter/Control Room to complete section 4, "End of Test Shutdown Procedure". Caution all personnel that the rocket engine will be hot and should not be touched.

3.3.16.   Turn off video recording.

4. END OF TEST SHUTDOWN PROCEDURE

4.1. System Purge:

4.1.1.   All personnel should have eye and ear protection. Entering the Test Cell also requires gloves to be equipped. Rocket and test stand will be hot, do not touch.

4.1.2.   Close N2 purge valves P1 and P2.

4.1.3.   Close supply valves S1 and S2.

4.1.4.   If no additional tests are to be performed at the same operating pressure as the previous test:
If additional tests to be performed, move to step 4.1.5.

4.1.4.1.   Close N2 high-pressure regulators (R1, R2, R3, R4).

4.1.4.2.   Slowly open hand vent valves (V1, V2, V3, V4).

4.1.4.3.   Close hand vent valves (V1, V2, V3, V4).

4.1.4.4.   Return N2 supply and purge regulators to 150psig (R1, R2, R3, R4).

4.1.5.   Return to Control Room and close door.

4.1.6.   Vent propellant lines by opening Valves 5/13 until venting of gas/liquid is no longer observed, then close Valves 5/13.

4.1.7.   Vent purge lines by opening Valves 6/14 until venting of N2 gas is no longer observed, then close Valves 6/14.

4.1.8.   Exit Control Room and move to Test Cell.

4.1.9.   Disconnect ignition wire from ignition spark plug in Test Cell.

4.1.10.   Close O2 and H2 bottles.

4.1.11.   Open purge line valves P1 and P2.

4.1.12.   Return to Control Room.

4.1.13.   Depress deadman's switch and arm igniter circuit.

4.1.14.   Vent O2 and H2 valves using Manual Control in LabView.

4.1.14.1.   Vent O2 by opening Valve 16 for 3 seconds, then close Valve 16.

4.1.14.2.   Purge engine with N2 by pulsing Valves 6/14.

4.1.14.3.   Vent H2 by opening Valve 15 for 3 seconds, then close Valve 15.

4.1.14.4.   Purge engine with N2 by pulsing Valves 6/14.

4.1.14.5.   Disarm igniter and release deadman's switch.

4.1.15.   Close purge line valves P1 and P2.

4.1.16.   Return to Control Room.

4.1.17.   Vent purge lines by opening Valves 6/14 until venting of N2 gas is no longer observed, then close Valves 6/14.

4.1.18.   Turn off Labview Manual Control.

4.1.19.   Exit Control Room, return to Test Cell.

4.1.20.   Close O2 and H2 regulators in Test Cell.

4.1.21.   Close valves H1 and H2

If additional tests are to be performed. Return to section 1, step 1.1, and fill out new test cover sheet, then start operations from section 2.

5. END OF DAY SHUTDOWN PROCEDURE
5.1. System Purge:
5.1.1.   Close N2 Supply bottles in Fuel Galley (Bottles 1-4)

5.1.2.   Operate LabVIEW valve sequential check.

5.1.3.   Open vent valves V1, V2, V3, V4.

5.1.4.   Close purge valves P1 and P2.

5.1.5.   Close vent valves V1, V2, V3, V4.

5.1.6.   Close regulators R1, R2, R3, R4.

5.2. Final Shutdown:
5.2.1.   Close N2 bottle 5.

5.2.2.   Drain ethanol from run tank, empty ethanol from dump system in fuel galley and test cell

5.2.3.   Reattach vent covers (6 in total)

5.2.4.   Check that propellant system supply hand valves S1 and S2 and fill valves F1 and F2 are closed. Lock out where indicated for S1, S2, F1, and F2

5.2.5.   Turn off propellant scale.

5.2.6.   Turn off video recording system.

5.2.7.   Turn off DAQ control system and supporting power supplies.

5.2.8.   Check that regulators in Fuel Galley R1, R2, R3, R4 are closed.

5.2.9.   If rocket engine is cool and there is liquid pooled in it, dry interior of rocket engine

5.2.10.   Secure doors to test cell, fuel galley and control cell

6. **CONTINGENCY PROCEDURES (Non Life Threatening):**

   6.1. Intermittent Firing:

   6.1.1.   Stop test by clicking and releasing red fire button in LabVIEW.

   6.1.2.   Continue to depress deadman's switch.

   6.1.3.   If propellant is still remaining and an attempt to fire again is desired, obtain clearance from Test Engineer that area is still clear and a retest can proceed.

   6.1.4.   Depress red fire button in LabVIEW.

   6.1.5.   If rocket engine does not fire or is intermittent in operation, release red fire button in Labview. Run End of Test shutdown procedure (Section 5).

   6.1.6.   Restart test and return to Start of Test Procedure (Section2)

   6.2. No Fire:

   6.2.1.   Stop test by clicking and releasing red fire button in LabVIEW.

   6.2.2.   Continue to depress deadman's switch.

   6.2.3.   Check 24VDC on ignition supply and valve supply.

   6.2.4.   Check relay operation by LabVIEW.

   6.2.5.   If propellant is still remaining and an attempt to fire again is made, obtain clearance from Test Engineer that area is still clear and a retest can proceed.

   6.2.6.   Depress red fire button in LabVIEW.

   6.2.7.   If rocket engine does not fire or is intermittent in operation, release red fire button in Labview. Run End of Test shutdown procedure (Section 5).

   6.2.8.   Restart test and return to Start of Test Procedure (Section2)

7. CONTINGENCY PROCEDURES (Life Threatening):
    7.1. The following procedure is for:
        Explosion of Rocket Engine
        Explosion of Propellant Run Tank
        Pressure Line Rupture
        Failure to shut down
        Test site fire
        Power loss

    7.1.1.   Release deadman's switch.

    7.1.2.   Wait 10 seconds.

    7.1.3.   Depress and hold deadman's switch to blow out any propellant still in lines.

    7.1.4.   Run LabView End of Day purge sequence.

    7.1.5.   Disarm ignition system via key switch.

    7.1.6.   Call the Life Threatening Hazard Call Tree in section 9

    7.1.7.   If still operating, let system burn out, and remain in cell until all gas cylinders empty.

    7.1.8.   If power loss remain in shelter until someone from the safety office can visually inspect area and confirm all clear for personnel to exit shelter.

8. SAFETY CALL TREE
    8.1. Life Threatening:
        8.1.1.   Campus Police: Ext. 5555. (Call if injury, uncontrolled fire, or death)

        8.1.2.   Safety Office, Phone Number: 575-835-5644

        8.1.3.   Michael J. Hargather, Phone Number: 585-738-7055

    8.2. Non Life Threatening:
        8.2.1.   Safety Office, Phone Number: 575-835-5644

        8.2.2.   Michael J. Hargather, Phone Number: 585-738-7055

Rocket Engine LabView Run Sequence

1) Opening valves: 1, 4. Time sequence: 3s
Valves open at end of sequence: 1, 4.

2) Opening valves: 15, Spark on. Time sequence: 0.250s.
Valves open at end of sequence: 1, 4, 15, spark on

3) Opening valves: 7, 8, 16. Time sequence: 0.750s.
Valves open at end of sequence: 1, 4, 7, 8, 15, 16, spark on

4) Closing valves: 15, Spark on. Time sequence: 0.250s.
Valves open at end of sequence: 1, 4, 7, 8, 16

5) Main run period. Time sequence: Run time minus 1s.
Valves open at end of sequence: 1, 4, 7, 8

6) Closing valves: 7, 8. Opening valves: 6, 14. Time sequence: 1s.
Valves open at end of sequence: 1, 4, 6, 14

7) Closing valves: 1, 4, 6, 14. Time sequence: sequence ends.
Valves open at end of sequence: none

B.4 Oxygen Cleaning Procedure

O2 Service Cleaning Procedure

Author: Stewart H. Youngblood
Written: February 3, 2015
Updated: August 12, 2015
Based on "CGA G-4.1 Cleaning Equipment for Oxygen Service"
Version 1.2
Updated:

Equipment:
- Eye protection
- Inspection/Handling gloves (Latex or Nitril). POWDER FREE
- Hair net or cap
- Strong white light source
- UV light source (2500 to 3700 angstrom units)
- Solvent (ethanol or acetone)
- Trichloroethylene (CRC Brakleen). Do not use toothbrushes with.
- Tweezers
- Lint free cloth or wipes (kim-wipes)
- Firm bristol toothbrush. Should be rinsed with solvent (Not Trichloroethylene) prior to use. Do not reuse for new parts
- Dry compressed gas (Dry air, nitrogen, electronics compressed gas). OIL FREE
- Distilled water (New sealed bottles, do not reuse water from previous cleanings)
- Ultra-Sonic cleaner
- Freezer Ziplock bags (gallon for big parts, quart for little parts)

Prep:
- Wear gloves, eye protection, and cap or hair net at all times
- Wear new pair of gloves for each step
- Heat distilled water
- All cleaning should be performed in fume hood. Solvents use should be collected and disposed of properly. Proper safety gear required.
- **EACH PHASE REQUIRES NEW PAIR OF GLOVES**

Remove all visible contaminants
1. Visually Inspect
    - Use strong white light
    - Technician should have 20/20 vision
2. Remove all visible debris
    - For particulate, use lint free wipes, tweezers, dry compressed gas
    - For oil/grease, clean by:
        1. Wash with trichloroethylene
        2. Rinse with solvent
        3. Wipe with lint free cloth/wipe

4. Wash with solvent
5. Dry part with dry compressed gas

Hot water wash

1. Wash
   - Use hot distilled water
   - Scrub using firm bristol tooth brush (focus on crevices, orifices, threads, etc)
2. Dry with dry compressed gas

Ultra-sonic and final cleaning

- Flush with trichloroethylene. (Focus on crevices, orifices, threads, etc)
- Ultrasonic clean using solvent for 20 minutes
- Ultrasonic clean in distilled water for 10 minutes
- Wear new set of gloves
- Dry with compressed gas
- Rinse cleaned part with solvent
- Dry with compressed gas
- Bag cleaned part in new ziplock bag

Final Inspection

1. Visually inspect with strong white light
2. Visually inspect with ultraviolet light (2500 to 3700 angstrom units)
3. With successful inspection, bag cleaned part and mark:
   - Date of inspection and inspectors name
   - Part description and part number
   - "Do not open until ready for use"

   FAILURE OF EITHER INSPECTION TEST REQUIRES RECLEANING

Allowable Contamination:
- Oil/grease or particulate matter detected should not exceed 47.5 grams per square foot ($500mg/m^2$) with no particle larger than 1000 microns and no more than 20 particles per square foot (250 particles/m^2)

Ethanol/N2O Fuel System Diagram

Supply Section

See legend on full system diagram

Last edited on: May 24, 2015
By: Jeff Phillip

Low P N2

Eth Pressure
Supply

Eth Purge
Supply

N2O Purge
Supply

N2O Pressure
Supply

N2O Pump
Pressure Supply

R5

Low
Pressure
N2 Supply
(Bottle 5)

1

2

3

4

V2

PG2

R2

PG1

V1

Ethanol
Pressure
Supply
(Bottle 2)

R1

N2O
Pressure
Supply
(Bottle 1)

PG3

P1

P2

PG4

V3

V4

R3

R4

Ethanol
Purge
Supply
(Bottle 3)

N2O
Purge
Supply
(Bottle 4)

Tank Section

See legend on full system diagram

Low P N2

Eth Pressure
Supply

Eth Purge
Supply

N2O Purge
Supply

N2O
Pressure
Supply

10

9

ETHANOL TANK

12

11

Eth Purge
Line

Low Pressure
N2

N2O TANK

PG5 P

F2

S2

Eth Line

N2O Line

**R6
80psi**

PG6 P

F1

S1

V6

N2O Purge
Line

N1

V5

N20 Bottle
(Bottle 6)

Ethanol
Container

Drain

Engine Section

Last edited on: May 24, 2015
By: Jeff Phillip

Engine

R8

16

H2 Bottle
(Bottle 8)

O2 Bottle
(Bottle 7)

R7

15

14

8

7

6

13

5

TC8 T

PG8 P

TC7 T

PG7 P

N2 Low
Pressure

Eth Purge
Line

Ethanol Line

N2O Line

N2O Purge
Line
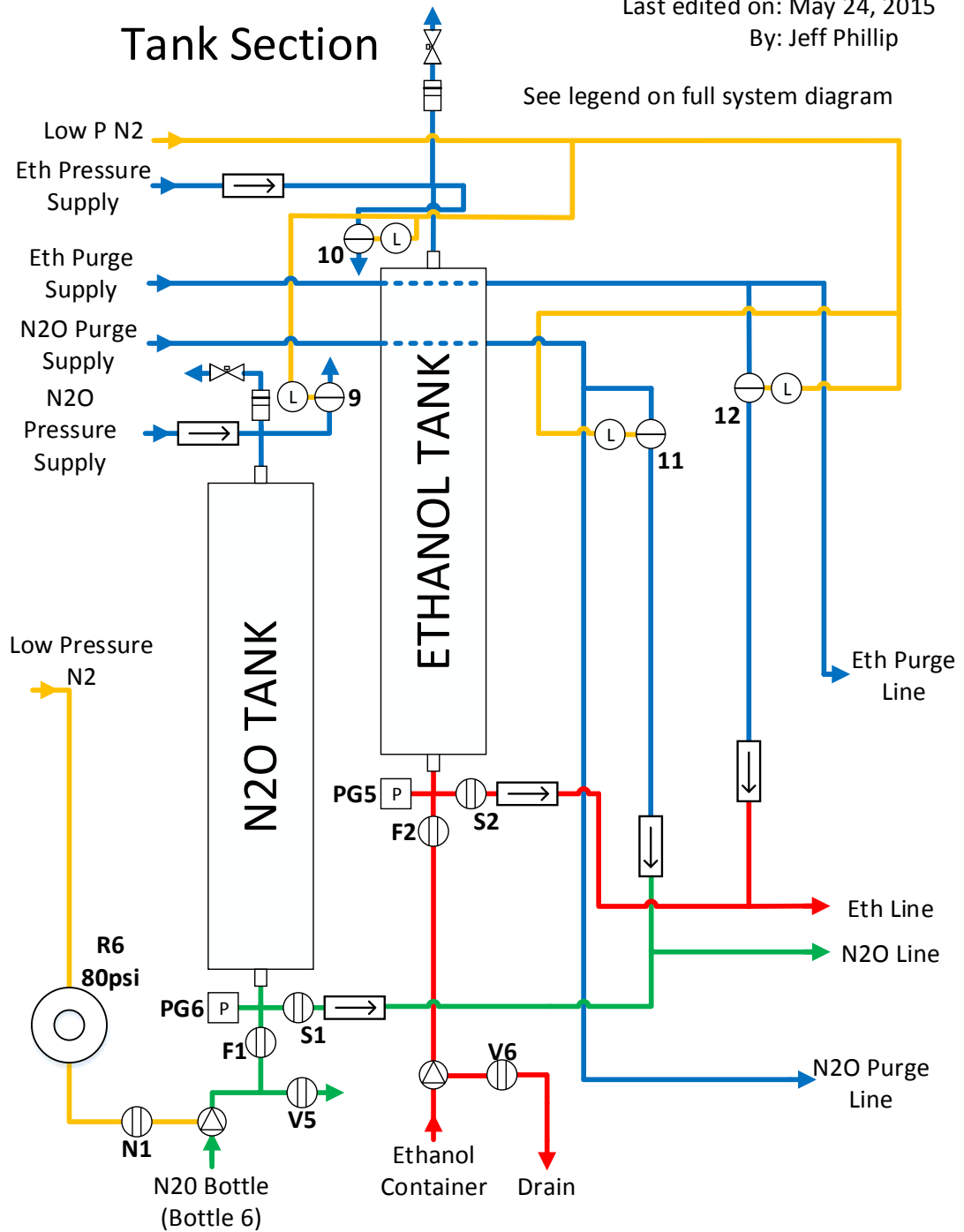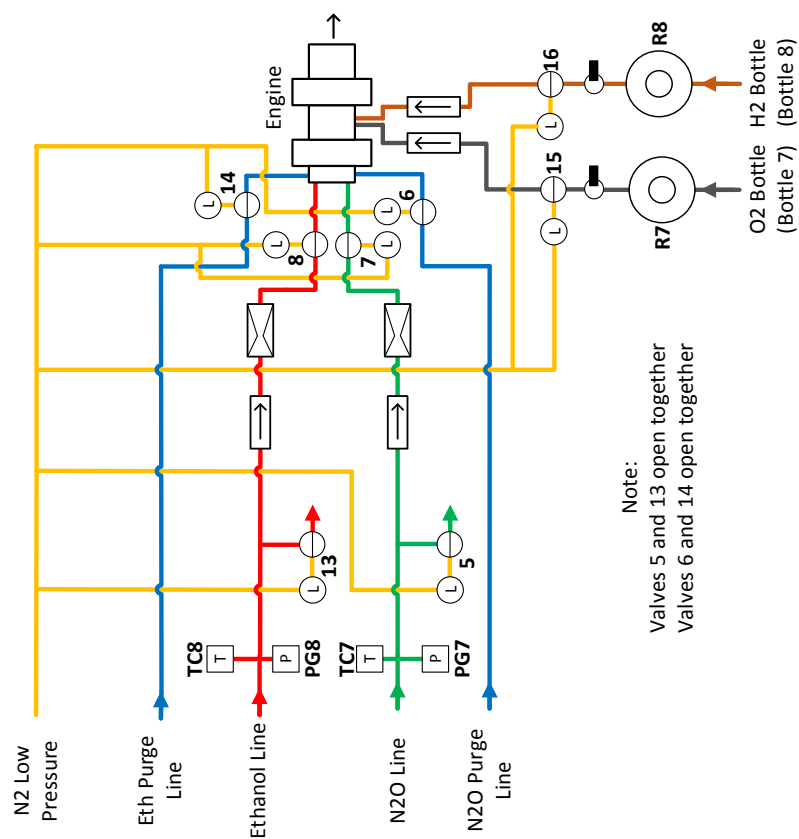
Note:
Valves 5 and 13 open together
Valves 6 and 14 open together

See legend on full system diagram

168

APPENDIX C

EXPERIMENTAL RESULTS

C.1 Uncertainty Equation Derivations

The uncertainty equation for the mass flow rate through a cavitating venturi is calculated by combining the reformatted cavitating venturi mass flow rate Equation C.1 with Equation C.2

$$\dot{m} = \frac{\pi}{4} D_t^2 * C_d \sqrt{\frac{2g\rho}{144}(P - P_v)} \tag{C.1}$$

$$\Delta Q = \sqrt{\left(\frac{\partial f}{\partial x}\Delta x\right)^2 + \left(\frac{\partial f}{\partial y}\Delta y\right)^2 + \dots} \tag{C.2}$$

This yielded Equation C.3:

$$\Delta \dot{m} = \left[\left(\frac{\partial \dot{m}}{\partial D_t}\Delta D_t\right)^2 + \left(\frac{\partial \dot{m}}{\partial C_D}\Delta C_D\right)^2 + \left(\frac{\partial \dot{m}}{\partial \rho}\Delta \rho\right)^2 + \right.$$
$$\left. + \left(\frac{\partial \dot{m}}{\partial P}\Delta P\right)^2 + \left(\frac{\partial \dot{m}}{\partial P_v}\Delta P_v\right)^2 \right]^{\frac{1}{2}} \tag{C.3}$$

The partial derivatives are solved individually and combined with the associated Δx. Using Equation C.1, the equations were rearranged as shown below:

$$\frac{\partial \dot{m}}{\partial D_t}\Delta D_t = \frac{\pi}{4} D_t * C_d \sqrt{\frac{2g\rho}{144}(P - P_v)} * 2\Delta D_t \tag{C.4}$$

$$= \dot{m} * 2\frac{\Delta D_t}{D_t} \tag{C.5}$$

$$\frac{\partial \dot{m}}{\partial C_D} \Delta C_D = \frac{\pi}{4} D_t^2 * \sqrt{\frac{2g\rho}{144}(P - P_v)} * \Delta C_D \tag{C.6}$$

$$= \dot{m} * \frac{\Delta C_D}{C_D} \tag{C.7}$$

$$\frac{\partial \dot{m}}{\partial \rho} \Delta \rho = \frac{\pi}{4} D_t^2 * C_D \sqrt{\frac{2g}{144}(P - P_v)} * \frac{1}{2\sqrt{\rho}} \Delta \rho \tag{C.8}$$

$$= \dot{m} * \frac{\Delta \rho}{2\rho} \tag{C.9}$$

$$\frac{\partial \dot{m}}{\partial P} \Delta P = \frac{\pi}{4} D_t * C_d \sqrt{\frac{2g\rho}{144}} * \frac{1}{2\sqrt{(P - P_v)}} \Delta P \tag{C.10}$$

$$= \dot{m} * \frac{\Delta P}{2(P - P_v)} \tag{C.11}$$

$$\frac{\partial \dot{m}}{\partial P_v} \Delta P = \frac{\pi}{4} D_t * C_d \sqrt{\frac{2g\rho}{144}} * -\frac{1}{2\sqrt{(P - P_v)}} \Delta P_v \tag{C.12}$$

$$= \dot{m} * \frac{-\Delta P_v}{2(P - P_v)} \tag{C.13}$$

Equations C.5, C.7 , C.9, C.11, and C.13 were plugged into Equation C.3. This yields Equation C.14:

$$\Delta \dot{m} = \left[\left(\dot{m} * 2\frac{\Delta D_t}{D_t} \right)^2 + \left(\dot{m} * \frac{\Delta C_D}{C_D} \right)^2 + \left(\dot{m} * \frac{\Delta \rho}{2\rho} \right)^2 + \right.$$
$$\left. + \left(\dot{m} * \frac{\Delta P}{2(P - P_v)} \right)^2 + \left(\dot{m} * \frac{-\Delta P_v}{2(P - P_v)} \right)^2 \right]^{\frac{1}{2}} \tag{C.14}$$

By bringing $\dot{m}$ to outside of the square root and rearranging Equation C.14, the uncertainty equation takes the final form shown in Equation C.15:

$$\Delta \dot{m} = |\dot{m}| \left[\left(2\frac{\Delta D_t}{D_t} \right)^2 + \left(\frac{\Delta C_D}{C_D} \right)^2 + \left(\frac{\Delta \rho}{2\rho} \right)^2 + \right.$$
$$\left. \left(\frac{\Delta P}{2(P - P_v)} \right)^2 + \left(\frac{-\Delta P_v}{2(P - P_v)} \right)^2 \right]^{\frac{1}{2}} \tag{C.15}$$

The total mass flow rate uncertainty is a function of the uncertainty of the mass flow rate of fuel and mass flow rate of oxidizer, shown in Equation C.16:

$$\Delta \dot{m}_{tot} = \sqrt{\Delta \dot{m}^2_{fuel} + \Delta \dot{m}^2_{oxidizer}} \qquad \text{(C.16)}$$

The uncertainty equation for the calculated ISP was derived by combining Equation C.17 with Equation 5.3. Following the same procedure as above, Equation C.18 was formulated.

$$I_{sp} = \frac{F}{\dot{m}_{tot} g} \qquad \text{(C.17)}$$

$$\Delta ISP = |ISP| \sqrt{\left(\frac{\Delta F}{F}\right)^2 + \left(\frac{\Delta \dot{m}_{tot}}{\dot{m}_{tot}}\right)^2} \qquad \text{(C.18)}$$

APPENDIX D

MATLAB/CANTERA ROCKET ENGINE MODELING CODE

D.1   MATLAB/Cantera Equilibrium and Property Calculator

D.2   Initial Model

D.2.1   Initialization and Data Processing

```
%%% Liquid Fueled Rocket Modeling Code %%%
%% Created by: Stewart Youngblood. Written: 12/23/13. Edited:1/26/2014
%
%This code is written to provide a simple model for a liquid fueled
   rocket
%which accounts for reactions between fuel and oxidizers in the
   combustion
%chamber and the nozzle.
%
%OUTPUTS:
%Plots of:
%1)Characteristic velocity, C_star,
%2)Combustion Chamber Stagnation Temperature, T0
%3)Nozzle Throat Temperature, T_t
%4)Exhaust Exit Temperature, Te
%5)Mole Fractions, ym
%5)Exit Velocity
%7)Thrust Coefficient, Cf
%8)Optimal Expansion Ratio, Aexit/Athroat (Aratio)
%9)Exit Mach Number, Me
%All plotted vs mixture ratio. Here mixture ratio is defined as
%mdot_oxidizer/mdot_fuel.
%
%INPUTS:
%1)Oxidizer
%2)Fuels:
%    -HDPE
%    -Propane
%    -Ethanol
%    -Isoctane
```

```matlab
%3)Estimated Chamber Pressure, Pchamber
%4)Ambient Conditions, Po, To
%
%Assumptions:
%1)Combustion takes place at a constant temperature and pressure in
    combustion
%chamber.
%2)Combustion consists of only  Fuel and Oxidizer. Looking at
    combustion at steady
%state and assume nitrogen purge gas has been blown out.
%
%Known Issues:
%1)With Ethanol_N2O.xml, cantera crashes if step size to small.
    Currently
%will only run with a step size of 0.05 or larger.
%2)Step Size is very important for graphs, smallest is best but code
    runs longer.
%3)Setting the minimum ratio too low for HDPE will result in cantera
%crashing due to negative temperature calculations. ratio_min=0.4 is
%minimum before cantera crashes.
%4)Freezes with Ioctane, haven't determined cause.


close all;
clc
clear all
format compact;
tic



%% INPUT
%Code Conditions
step = 0.1;
ratio_min =8.55;
ratio_max = 8.55;
ratio = ratio_min:step:ratio_max; % Mixture Ratio
%Ambient Conditions
Po = 101325%85900; %Pa. Approximate atmospheric air pressure at 4500ft.
To = 298; %K
PSI_Pa = 0.000145037738;


%Test Properties
Pexit = Po;
Tpre = To;
Pchamber = 1000/PSI_Pa; %Pa. Are assuming chamber pressure.
Oxidizer = 'N2O';
Fuel = 'Ethanol';
```

```matlab
%% OUTPUT
[C_star,To_K,T_t_K,Te_K,Ve,ym,Aratio,Me,Cf,Ke,Isp] = Get_Properties(
    Pexit,Tpre,Pchamber,Fuel, Oxidizer,ratio);

%% PLOTTING
%Converting
 To_F = (To_K-273).*1.8 + 32;
 T_t_F = (T_t_K-273).*1.8 + 32;
 Te_F = (Te_K-273).*1.8 + 32;
Ve_ft = Ve*3.28;

% C* T_t and To plots
AF_ratio = ratio;
figure;
hold on;
plot(AF_ratio,C_star*3.28,'b');
plot(AF_ratio,To_F,'r');
plot(AF_ratio,T_t_F,'k');
plot(AF_ratio,Te_F,'m');
plot(AF_ratio,Ve_ft,'g');
title('Engine Performance vs Mixture Ratio for 1000PSI Chamber Pressure
    ');
xlabel('Mixture Ratio');
ylabel('Temperature ( F), C*(ft/s), Velocity (ft/s)');
legend('C*','T_{o}', 'T_{throat}', 'T_{exit}', 'V_{exit}');
axis([ratio_min ratio_max 0 6000]);
grid;
PlotFixer2014()
hold off;

%mole fractions plot
% figure;
% hold on;
% plot(AF_ratio, ym(:,1),'b');
% plot(AF_ratio, ym(:,2),'g');
% plot(AF_ratio, ym(:,3),'r');
% plot(AF_ratio, ym(:,4),'c');
% plot(AF_ratio, ym(:,5),'m');
% plot(AF_ratio, ym(:,6),'y');
% plot(AF_ratio, ym(:,7),'k');
% plot(AF_ratio, ym(:,8),'g--');
% plot(AF_ratio, ym(:,9),'b--');
% plot(AF_ratio, ym(:,10),'r--');
% plot(AF_ratio, ym(:,11),'c--');
% plot(AF_ratio, ym(:,12),'k--');

% title('Product Mole Fractions vs Mixture Ratio');
% xlabel('Mixture Ratio');
% ylabel('Mole Fractions');
% legend('H' ,'H_{2}', 'O' ,'O_{2}', 'OH', 'CO', 'CO_{2}', 'H_{2}O', '
```

174

```
   N_{2}', 'NO', 'N2O', Fuel);
% axis([ratio_min ratio_max 0 .6]);
% grid;
% PlotFixer2014()
% hold off;


figure;
hold on;
plot(AF_ratio, Aratio,'b');
plot(AF_ratio, Me,'k');
plot(AF_ratio, Cf,'g');
plot(AF_ratio, Isp/100,'R');
title('Engine Performance vs. Mixture Ratio for 1000PSI Chamber
   Pressure');
xlabel('Mixture Ratio');
ylabel('Area Ratio, Cf, Mach Number, Isp/100');
legend('A_{exit}/A*','M', 'Cf', 'Isp(s)/100');
grid;
% axis([1 10 0 11]);
hold off;
PlotFixer2014()
toc
```

D.2.2   Rocket Engine Model

```
function [C_star,To,T_t,Te,Ve,ym,Aratio,Me,Cf,Ke,Isp] = Get_Properties(
   Pexit,Tpre,Pchamber,Fuel,Oxidizer,ratio)
%% Created by: Stewart Youngblood. Written: 12/23/14. Edited:1/27/14
%This function calculates the gas flow from the combustion
%chamber to the nozzle exit and accounts for intial reaction in the
%combustion chamber and reactions through the nozzle.
%
%INPUT:
%1)Exit Pressure - Pexit (Pa)
%2)Temperature pre-combustion - Tpre (K)
%3)Assumed Chamber combustion pressure - Pchamber (Pa)
%4)Fuel (String)
%5)Oxidizer (String)
%6)Mixing Ratio - ratio (Array)
%
%OUPUT:
%1)Characteristic Velocity - C_star
%2)Stagnation Temperature - To (K)
%3)Throat Temperature - T_t (K)
%4)Exit Temperature - Te (K)
%5)Exit Velocity - Ve (m/s)
%6)Mole Fractions of Exhaust Gas - ym
%7)Area Ratio of Throat to Nozzle - Aratio
```

```matlab
%8)Exit Mach Number - Me
%
%Note: Code saves many properties as it cycles through. Can call upon
   more
%properties then those outputted if needed, look in Array Construction
   for
%properties saved.

%% INITIALIZATION
%---ARRAY CONSTRUCTION---%
To = zeros(length(ratio),1);
Po = zeros(length(ratio),1);
Cpo = zeros(length(ratio),1);
Cvo = zeros(length(ratio),1);
rho_o = zeros(length(ratio),1);
ho = zeros(length(ratio),1);
Ko = zeros(length(ratio),1);
Ro = zeros(length(ratio),1);
co = zeros(length(ratio),1);
Cp = zeros(length(ratio),1);
Cv = zeros(length(ratio),1);
rho_t = zeros(length(ratio),1);
T_t = zeros(length(ratio),1);
P_t = zeros(length(ratio),1);
v_t = zeros(length(ratio),1);
ct = zeros(length(ratio),1);
K = zeros(length(ratio),1);
R = zeros(length(ratio),1);
Ke = zeros(length(ratio),1);
Te = zeros(length(ratio),1);
Re = zeros(length(ratio),1);
rho_e = zeros(length(ratio),1);
he = zeros(length(ratio),1);
Ve = zeros(length(ratio),1);
ce = zeros(length(ratio),1);
C_star = zeros(length(ratio),1);
Cf = zeros(length(ratio),1);

Aratio = zeros(length(ratio),1);
Me = zeros(length(ratio),1);
Isp = zeros(length(ratio),1);

%---GAS OBJECTS---%
switch Fuel
    case 'Propane'
        gas = IdealGasMix('GRI30.xml');
        iFUEL = speciesIndex(gas,'C3H8');
        iOXI = speciesIndex(gas,Oxidizer);
        species = {'H' 'H2' 'O' 'O2' 'OH' 'CO' 'CO2' 'H2O' 'N2' 'NO' '
            N2O' 'C3H8'};
```

```matlab
        ym = zeros(length(ratio),length(species));

    case 'Ethanol'
        %gas = IdealGasMix('ethanol_mech.xml');
        %gas = IdealGasMix('Ethanol_N2OSimple.xml');
        gas = IdealGasMix('Ethanol_N2O.xml');
        iFUEL = speciesIndex(gas,'C2H5OH');
        iOXI = speciesIndex(gas,Oxidizer);
        species = {'H' 'H2' 'O' 'O2' 'OH' 'CO' 'CO2' 'H2O' 'N2' 'NO' '
           N2O' 'C2H5OH'};
        ym = zeros(length(ratio),length(species));

        %NOTE: Have simple xml file with only 12 species for Ethanol/
           N2O
        %reaction and have more advanced Ethanol File with 50 plus
           species.
        %The larger xml predicts at a lower mixing ratio. Neither file
           has
        %kinetics, so will add xml with kinetics

    case 'Ioctane'
        gas = IdealGasMix('IoctaneSkelMech.xml');
        iFUEL = speciesIndex(gas,'ic8h18');
        iOXI = speciesIndex(gas,Oxidizer);
        species = {'h' 'h2' 'o' 'o2' 'oh' 'co' 'co2' 'h2o' 'n2' 'no' '
           n2o' 'ic8h18'};
        ym = zeros(length(ratio),length(species));

    case 'HDPE'
        gas = IdealGasMix('me140_N2O.xml');
        iFUEL = speciesIndex(gas,'C2H4');
        iOXI = speciesIndex(gas,Oxidizer);
        species = {'H' 'H2' 'O' 'O2' 'OH' 'CO' 'CO2' 'H2O' 'N2' 'NO' '
           N2O' 'C2H4'};
        ym = zeros(length(ratio),length(species));

        %Enthalp Adjustment Calculations for using C2H4
        mmCH2=.0140267; %kg/mol
        mmC2H4=2*mmCH2;
        HHV_CH2=46500000*.0140267; %J/mol
        hf_CO2=-393509; %J/mol
        hf_H2O=-285830; %liquid J/mol
        hf_C2H4m=52280/mmC2H4; %J/kg
        hf_CH2=HHV_CH2+hf_CO2+hf_H2O; %J/mol
        hf_CH2m=hf_CH2/mmCH2;
        deltaH=hf_CH2m-hf_C2H4m; %J/kg
end
nsp = nSpecies(gas);
```

```matlab
%% FLUID MODEL
%Iterating through ratios. Must create an individual gas for each ratio
for i = 1:length(ratio)
    switch Fuel
        case 'Propane'
            LHV = 46.334e6;                % Lower heating value of fuel,
                from Stone.
            x_oxifuel = zeros(nsp,1);    % Molefraction array with
                zeros.
            x_oxifuel(iFUEL) = 1;        % Set fuel to phi.
            x_oxifuel(iOXI) = ratio(i);       % Set amount of oxidizer
                based on ratio

            %Set gas pre-reaction at ambient temperature and pressure.
            gas = set(gas,'T',Tpre,'P',Pchamber,'X',x_oxifuel);

        case 'Ethanol'
            x_oxifuel = zeros(nsp,1);    % Molefraction array with
                zeros.
            x_oxifuel(iFUEL) = 1;        % Set fuel to phi.
            x_oxifuel(iOXI) = ratio(i);       % Set amount of oxidizer
                based on ratio

            %Set gas pre-reaction at ambient temperature and pressure.
            gas = set(gas,'T',Tpre,'P',Pchamber,'X',x_oxifuel);

        case 'Ioctane'
            x_oxifuel = zeros(nsp,1);    % Molefraction array with
                zeros.
            x_oxifuel(iFUEL) = 1;        % Set fuel to phi.
            x_oxifuel(iOXI) = ratio(i);       % Set amount of oxidizer
                based on ratio

            %Set gas pre-reaction at ambient temperature and pressure.
            gas = set(gas,'T',Tpre,'P',Pchamber,'X',x_oxifuel);

        case 'HDPE'
            x_oxifuel = zeros(nsp,1);    % Molefraction array with
                zeros.
            x_oxifuel(iFUEL) = 1;        % Set fuel to phi.
            x_oxifuel(iOXI) = ratio(i);       % Set amount of oxidizer
                based on ratio

            %Set gas pre-reaction at ambient temperature and pressure.
            gas = set(gas,'T',Tpre,'P',Pchamber,'X',x_oxifuel);

            %adjust enthalpy from C2H4 to CH2 fuel
            y = massFractions(gas);
            H_new = enthalpy_mass(gas)+y(12).*(deltaH); %in J/kg
```

```matlab
        equilibrate(gas,'TP');
        gas=set(gas,'H', H_new, 'P', Pchamber);
    end

    %Equilibrate Gas. Do so at constant Enthalpy and Pressure
    gas = equilibrate(gas,'HP');

    %Stagnation Properties
    To(i) = temperature(gas);
    Po(i) = pressure(gas);
    Cpo(i) = cp_mass(gas);
    Cvo(i) = cv_mass(gas);
    rho_o(i) = density(gas);
    ho(i) = enthalpy_mass(gas);


    [y] = moleFraction(gas, species);

    for n = 1:length(species)
        ym(i,n) = y(n);
    end

    %---Throat Properties---%
    %Pass in gas object, outputs throat temperature and pressure
    [T_t(i), P_t(i)] = Throat_Prop(gas);

    gas = set(gas,'T',T_t(i),'P',P_t(i));
    Cp(i)=cp_mass(gas);
    Cv(i)=cv_mass(gas);
    rho_t(i)=density(gas);
    v_t(i) = soundspeed(gas);

    %---Exit Properties---%
    %Pass in gas object and exit pressure, outputs exit gas properties
    [Te(i), Ke(i), Re(i)] = Exit_Props(gas, Pexit);

    gas = set(gas,'T',Te(i),'P',Pexit);
    he(i) = enthalpy_mass(gas);
    rho_e(i) = density(gas);

    %---EXIT VELOCITY---%
    Ve(i) = sqrt(2*(ho(i) - he(i)));
    ce(i) = soundspeed(gas);
    Me(i) = Ve(i)./ce(i);

    %---AREA RATIO---%
    Aratio(i) = rho_t(i)*v_t(i)/(rho_e(i)*Ve(i));

    %---C_STAR CALCULATION--%
    Ko(i) = Cpo(i)/Cvo(i);
    Ro(i) = (Cpo(i)-Cvo(i));
```

```
        co(i) = sqrt(Ko(i)*Ro(i)*To(i));
        K(i) = Cp(i)/Cv(i);
        R(i) = (Cp(i)-Cv(i));
        ct(i) = sqrt(K(i)*R(i)*T_t(i));

        C_star(i) = (co(i)/Ko(i)) * (rho_o(i)/rho_t(i)) * (co(i)/ct(i));

        %---THRUST COEFFICIENT---%
        Cf(i) = Ve(i)/C_star(i);

        %---ISP---%
        Isp(i) = (C_star(i)*Cf(i))/9.8066;

        %Step Count
        j = length(ratio);
        steps_left = j-i
end




end
```

D.3 Advanced Model

D.3.1 Initialization and Data Processing

```
%%% Liquid Fueled Rocket Modeling Code V3 %%%
%% Created by: Stewart Youngblood. Written: 4/14/14. Edited:
%
%This code is written to provide a moderate model for a liquid fueled
   rocket
%which accounts for reactions between fuel and oxidizers in the
   combustion
%chamber and the nozzle. Calculations are for constant propallent rate,
%with mixture ratio varied via propellant proportions.
%
%Notes:
%1)Can output both single arrays and plots of multiple arrays of
   calculated
%system properties. As of 4/2/2014, set to run multiple data arrays.
   Single
%array plotting code is commented out. To run for single array use,
   comment
%out the large array plot section, uncomment the single array section,
   and
%for min and max fuel flows, put the same rates.
```

```
%
%2)Will be creating seperate code soon for running simulation for
   rocket
%with single situation parameters.
%
%3)Current XML file for ethanol and nitrous lacks kinetics mechanisms
   and
%relies on cantera for guessing. Will be updating XML file soon!

%OUTPUTS:
%Plots of:
%1)Combustion Chamber Stagnation Pressure, Pchamber
%2)Combustion Chamber Stagnation Temperature, To
%3)Nozzle Throat Temperature, T_t
%4)Exhaust Exit Temperature, Te
%5)Exit Velocity
%6)Optimal Expansion Ratio, Aexit/Athroat (Aratio)
%7)Exit Mach Number, Me
%8)Thrust
%9)Coefficient of Thrust error from calculating via equation vs flow
%properties, Cf_error
%10)Characterisitc Velocity error from calculating via equation vs flow
%properties, Cstar_error
%11)Specific heat ratio of the exit gases, K_exit
%
%All plotted vs mixture ratio. Here mixture ratio is defined as
%mdot_oxidizer/mdot_fuel.
%
%INPUTS:
%1)Oxidizer
%2)Fuels:
%    -Propane
%    -Ethanol
%3)Fuel Flow Rate Range
%4)Throat Diameter
%5)Ambient Conditions, Po, To
%
%Assumptions:
%1)Combustion takes place at a constant temperature and pressure in
   combustion
%chamber. Will soon be updating this with a droplet evap. model
%2)Combustion consists of only Fuel and Oxidizer. Looking at combustion
    at steady
%state and assume nitrogen purge gas has been blown out.
%
%Known Issues:
%1)With Ethanol_N2O.xml, cantera crashes if step size to small.
   Currently
%will only run with a step size of 0.05 or larger.
%2)Step Size is very important for graphs, smallest is best but code
```

runs longer.

```matlab
close all;
clc
clear all
format compact;
tic

%% CONSTANTS

rho_eth = 789; %kg/m^3. From http://encyclopedia.airliquide.com
rho_N2O = 1230.5; %kg/m^3. From http://encyclopedia.airliquide.com
PSI_Pa = 0.000145037738;
N_lbThrust = 0.2248;

global Pamb Tamb
%% INPUT

%%CODE CONDITIONS%%
%Ratio Array
ratio_step = 0.1;
ratio_min = 4.71;
ratio_max = 4.71;
ratio = ratio_min:ratio_step:ratio_max; % Mixture Ratio

%Propellant Flow Array
mdot_step = 0.05;
mdot_min = 0.508; %lb/s
mdot_max = 0.508; %lb/s

mdot_lbm = mdot_min:mdot_step:mdot_max; %lb/s
mdot_kg = mdot_lbm./2.2; %kg/s

%Ambient Conditions
Pamb = 85.9*1000;%101350; %Pa. 85.9kPa Approximate atmospheric air
    pressure at 4500ft.
Tamb = 294.15; %K


%Test Properties
Pexit = Pamb;
Tpre = Tamb;
Pinit = Pamb;

%Engine Parameters
D_NozExit = 1.02*(0.0254); %Input in inches but units for code is
    meters
```

```matlab
D_throat = 0.333*(0.0254); %Input in inches but units for code is
    meters


%Nozzle Area Ratio
Aratio = (D_NozExit^2)/(D_throat^2);
%Fuel and Oxidizer
Oxidizer = 'N2O';
Fuel = 'Ethanol';

%Time Estimate
%~2000sec per mixture ratio run through per mdot
RunTime_min = length(mdot_kg)*2000/60

%% OUTPUT
[Pchamber,To_K,T_t_K,Te_K,Ve,Aratio,Me,Thrust,rho_o,Cf,Cstar,Isp,K_exit
    ] = Get_Properties_V3(Aratio, Tpre, Pinit, Fuel, Oxidizer, mdot_kg,
     ratio, D_throat);


P = Pchamber*PSI_Pa;
Thr = Thrust*N_lbThrust;
%% PLOTTING
%%%LARGE ELEMENT ARRAYS%%%

%Prep Labeling
 lAF_ratio = ratio;

%Color Map
Cstr = ['r' 'g' 'b' 'k' 'y' 'm' 'c'];

%Converting numbers to Strings
mdot_plot = flipud(mdot_lbm(:));
flowstr = num2str(mdot_plot);
Dstr = num2str(D_throat*39.37);

%Converting Units. Kelvin to Farenheit
 To_F = (To_K-273).*1.8 + 32;
 T_t_F = (T_t_K-273).*1.8 + 32;
 Te_F = (Te_K-273).*1.8 + 32;

%---PRESSURE PLOTS---%
%Plotting
figure;
hold on;
m = length(mdot_plot);

for n = 1:length(mdot_plot)
    plot(AF_ratio,(Pchamber(:,m)*PSI_Pa),Cstr(m))
    m = m-1;
end
```

183

```matlab
%Labeling
title(['Chamber Pressure vs Mixture Ratio. Throat Diam(in):', Dstr]);
xlabel('Mixture Ratio');
ylabel('Chamber Pressure (PSI)');

%Legend Titling
hleg = legend(flowstr);
htitle = get(hleg,'Title');
legstr = sprintf(['  Propellant \n' ...
    '     Flow (lbm/s)']);
set(htitle, 'String', legstr);
set(htitle, 'FontSize', 18);

grid;
PlotFixer2014()
hold off




%---THRUST PLOTS---%
%Plotting
figure;
hold on;
m = length(mdot_plot);

for n = 1:length(mdot_plot)
    plot(AF_ratio,(Thrust(:,m)*N_lbThrust),Cstr(m))
    m = m-1;
end

%Labeling
title(['Thrust vs Mixture Ratio. Throat Diam(in):', Dstr]);
xlabel('Mixture Ratio');
ylabel('Thrust (lbs)');

%Legend Titling
hleg = legend(flowstr);
htitle = get(hleg,'Title');
legstr = sprintf(['  Propellant \n' ...
    '     Flow (lbm/s)']);
set(htitle, 'String', legstr);
set(htitle, 'FontSize', 18);

grid;
PlotFixer2014()
hold off

%---SPECIFIC IMPULSE---%
figure;
```

184

```matlab
hold on;
m = length(mdot_plot);

for n = 1:length(mdot_plot)
    plot(AF_ratio,(Isp(:,m)),Cstr(m))

    m = m-1;
end

%Labeling
title(['Specific Impulse vs Mixture Ratio. Throat Diam(in):', Dstr]);
xlabel('Mixture Ratio');
ylabel('Specific Impulse (s)');

%Legend Titling
hleg = legend(flowstr);
htitle = get(hleg,'Title');
legstr = sprintf(['  Propellant \n' ...
    '     Flow (lbm/s)']);
set(htitle, 'String', legstr);
set(htitle, 'FontSize', 18);

grid;
PlotFixer2014()
hold off




%---CHAMBER TEMPERATURE PLOTS---%
%Plotting
figure;
hold on;
m = length(mdot_plot);

for n = 1:length(mdot_plot)
    plot(AF_ratio,(To_F(:,m)),Cstr(m))
    m = m-1;
end

%Labeling
title(['Chamber Temperature vs Mixture Ratio. Throat Diam(in):', Dstr])
    ;
xlabel('Mixture Ratio');
ylabel('Temperature ( F )');

%Legend Titling
hleg = legend(flowstr);
htitle = get(hleg,'Title');
legstr = sprintf(['  Propellant \n' ...
    '      Flow (lbm/s)']);
```

```matlab
set(htitle, 'String', legstr);
set(htitle, 'FontSize', 18);

grid;
PlotFixer2014()
hold off




%---THROAT TEMPERATURE---%
%Plotting
figure;
hold on;
m = length(mdot_plot);

for n = 1:length(mdot_plot)
    plot(AF_ratio,(T_t_F(:,m)),Cstr(m))
    m = m-1;
end

%Labeling
title(['Throat Temperature vs Mixture Ratio. Throat Diam(in):', Dstr]);
xlabel('Mixture Ratio');
ylabel('Temperature ( F )');

%Legend Titling
hleg = legend(flowstr);
htitle = get(hleg,'Title');
legstr = sprintf(['  Propellant \n' ...
    '    Flow (lbm/s)']);
set(htitle, 'String', legstr);
set(htitle, 'FontSize', 18);

grid;
PlotFixer2014()
hold off




%---EXIT TEMPERATURE---%
%Plotting
figure;
hold on;
m = length(mdot_plot);

for n = 1:length(mdot_plot)
    plot(AF_ratio,(Te_F(:,m)),Cstr(m))
    m = m-1;
end
```

```matlab
%Labeling
title(['Exit Temperature vs Mixture Ratio. Throat Diam(in):', Dstr]);
xlabel('Mixture Ratio');
ylabel('Temperature ( F )');

%Legend Titling
hleg = legend(flowstr);
htitle = get(hleg,'Title');
legstr = sprintf(['  Propellant \n' ...
    '     Flow (lbm/s)']);
set(htitle, 'String', legstr);
set(htitle, 'FontSize', 18);

grid;
PlotFixer2014()
hold off




%---AREA RATIO---%
%Plotting
figure;
hold on;
m = length(mdot_plot);

for n = 1:length(mdot_plot)
    plot(AF_ratio,(Aratio(:,m)),Cstr(m))
    m = m-1;
end

%Labeling
title(['Area Ratio vs Mixture Ratio. Throat Diam(in):', Dstr]);
xlabel('Mixture Ratio');
ylabel('Area Ratio');

%Legend Titling
hleg = legend(flowstr);
htitle = get(hleg,'Title');
legstr = sprintf(['  Propellant \n' ...
    '     Flow (lbm/s)']);
set(htitle, 'String', legstr);
set(htitle, 'FontSize', 18);

grid;
PlotFixer2014()
hold off


%---Cf---%
%Plotting
```

```matlab
figure;
hold on;
m = length(mdot_plot);


for n = 1:length(mdot_plot)
    plot(AF_ratio,(Cf(:,m)),Cstr(m))

    m = m-1;
end

%Labeling
title(['Coefficient of Thrust vs Mixture Ratio. Throat Diam(in):', Dstr
    ]);
xlabel('Mixture Ratio');
ylabel('Coefficient of Thrust');

%Legend Titling
hleg = legend(flowstr);
htitle = get(hleg,'Title');
legstr = sprintf(['  Propellant \n' ...
    '    Flow (lbm/s)']);
set(htitle, 'String', legstr);
set(htitle, 'FontSize', 18);

grid;
PlotFixer2014()
hold off


%---Cstar---%
%Plotting
figure;
hold on;
m = length(mdot_plot);

for n = 1:length(mdot_plot)
    plot(AF_ratio,(Cstar(:,m).*3.28),Cstr(m))

    m = m-1;
end

%Labeling
title(['Cstar vs Mixture Ratio. Throat Diam(in):', Dstr]);
xlabel('Mixture Ratio');
ylabel('Cstar (ft/s)');

%Legend Titling
hleg = legend(flowstr);
htitle = get(hleg,'Title');
legstr = sprintf(['  Propellant \n' ...
```

```matlab
    '      Flow (lbm/s)']);
set(htitle, 'String', legstr);
set(htitle, 'FontSize', 18);


grid;
PlotFixer2014()
hold off


%---EXIT MACH---%
figure;
hold on;
m = length(mdot_plot);

for n = 1:length(mdot_plot)
    plot(AF_ratio,(Me(:,m)),Cstr(m))

    m = m-1;
end

%Labeling
title(['Exit Mach vs Mixture Ratio. Throat Diam(in):', Dstr]);
xlabel('Mixture Ratio');
ylabel('Mach Number');

%Legend Titling
hleg = legend(flowstr);
htitle = get(hleg,'Title');
legstr = sprintf(['  Propellant \n' ...
    '      Flow (lbm/s)']);
set(htitle, 'String', legstr);
set(htitle, 'FontSize', 18);

grid;
PlotFixer2014()
hold off


%%%Single Element Arrays%%%
%---THRUST AND PRESSURE PLOTS---%
m = 1;
    AF_ratio = ratio;
    figure;
    hold on;
    plot(AF_ratio,(Pchamber(:,m)*PSI_Pa),'r')
    plot(AF_ratio,(Thrust(:,m)*N_lbThrust),'b');
    plot(AF_ratio,(Isp(:,m)),'g');

    flowstr = num2str(mdot_lbm(m));
```

```matlab
    title(['Engine Performance vs Mixture Ratio. Propellant Flow Rate (
        lbm/s):', flowstr]);
    xlabel('Mixture Ratio');
    ylabel('Chamber Pressure (PSI), Thrust (lbs), Isp (s)');
    legend('Pchamber','Thrust','Isp');
    grid;
    PlotFixer2014()
  hold off;
m=1;
figure;
hold on;
plot(AF_ratio, Aratio(:,m),'b');
plot(AF_ratio, Me(:,m),'r');
plot(AF_ratio, Cf,'g');
plot(AF_ratio,K_exit,'k');
title(['Engine Performance vs Mixture Ratio. Propellant Flow Rate (lbm/
    s):', flowstr]);
xlabel('Mixture Ratio');
ylabel('Area Ratio, Mach Number, Cf');
legend('A_{exit}/A*','Mexit', 'Cf');
grid;
% axis([1 10 0 11]);

PlotFixer2014()
hold off;
% % figure;
% % hold on;
% % plot(AF_ratio, Cstar_error,'b');
% % plot(AF_ratio,Cf_error,'r');
% % xlabel('Mixing Ratio');
% % ylabel('Error (%)');
% % legend('C*','Cf');
% % grid;
% % % axis([1 10 0 11]);
% % hold off;
% % PlotFixer()
%
%T_t and To plots
m=1
AF_ratio = ratio;
figure;
hold on;
plot(AF_ratio,To_F(:,m),'r');
plot(AF_ratio,T_t_F(:,m),'k');
plot(AF_ratio,Te_F(:,m),'m');
plot(AF_ratio,Cstar*3.28,'b');
title(['Engine Performance vs Mixture Ratio. Propellant Flow Rate(lbm/s
    ):', flowstr]);
    xlabel('Mixture Ratio');
ylabel('Temperature ( F), C* (ft/s)');
```

```matlab
legend('T_{o}', 'T_{throat}', 'T_{exit}', 'C*');
axis([ratio_min ratio_max 0 6000]);
grid;
PlotFixer2014()
hold off;

%mole fractions plot
%Has issue with matirx dimensions. Not important at the moment
% figure;
% hold on;
% plot(AF_ratio, ym(:,1),'b');
% plot(AF_ratio, ym(:,2),'g');
% plot(AF_ratio, ym(:,3),'r');
% plot(AF_ratio, ym(:,4),'c');
% plot(AF_ratio, ym(:,5),'m');
% plot(AF_ratio, ym(:,6),'y');
% plot(AF_ratio, ym(:,7),'k');
% plot(AF_ratio, ym(:,8),'g--');
% plot(AF_ratio, ym(:,9),'b--');
% plot(AF_ratio, ym(:,10),'r--');
% plot(AF_ratio, ym(:,11),'c--');
% plot(AF_ratio, ym(:,12),'k--');
%
% title('Product Mole Fractions vs Mixing Ratio');
% xlabel('Mixing Ratio');
% ylabel('Mole Fractions');
% legend('H' ,'H_{2}', 'O' ,'O_{2}', 'OH', 'CO', 'CO_{2}', 'H_{2}O', '
    N_{2}', 'NO', 'N2O', Fuel);
% axis([ratio_min ratio_max 0 .6]);
% grid;
% PlotFixer()
% hold off;


% figure;
% hold on;
% plot(AF_ratio, Aratio,'b');
% plot(AF_ratio, Me,'r');
% title('Area Ratio vs. Mixing Ratio');
% xlabel('Mixing Ratio');
% ylabel('Area Ratio, Mach Number');
% legend('A_{exit}/A*','M');
% grid;
% % axis([1 10 0 11]);
% hold off;
% PlotFixer()

toc
```

D.3.2 Rocket Engine Model, Advanced

```matlab
function [Po,To,T_t,Te,Ve,Aratio,Me,Thrust,rho_o,Cf,C_star,Isp,Ke] =
    Get_Properties_V3(Aratio,Tpre,Pinit,Fuel,Oxidizer,mdot,ratio,
    D_throat)
%% Created by: Stewart Youngblood. Written: 4/14/14. Edited:6/1/2014
%This function calculates the gas flow from the combustion
%chamber to the nozzle exit and accounts for intial reaction in the
%combustion chamber and reactions through the nozzle.
%
%INPUT:
%1)Exit Pressure - Pexit (Pa)
%2)Temperature pre-combustion - Tpre (K)
%3)Chamber Pre-Ignition Pressure - Pchamber (Pa)
%4)Fuel (String)
%5)Oxidizer (String)
%6)Propellant Mass Flow - mdot(Array)
%7)Mixing Ratio - ratio (Array)
%
%OUPUT:
%1)Stagnation Pressure - Pchamber
%2)Stagnation Temperature - To (K)
%3)Throat Temperature - T_t (K)
%4)Exit Temperature - Te (K)
%5)Exit Velocity - Ve (m/s)
%6)Area Ratio of Throat to Nozzle - Aratio
%7)Exit Mach Number - Me
%8)Thrust
%Note: Code saves many properties as it cycles through. Can call upon
   more
%properties then those outputted if needed, look in Array Construction
   for
%properties saved.

%Notes: Found that was wrongly inputting mole fractions as Mass
   fractions.
%Have corrected issue, didn't catch because molecular weights so
   similar
%between ethanol and N2O

%% INITIALIZATION

%---ARRAY CONSTRUCTION---%
To = zeros(length(ratio),length(mdot));
Po = zeros(length(ratio),length(mdot));
Cpo = zeros(length(ratio),length(mdot));
Cvo = zeros(length(ratio),length(mdot));
rho_o = zeros(length(ratio),length(mdot));
ho = zeros(length(ratio),length(mdot));
```

```matlab
Ko = zeros(length(ratio),length(mdot));
Ro = zeros(length(ratio),length(mdot));
co = zeros(length(ratio),length(mdot));
Cp = zeros(length(ratio),length(mdot));
Cv = zeros(length(ratio),length(mdot));
rho_t = zeros(length(ratio),length(mdot));
T_t = zeros(length(ratio),length(mdot));
P_t = zeros(length(ratio),length(mdot));
v_t = zeros(length(ratio),length(mdot));
ct = zeros(length(ratio),length(mdot));
K = zeros(length(ratio),length(mdot));
R = zeros(length(ratio),length(mdot));
Ke = zeros(length(ratio),length(mdot));
Te = zeros(length(ratio),length(mdot));
Re = zeros(length(ratio),length(mdot));
rho_e = zeros(length(ratio),length(mdot));
he = zeros(length(ratio),length(mdot));
Ve = zeros(length(ratio),length(mdot));
ce = zeros(length(ratio),length(mdot));
C_star = zeros(length(ratio),length(mdot));
Cf = zeros(length(ratio),length(mdot));
C_star_calc = zeros(length(ratio),length(mdot));
Cf_calc = zeros(length(ratio),length(mdot));
Cf_error = zeros(length(ratio),length(mdot));
Cstar_error = zeros(length(ratio),length(mdot));
%Aratio = zeros(length(ratio),length(mdot));
Me = zeros(length(ratio),length(mdot));
Thrust = zeros(length(ratio),length(mdot));
Isp = zeros(length(ratio),length(mdot));
Cp_exit = zeros(length(ratio),length(mdot));
Cv_exit = zeros(length(ratio),length(mdot));
P_exit = zeros(length(ratio),length(mdot));

%---GAS OBJECTS---%
switch Fuel
    case 'Propane'
        gas = IdealGasMix('GRI30.xml');
        iFUEL = speciesIndex(gas,'C3H8');
        iOXI = speciesIndex(gas,Oxidizer);
        species = {'H' 'H2' 'O' 'O2' 'OH' 'CO' 'CO2' 'H2O' 'N2' 'NO' '
            N2O' 'C3H8'};
        ym = zeros(length(ratio),length(mdot),length(species));

    case 'Ethanol'
        %gas = IdealGasMix('ethanol_mech.xml');
        %gas = IdealGasMix('Ethanol_N2OSimple.xml');
        gas = IdealGasMix('Ethanol_N2O.xml');
        iFUEL = speciesIndex(gas,'C2H5OH');
        iOXI = speciesIndex(gas,Oxidizer);
        species = {'H' 'H2' 'O' 'O2' 'OH' 'CO' 'CO2' 'H2O' 'N2' 'NO' '
```

```matlab
            N2O' 'C2H5OH'};
        ym = zeros(length(ratio),length(mdot),length(species));

        %NOTE: Have simple xml file with only 12 species for Ethanol/
            N2O
        %reaction and have more advanced Ethanol File with 50 plus
            species.
        %The larger xml predicts at a lower mixing ratio. Neither file
            has
        %kinetics, so will add xml with kinetics

end
nsp = nSpecies(gas);




%% FLUID MODEL
%Iterating through ratios. Must create an individual gas for each ratio
for k = 1:length(mdot)
    for i = 1:length(ratio)
        switch Fuel
            case 'Propane'
                LHV = 46.334e6;                 % Lower heating value of
                    fuel, from Stone.
                y_oxifuel = zeros(nsp,1);    % Massfraction array with
                    zeros.
                y_oxifuel(iFUEL) = (mdot(k)/(1 + ratio(i)));%/44.1;  %
                    Mass
                y_oxifuel(iOXI) = (ratio(i)/(1 + ratio(i)))*mdot(k);%
                    /44.013;  % Set amount of oxidizer based on ratio


            case 'Ethanol'
                y_oxifuel = zeros(nsp,1);    % Massfraction array with
                    zeros.
                y_oxifuel(iFUEL) = (mdot(k)/(1 + ratio(i)));%/46.06844;
                     Mass
                y_oxifuel(iOXI) = (ratio(i)/(1 + ratio(i)))*mdot(k);%
                    /44.013;  % Set amount of oxidizer based on ratio



        end
        %---MASS FLOW---%
        %mdot(i,k) = mdot(k) + ratio(i)*mdot(k);

        %---EQUILIBRIATE GAS---%
        At = (pi/4)*D_throat^2;
        [Pchamb] = Chamber_CombV2(Tpre, Pinit, At, mdot(k), Fuel,
            y_oxifuel);
```

```matlab
gas = set(gas,'T',Tpre,'P',Pchamb,'Y',y_oxifuel);
gas = equilibrate(gas,'HP');

%Note: Need to address gamma throat finder as the iteration is
%producing a gamma that is slightly off do to step size of

%---STAGNATION PROPERTIES---%
To(i,k) = temperature(gas);
Po(i,k) = pressure(gas);
Cpo(i,k) = cp_mass(gas);
Cvo(i,k) = cv_mass(gas);
rho_o(i,k) = density(gas);
ho(i,k) = enthalpy_mass(gas);


%%---MOLE FRACTIONS---%
%[y] = moleFraction(gas, species);

%     for n = 1:length(species)
%          ym(i,n) = y(n);
%     end


%---THROAT PROPERTIES---%
%Pass in gas object, outputs throat temperature and pressure
[T_t(i,k), P_t(i,k)] = Throat_Prop(gas);

gas = set(gas,'T',T_t(i,k),'P',P_t(i,k));
Cp(i,k)=cp_mass(gas);
Cv(i,k)=cv_mass(gas);
rho_t(i,k)=density(gas);
v_t(i,k) = soundspeed(gas);


%---EXIT PROPERTIES---%
%Pass in gas object and exit pressure, outputs exit gas
   properties
%Error is here iwth pressure integration. dP of 1kpa is to
   large a
%step size, putting gas at a state thats resulting in errors
   down
%stream of ~6%. Need to adjust integration method so uses
   perhaps
%bisection for the pressure iteration.
[Te(i,k), Ke(i,k), Re(i,k), P_exit(i,k)] = Exit_Props(gas,
   Aratio,ho(i,k));

gas = set(gas,'T',Te(i,k),'P',P_exit(i,k));
he(i,k) = enthalpy_mass(gas);
```

```
rho_e(i,k) = density(gas);
Cp_exit(i,k) = cp_mass(gas);
Cv_exit(i,k) = cv_mass(gas);


%---EXIT VELOCITY---%
Ve(i,k) = sqrt(2*(ho(i,k) - he(i,k)));
ce(i,k) = soundspeed(gas);
Me(i,k) = Ve(i,k)./ce(i,k);


%---AREA RATIO---%
%Aratio(i,k) = rho_t(i,k)*v_t(i,k)/(rho_e(i,k)*Ve(i,k));
%result = Aratio_Kvar(Aratio(i,k), Ke(i,k), 'MACH NUMBER');
%Me(i,k) = result(2);

%---C_STAR CALCULATION--%
Ko(i,k) = Cpo(i,k)/Cvo(i,k);
Ro(i,k) = (Cpo(i,k)-Cvo(i,k));
co(i,k) = sqrt(Ko(i,k)*Ro(i,k)*To(i,k));
K(i,k) = Cp(i,k)/Cv(i,k);
R(i,k) = (Cp(i,k)-Cv(i,k));
ct(i,k) = sqrt(K(i,k)*R(i,k)*T_t(i,k));

C_star(i,k) = (co(i)/Ko(i,k)) * (rho_o(i,k)/rho_t(i,k)) * (co(i
    ,k)/ct(i,k));

C_star_calc(i,k) = Po(i,k)*At/mdot(k);


%---THRUST COEFFICIENT---%
Cf(i,k) = Ve(i,k)/C_star(i,k);


%---THRUST---%
Thrust(i,k) = Ve(i,k)*mdot(k);

Cf_calc(i,k) = Thrust(i,k)/(Po(i,k)*At);


%---ERROR CALCULATIONS---%
Cf_error(i,k) = 100 * abs(Cf(i,k)-Cf_calc(i,k))/Cf(i,k);
Cstar_error(i,k) = 100 * abs(C_star_calc(i,k)-C_star(i,k))/
    C_star(i,k);

%---ISP CALCULATIONS---%
Isp(i,k) = Thrust(i,k)/(mdot(k)*9.8066);


%Step Count
```

```
        j = length(ratio);
        steps_left = j-i
    end
end
end
```

D.3.3   Combustion Chamber Pressure Calculator

```
function [Pmid] = Chamber_CombV2(Tpre, Pinit, At, mdot, Fuel, y_oxifuel
    )
%% Created by: Stewart Youngblood. Written: 4/14/14. Edited:
%This function calculates the combustion chamber stagnation properties
%(Po,To)using the isentropic choke flowed equation. Uses the bisection
    method to
%iterate through until the choked mass flow is equal to the injected
%propellant mass flow, at which point the system will be "steady state"
     at
%that pressure and temperature
%
%INPUT:
%1)Gas Object - gas_pre
%2)Throat Diameter - D_throat
%3)Propellant Mass Flow - mdot
%4)Gas object composition - x_oxifuel
%
%OUTPUT:
%1)PostCombustion Gas State - gas_post

%Constants
Rs = 8.314; %J/K*mol
M = 1;

%Initialization
switch Fuel
    case 'Propane'
        gas = IdealGasMix('GRI30.xml');

    case 'Ethanol'
        %gas = IdealGasMix('ethanol_mech.xml');
        %gas = IdealGasMix('Ethanol_N2OSimple.xml');
        gas = IdealGasMix('Ethanol_N2O.xml');

        %NOTE: Have simple xml file with only 12 species for Ethanol/
            N2O
        %reaction and have more advanced Ethanol File with 50 plus
            species.
        %The larger xml predicts at a lower mixing ratio. Neither file
            has
        %kinetics, so will add xml with kinetics
```

```
        end

    %Set gas pre-reaction at ambient temperature and pressure.
    gas = set(gas,'T',Tpre,'P',Pinit,'Y',y_oxifuel);
    m_choked = 0;
    Ptest = pressure(gas);
    Tinit = temperature(gas);
    toler = 10^-6;

    %Bisection Variables
    P_high = 1000*Ptest;
    P_low = Ptest;
    Pmid = (P_high+P_low)/2;

    %Pmid = Ptest;

    while abs(mdot - m_choked)>toler

        %Update Guess
        Pmid = (P_high + P_low)/2;

        %Pmid = Pmid+10000;
        %Set Gas properties
        gas = set(gas, 'T', Tinit, 'P', Pmid, 'Y', y_oxifuel);

        %Equilibrate Gas. Do so at constant Enthalpy and Pressure
        gas = equilibrate(gas,'HP');

        %Get Properties
        To = temperature(gas);
        MW = meanMolarMass(gas);

        [gamma, Tthroat, Pthroat] = ChokedThroat_gamma(gas);

        R = Rs*1000/MW;
        %Calculate Choked Mass Flow
        %m_choked = (At*Pmid/sqrt(To)) * sqrt(gamma/(R*1000/MW)) *(1 + 0.5
            *(gamma-1))^-((gamma+1)/((gamma-1)/2));
        m_choked = (At * Pmid/sqrt(To)) * sqrt(gamma/R) * M * (1 + .5 * (
            gamma-1) * M^2 )^-((gamma + 1)/(gamma - 1)/2);


        if m_choked > mdot
            P_high = Pmid;
        else
            P_low = Pmid;
        end

        %Running Check
```

```
        (mdot - m_choked)

end


% gas = set(gas, 'T', Tinit, 'P', Pmid, 'Y', x_oxifuel);
%
% %Equilibrate Gas. Do so at constant Enthalpy and Pressure
% gas = equilibrate(gas,'HP');

end
```

D.3.4   Combustor Model

D.4   Rocket Model Base Code Functions

D.4.1   Engine Throat Flow Property Calculator Module

```
function[gamma, Tthroat, Pthroat] = Throat_Prop(gas)
%% Created by: Stewart Youngblood. Written: 3/2/14. Edited:6/1/2014
%SOLUTION METHOD:
%1st) Guess T, iterate P until have equal entropy
%2nd) Check if H + 1/2(speed of sound)^2 = Ho

%Constants
global Pamb

%Gas State for iterations
T_test = temperature(gas);
P_test = pressure(gas);
So = entropy_mass(gas);
Ho = enthalpy_mass(gas);

%Iteration Variables
Hto = Ho + 1;
toler_s = 10^-8;
Phigh = P_test;
Plow = Pamb/1000;

Pmid = (Phigh + Plow)/2;

while Ho<=Hto
    T_test = T_test - 1;
    gas = set(gas,'T',T_test,'P',Pmid);
    Stest = entropy_mass(gas);

    %Prep Entropy Bisection Variables
    Phigh = P_test;
```

```
        Plow = Pamb/1000;

    while abs(So-Stest) > toler_s

        %Update guess
        Pmid = (Phigh+Plow)/2;

        %P_test = P_test - 1000;
        gas = set(gas,'T',T_test,'P',Pmid);
        Stest = entropy_mass(gas);

        if Stest < So
            Phigh = Pmid;
        else
            Plow = Pmid;
        end

        %Run Check
        %So-Stest
    end
    gas = equilibrate(gas,'TP');
    c = soundspeed(gas);
    Hto = enthalpy_mass(gas) + 0.5.*c.^2;
end

%Gamma Calculations
Cp = cp_mass(gas);
Cv = cv_mass(gas);
gamma = Cp/Cv;

%Throat Properties
Tthroat = temperature(gas);
Pthroat = pressure(gas);


end
```

D.4.2   Nozzle Exit Flow Property Calculator Module

```
function[Te, Ke, Re] = Exit_Props(gas, Pexit)
%% Created by: Stewart Youngblood. Written: 12/23/14. Edited:
%SOLUTION METHOD
%Iterate using bisection method T until entropy at exit equals entropy
   at throat.
%Assuming expansion is to ambient pressure and isentropic nozzle
toler = 1e-8;

So = entropy_mass(gas)-1;
Stest = entropy_mass(gas);
```

```matlab
T_high = temperature(gas);
T_low = 298;
Tmid = (T_high + T_low)/2;


while abs(So - Stest)>toler
    gas = set(gas,'T',Tmid,'P',Pexit);
    gas = equilibrate(gas,'TP');
    Stest = entropy_mass(gas);
    if Stest > So
        T_high = Tmid;
    else
        T_low = Tmid;
    end
    %Update guess
    Tmid = (T_high+T_low)/2;

end

%%NOTE:
%If bisection method above fails to converge or fails at equilibrate(
   gas),
%use below iteration. Below method is slowly, but more robust.

%     T_test = temperature(gas);
%     So = entropy_mass(gas);
%     Sp = entropy_mass(gas)+1;
%
%     while So<Sp
%         T_test = T_test - 1;
%         gas = set(gas,'T',T_test,'P',Pexit);
%         gas = equilibrate(gas,'TP');
%         Sp = entropy_mass(gas);
%     end
%
 Cp_e = cp_mass(gas);
 Cv_e = cv_mass(gas);

%Pass out Te, ke, Re for arrays
%Te = T_test;
Te = Tmid;
Re = Cp_e-Cv_e;
Ke = Cp_e/Cv_e;


end
```

D.4.3   Ethanol Property Module

```matlab
function [K_eth, Cp_eth] = thermalProps_Ethanol(Tbar)
%% Created By: Stewart Youngblood. Written:2/19/2014. Edited:
%
%This function takes in Tbar (average of droplet temperature and
%surrounding temperature) and plugs it into two polynomials. One
   polynomial
%for the specific heat Cp, the other for thermal conductivity K.

%OUTPUTS:
%1)K_eth, (W/m*K)
%2)Cp_eth, (KJ/Kmol*K)


%% CP Polynomial
a1 = 6.990;
a2 = 39.741;
a3 = -11.926;
a4 = 0;
a5 = 0;

%MW of Ethanol
MW = 46.07;
theta = Tbar/1000;

Cp_eth = 1000*4.184*(a1 + a2*(theta) + a3*(theta^2) + a4*(theta^3) + a5
   *(theta^(-2)))/MW;


%% Thermal Conductivity Fit Polynomial
a1 = -2.46663E-2;
a2 = 1.5589255E-4;
a3 = -8.22954822E-8;
a4 = 0;
a5 = 0;
a6 = 0;
a7 = 0;

K_eth = a1 + a2*Tbar + a3*Tbar^2 + a4*Tbar^3 + a5*Tbar^4 + a6*Tbar^5 +
   a7*Tbar^6;


end
```

D.4.4 Nitrous Oxide Property Module

```matlab
function [property] = N2O_Properties(T, option)
%% Created by: Stewart Youngblood. Written: 6/19/2014. Edited:
%This function solves the polynomial thermo and transport property
%equations for liquid nitrous oxide. Assumes only temperature dependent
```

```matlab
%properties.
%
%INPUT:
%1) Temperature of Liquid Nitrous oxide - T_liq
%2) Property to solve for - option (String)
%
%OUTPUT:
%1) Property solved for - property
%
%Available Properties
%1)
%2)
%3)
%
%Notes:
% Polynomial equations and constants for equations from "Thermophysical
% properties of nitrous oxide" by IHS, ESDU. Issue # 91022, Sepetember
%   1991


%% INITIALIZATION

%Constants
T_Crit = 309.57; %K, Critical Temperature
P_crit = 7251; %kPa, Critical Pressure
rho_crit = 452; %kg/m^3, Critical Density
Tr = T/T_Crit;

%% PROPERTIES CALCS

switch option
    case 'Vapour_Pressure'

    case 'SatLiquid_Density'

    case 'SatVapour_Density'

    case 'Enthalpy_SatLiquid'
        %Range of Applicability -90C to 35C
        b1 = -200;
        b2 = 116.043;
        b3 = -917.225;
        b4 = -794.779;
        b5 = -589.587;

        h_L = b1 + b2*(1-Tr)^(1/3) + b3*(1-Tr)^(2/3) + b4*(1-Tr) + b5
            *(1-Tr)^4/3;

        property = h_L;

    case 'Enthalpy_Vaporization'
```

203

```matlab
        %Range of Applicability -90C to 35C
        b1 = -200;
        b2 = 116.043;
        b3 = -917.225;
        b4 = -794.779;
        b5 = -589.587;

        h_L = b1 + b2*(1-Tr)^(1/3) + b3*(1-Tr)^(2/3) + b4*(1-Tr) + b5
            *(1-Tr)^4/3;
        %Range of Applicability -90C to 36C
        b1 = -200;
        b2 = 440.055;
        b3 = -459.701;
        b4 = 434.081;
        b5 = -485.338;

        h_G = b1 + b2*(1-Tr)^(1/3) + b3*(1-Tr)^(2/3) + b4*(1-Tr) + b5
            *(1-Tr)^4/3;

        h_vap = h_G - h_L;

        property = h_vap;

    case 'Enthalpy_SatVapor'
        %Range of Applicability -90C to 36C
        b1 = -200;
        b2 = 440.055;
        b3 = -459.701;
        b4 = 434.081;
        b5 = -485.338;

        h_G = b1 + b2*(1-Tr)^(1/3) + b3*(1-Tr)^(2/3) + b4*(1-Tr) + b5
            *(1-Tr)^4/3;

        property = h_G;

    case 'Cp_SatLiquid'

    case 'Cp_SatVapour'
        %Isobaric assumption
    case 'DynViscosity_SatLiquid'

    case 'DynViscosity_SatVapour'

    case 'ThermConduct_SatLiquid'

    case 'ThermConduct_SatVapour'

    case 'Surface_Tension'
```

```matlab
        case 'Cp_IdealGas'
            %Isobaric Assumption
        case 'Enthalpy_IdealGas'

        case 'DynViscosity_DiluteGas'

        case 'ThermConduct_DiluteGas'

    end


    end
```

REFERENCES

[1] J.D. Lindbolm. Analysis of nitrous oxide as a propellant with selected fuels. Master's thesis, New Mexico Institute of Mining and Technology, 2013.

[2] George P. Sutton and O. B. Oscar Biblarz. *Rocket Propulsion Elements*. Wiley and Sons, 7th edition, 2001.

[3] Vadim Zakirov, Martin Sweeting, Timothy Lawrence, and Jerry Sellers. Nitrous oxide as a rocket propellant. *Acta Astronautica*, 48(5-12):pp 353–362, 2001.

[4] Philippe Grenard, Carola Bauer, Aaron Koch, and Holger Winkler. Evaluation of rocket launches' effect on climate. ONERA, 2013.

[5] Chung K. Law. Fuel options for next-generation chemical propulsion. *AIAA*, 50(1):pp. 19–36, January 2012.

[6] Sanford Gordon and Bonnie J. McBride. *Computer Program for Calculation of Complex Chemical Equilibrium Compositions and Application: Analysis*, 1994.

[7] A.A. Alexeenko, N.E. Gimelshein, D.A.Levin, R.J. Collins, R. Rao, G.V. Candler, S.F. Gimelshein, J.S. Hong, and T.schilling. Modeling of flow and radiation in the atlas plume. *Thermophysics and Heat Transfer*, 16:pp. 50–57, 2002.

[8] David Munday, andJumhui Liu Ephraim Gutmark, and K. Kailasanath. Flow structure of supersonic jets from conical c-d nozzles. *AIAA*, 2009.

[9] Bhanu Swaroop Gaddam and Amar. Subramanya. Preliminary rocket exhaust plume analysis and compatible acoustic ignition technology. International Conference on Mechanical, Automobile and Biodiesel Engineering, 2012.

[10] Carola Bauer, Aaron Koch, Francesco Minutolo, and Philippe Grenard. Engineering model for rocket exhaust plumes verified by cfd results. ONERA, 2014.

[11] Henry L. Alden and Roger H. Habert. Gas dynamics of high-altitude rocket plumes, July 1964.

[12] B. Abramzon and W.A. Sirignano. Droplet vaporization model for spray combustion calculations. *Heat Mass Transfer*, Vol. 32, No. 9:pp. 1605–1618, May 1989.

[13] S.R.Turns. *An Introduction to Combustion*. McGraw-Hill, 3rd edition, 2011.

[14] S.K. Aggarwal and H.C. Mongia. Multicomponenet and high-pressure effects on droplet vaporization. *ASME*, Voume 124:pp. 248–255, April 2002.

[15] R Viskanta and M.P. Menguc. Radiation heat transfer in combustion systems. *Energy Combustion Science*, 13:pp.97–160, 1987.

[16] David Goodwin. *Cantera C++ User Guide*. Caltech, 2002.

[17] Deep Gupta. Comparison of combustion calculations using cantera and chemkin. Technical report, Indian Institute of Technology of Bombay, 2008.

[18] P. Bangalore Venkatech, Entremont J.D, S.E. Meyer, S.P.M Bane, and M.C. Grubelich. High-pressure combustion and deflagration-to-dtonation transition in ethylene/nitrous oxide mixtures. 8th U.S. National Combustion Meeting, 2013.

[19] Nick M. Marinov. A detailed chemical kinetic model for high temperature ethanol oxidation. Technical report, Lawerence Livermore National Lab, October 1998.

[20] H.E. Dillon and S.G. Penoncello. A fundamental equation for the calculations of the thermodynamic properties of ethanol. Technical report, University of Idaho, June 2003.

[21] Randolph C. Wilhoit, Jing Chao, and Kenneth R. Hall. Thermodynamic properties of key organic oxygen compounds in the carbon range c1 to c4. Technical report, Texas A&M University, 1985.

[22] G.H. Walterm. Thermophysical properties of nitrous oxide. Paper 91022, IHS ESDU, September 1991.

[23] Zola Fox. Cavitating venturis for small pulsing rocket engines. *Space/Aeronautics*, 38(7), December 1962.

[24] Leroy J. Krzycki. *How to Design, Build and Test Small Liquid-Fuel Rocket Engines*. Rocketlab, 1967.

[25] Gerald Hagemann, Hans Immich, Thong Van Nguyen, and Gennady E. Dumnov. Advanced rocket nozzles. *Propulsion and Power*, 14(5):pp. 620–634, 1998.

[26] George A. Repas. Hydrogen-oxygen torch ignitor. Technical report, NASA, March 1994.

[27] Arie Peretz, Omry Einav, Ben-Ami Hashmonay, Avi Birnholz, and Zeev Sobe. Development of laboratory-scale hybrid engine test facility. *Propulsion and Power*, 27(1):pp. 190–196, 2011.

[28] David Helderman. Measurement and analysis in a subscale rocket combustor. Master's thesis, Purdue University, 2009.

[29] Benjamin S. Waxman, Jonah E. Zimmerman, Drian J. Cantwell, and Gregory G. Zilliac. Effects of injector design on combustion stability in hybrid rocket using self-pressurizing oxidizers. 50th AIAA/ASME/SAE/ASEE Joint Propulsion Conference, July 2014.

[30] Nathaniel Oliver. Me 140 rocket setup description, September 2013.

[31] Mark Grubelich. Personal communication, July 2015.

[32] Mark Grubelich, John Rowland, and Larry Reese. A hybrid rocket engine design for simple low cost sounding rocket use. AIAA 29th Joint Propulsion Conference and Exhibit, June 1993.

[33] Shinichiro Tokudome, Tsuyoshi Yagashita, Ken Goto, Hiroto Habu, Naohiro Suzuki, Fuyuko Fukuyoshi, Yasuhiro Daimoh, and Fumio Okuno. Experimental study of nitrous oxide/ethanol propulsion system: Technology demonstration with a bbm. Eurpoean Conference for Aeronautics and Space Sciences 2013 Meeting, July 2013.

[34] James E. Cocchiaro and Jerry M. Ward. Dod explosives safety standard for energetic liquids program, 1998.

[35] SS Paulsen. Pressure systems stored-energy threshold risk analysis. Technical report, Department of Energy, August 2009.

[36] Claude Merrill. Nitrous oxide explosive hazards. Technical report, Air Force Research Laboratory, 2008.

[37] Konrad Munke. Nitrous oxide trailer rupture, October 2001.

[38] Asia Industrial Gases Association. Oxygen pipeline and piping systems, 2012.

[39] European Industrial Gas Association. Code of practice nitrous oxide, 2007.

[40] Advanced Specialty Gas Equipment. Gas compatibility, 2014.

[41] Compressed Gas Association. Cga g-4.1: Cleaning equipment for oxygen service, 1985.

[42] Paul W. Cooper. *Explosive Engineering*. Wiley-VCH, 1996.

[43] JM Dewey. The tnt equivalence of an optimum propane?oxygen mixture. *Physics D: Applied Physics*, 38:pp. 4245–4251, 2005.

[44] Joong M. Yang. An improved analytical approach to determine the explosive effects of flammable gas-air mixtures. Technical report, Lawerence Livermore National Laboratory, November 2005.

[45] Daniel A. Crowl. *Understanding Explosions*. American Institute of Chemical Engineers, 2003.

[46] K Niklasinski. Application of cantera in liquid rocket engine performance calculations, November 2013.

[47] Dieter K. Huzel and David H. Huang. *Design of Liquid Propellant Rocket Engines*. NASA, 1967.

[48] Sanford Gordon and Bonnie J. McBride. *Computer Program for Calculation of Complex Chemical Equilibrium Compositions and Application: Users Manual and Program Description*. NASA, 1996.

[49] NCP Alcohols. Msds: Ethanol 200proof. Technical report, May 2012.

[50] Melissa Lyons. Personal communication, August 2015.

[51] Asia Industrial Gases Association. Safe practice for storage and handling of nitrous oxide, 2013.

[52] Parker Hannifi Corporation. *Parker O-Ring Handbook*, 2007.

[53] Robert A. Braeunig. Rocket and space technology, 2012.

[54] Ideal AeroSmith. Flow calculations for gases, 2014.

[55] Jeff Phillip. Propellant supply system, full diagram. May 2015.

[56] Thermal-Fluids Central. Thermophysical properties: Ethanol. Thermal-Fluids Central, July 2010.

[57] Ideal AeroSmith. Flow calculations for liquids, 2014.

Design and Testing of a Liquid Nitrous Oxide and Ethanol
Fueled Rocket Engine

by

Stewart H. Youngblood